

THESIS

NUCLEOPHOSMIN DEPOSITION DURING mRNA 3' END PROCESSING
INFLUENCES POLY(A) TAIL LENGTH AND mRNA EXPORT

Submitted by

Fumihiko Sagawa

Graduate Degree Program in Cell and Molecular Biology

In partial fulfillment of the requirements

For the Degree of Master of Science

Colorado State University

Fort Collins, Colorado

Spring 2011

Master's Committee:

Advisor: Jeffrey Wilusz

Co-Advisor: Carol J. Wilusz

A.S.N. Reddy
Douglas Thamm

ABSTRACT

NUCLEOPHOSMIN DEPOSITION DURING mRNA 3' END PROCESSING INFLUENCES POLY(A) TAIL LENGTH AND mRNA EXPORT

During polyadenylation the multi-functional protein nucleophosmin is deposited onto all cellular mRNAs analyzed. Premature termination of poly(A) tail synthesis using cordycepin abrogates deposition of the protein onto the mRNA, indicating natural termination of poly(A) addition is required for nucleophosmin binding. Nucleophosmin appears to be a *bona fide* member of the complex involved in 3' end processing as it is directly associated with the AAUAAA-binding CPSF-160 protein and can be co-immunoprecipitated with other polyadenylation factors. Furthermore, reduction in the levels of nucleophosmin results in hyperadenylation of mRNAs, consistent with alterations in poly(A) tail chain termination. Finally, knock down of nucleophosmin results in retention of poly(A)+ RNAs in the cell nucleus, indicating that nucleophosmin binding influences mRNA export. Collectively these data suggest that nucleophosmin plays an important role in poly(A) tail length determination and helps network 3' end processing with other aspects of nuclear mRNA maturation.

ACKNOWLEDGEMENTS

First and most of all, I would like to thank my advisors, Jeff and Carol for their unconditional morale and professional support throughout my five-year graduate school time. They have enriched my laboratory experience with their uniquely combined repertoires from the spot-on scientific expertise and thorough guidance, to joyous lab environments and countless moments of what we call 'Wilusz²-ness'. The Wilusz² lab was always encouraging and exciting, even when I would come back at night to continue experiments and find our -80°C freezers were alarming / dying with lab temperatures in the Micro Building reaching 40°C. I am also grateful to have Doug Thamm and A.S.N. Reddy as committee members. They have been patiently putting up with me in both the good and agonizing times - and have significantly expanded the horizons of my project with their knowledge. Finally I am, needless to say, quite fortunate to have fellow/neighbor lab members, past and present, to help propel my project with experimental tips, immense/intense 'brainshooting' and harmonizing the lab with science and fun. It has been irreplaceable to chill out with my friends, no matter where or what they are.

TABLE OF CONTENTS

Abstract.....	ii
Acknowledgements.....	iii
Table of Contents.....	iv
List of Figures.....	v
List of Tables.....	vi
Introduction.....	1
Results	
Polyadenylation mediated by a variety of cellular polyadenylation signals causes deposition of nucleophosmin on transcripts.....	21
Nucleophosmin is deposited on mRNAs as a result of the natural process of termination of polyadenylation.....	24
Nucleophosmin interacts with factors directly implicated in the determination of poly(A) tail length.....	26
Knock down of nucleophosmin in cells results in hyperadenylation of mRNAs in HeLa cells.....	29
Hyperadenylation of RNA could be recapitulated in an <i>in vitro</i> polyadenylation assays from NPM knock down extracts.....	33
Knock down of nucleophosmin in dividing cells results in reduced mRNA export in the cytoplasm.....	40
NPM depletion does not influence the relative use of alternative polyadenylation sites.....	40
NPM knock down leads to slow growth in HeLa cells.....	45
Attempts/alternatives to purify a 14kDa protein that may also be a component of the polyadenylation mark.....	47
Microarray analyses on mRNAs following the transient depletion of NPM in HeLa cells.....	50
Discussion.....	54
Experimental Procedures.....	59
References.....	73

LIST OF FIGURES AND TABLES

Figures

1. Diagram of AAUAAA core polyadenylation signal surrounding the cleavage site.....	2
2. Diagram of cleavage/polyadenylation processing.....	6
3. Diagram of co-transcriptional nuclear processing.....	10
4. Model of poly(A) tail dynamics after DNA damage.....	16
5. Nucleophosmin is directly deposited on cellular poly(A) ⁺ RNAs both <i>in vitro</i> polyadenylation system and dividing cells.....	22
6. Sequences of various polyadenylation signals.....	23
7. Deposition of NPM on RNAs is associated with natural termination of poly(A) synthesis.....	25
8. NPM is associated with the core polyadenylation factor CPSF.....	27
9. Verification of stable NPM knock down in HeLa cells by an NPM-specific shRNA.....	29
10. Stable knock down of NPM results in an increase in mRNA poly(A) tail length in cells.....	30
11. Transient transfection with independent NPM shRNA does not result in an increase of polyadenylated forms of 25S rRNA.....	30
12. Transient knock down using NPM shRNAs does not induce the hyperadenylation of GAPDH or β -actin mRNAs.....	31
13. Transient NPM knock down using NPM shRNAs results in the hyperadenylation of puromycin N-acetyltransferase (PAC) mRNAs.....	32
14. Hyperadenylation can be demonstrated in nuclear extract-based polyadenylation assays when NPM is depleted.....	34
15. PARN deadenylase is not involved in hyperadenylation defects of NPM knock down.....	36
16. WT and NPM KD HeLa nuclear extracts are similarly sensitive to addition of exogenous poly(A).....	38
17. NPM knock down does not affect the expression level of CPSF160, PAP, PABPN1 and α -tubulin.....	39
18. Reduction of NPM levels results in the accumulation of poly(A) ⁺ RNAs in the nucleus.....	41
19. NPM knock down does not affect the subcellular localization of 25S rRNA.....	42
20. Schematic diagram of alternative polyadenylation sites in tumor cells, RPA assay to detect the sites and CCND1 and IMP1 mRNAs with known alternative polyadenylation sites.....	43
21. NPM knock down does not lead to alternative polyadenylation site usage.....	44
22. The NPM knock down HeLa cell lines divide significantly slower than WT or LKO control HeLa cell lines, but similarly sensitive to 5FU treatment.....	46
23. Biotinylated SVL RNA is polyadenylated in our <i>in vitro</i> polyadenylation assays.....	48
24. List of candidates narrowed down for a 14kDa protein which behaves similarly to NPM in our <i>in vitro</i> polyadenylation assays.....	50
25. List of top ranked GO terms associated mRNAs that are misregulated upon transient NPM knock down in HeLa cells.....	51
26. List of top 50 ranked mRNAs up-regulated or down-regulated following transient NPM knock down in HeLa cells.....	52

Tables

1. List of oligonucleotides used for q-RT PCR assays.....	59
2. List of oligonucleotides hybridized to generate transcription templates for MC4R and PAPOLG polyadenylation signals.....	60
3. List of oligonucleotides used to clone RPA probes.....	61
4. List of oligonucleotides used to clone northern probes.....	62
5. List of oligonucleotides used to hybridize to 3' UTR of mRNAs to trim the 3' UTR length in RNase H/northern assays.....	64
6. List of oligonucleotides used for LLM-Pat assays.....	67
7. List of oligonucleotides used to detect mRNA by RT-PCR assays.....	68

Introduction

With the completion of The Human Genome Project, researchers seemed to have the blueprint for what makes a human a human, rather than a mouse or a chimpanzee. However, what was actually revealed is the striking similarities in gene content and sequence between evolutionarily distinct organisms. This finding emphasizes the huge role that regulation of gene expression must play in defining cellular characteristics.

The regulation of gene expression takes place at both the transcriptional and post-transcriptional levels. Because accurate regulation is critical to all aspects of cell metabolism, the precise and detailed characterization of these regulatory networks greatly augments our understanding of a wide range of biological events that includes cancer, the molecular basis of disease and therapeutic approaches. Post-transcriptional processing has gained significant attention as a key participant in the regulation of gene expression in eukaryotic cells. One such process is the maturation of nascent RNA transcripts into mRNPs.

Three main co-transcriptional events in mammalian cells are required to process pre-mRNAs into mature mRNAs – capping, splicing and 3' end formation (Shatkin, 1976; McCracken et al., 1997a; b; Long and Caceres, 2009; Keller et al., 1991; Neilson and Sandberg, 2010). Capping is the process in which a 7-methyl-guanosine triphosphate is introduced at the 5' end of pre-mRNAs in a 5'-5' linkage (Shatkin, 1976). Splicing is the process in which introns are removed and exons are joined together (Long and Caceres, 2009). 3' end formation, which is the main focus of this thesis, comprises two events – cleavage and polyadenylation. Cleavage defines the 3' end of the transcript and

generates a 5' product which eventually becomes the mature mRNA. The 3' product is degraded, but nevertheless plays an important role in transcription termination (West et al., 2008; Luo and Bentley, 2004). Polyadenylation is the addition of 150-200 adenines to the 3' end of the 5' cleavage product. Upon the completion of nuclear mRNA processing, mRNA is transported to cytoplasm where it can be localized, translated and eventually degraded.

Cis elements in cleavage/polyadenylation

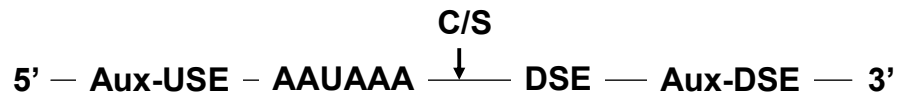


Figure 1: Diagram of AAUAAA core polyadenylation signal surrounding the cleavage site

Typical mammalian polyadenylation signals may contain an Auxiliary UpStream Element (Aux-USE), AAUAAA core upstream element, Cleavage Site (C/S), U-rich sequence which is commonly known as the DownStream Element (DSE) and Auxiliary-DownStream Element (Aux-DSE). See the main text for further information.

In eukaryotic cells, there are four elements required for efficient polyadenylation (Figure 1). They are the core polyadenylation signal, AAUAAA, which is found 10-30 nt upstream of the actual cleavage site and a U-rich or GU-rich sequence which lies downstream of the cleavage site (the Downstream Sequence Element (DSE)). The cleavage site is also the point of polyadenylation and is thus often called polyadenylation site.

The core polyadenylation signal, AAUAAA was first discovered by comparing the sequences upstream of the cleavage site in mammalian pre-mRNAs (Proudfoot and Brownlee, 1976) and since then has been observed in a significant proportion of polyadenylated mRNAs. AAUAAA is the most common motif (present in close to 50% of

mRNAs) whereas AUUAAA is the most frequent variant among others (~15%) (Hu et al., 2005) and its activity is comparable to that of AAUAAA *in vitro*. Mutation of any of other nucleotides leads to strong inhibition of processing *in vitro* (Wickens and Stephenson., 1984; Wilusz et al., 1989). There are other non-canonical and relatively rare poly(A) signals including 11 other variants – UAUAAA, AGUAAA, AAGAAA, AAUAUA, AAUACA, CAUAAA, GAUAAA, AAUGAA, UUUAAA, ACUAAA and AAUAGA (Hu et al., 2005; Beaulieu et al., 2000). These studies describe that AWUAAA (where W can be A or U) is the canonical polyadenylation motif upstream of the cleavage site. Recent genome-wide deep sequencing techniques (Ozsolak et al., 2010) also confirmed that the upstream sequence surrounding the polyadenylation site contains an AAWAAA motif near the annotated 3' ends of genes, which closely resembles the canonical AWUAAA motif found by other groups. The Milos laboratory also discovered that a UUUUUUUUUU motif can also be specifically positioned at about 21nt upstream to the polyadenylation site. This newly discovered UUUUUUUUUU polyadenylation signal, however, is exclusively found in non-coding RNAs, is not generally found in mRNAs and does not co-exist with canonical AWUAAA signals.

In addition to the core polyadenylation signals, there are also non-canonical polyadenylation signals. Bioinformatics studies show that nearly 30% of polyadenylation events do not use AWUAAA-containing polyadenylation signals (Ji and Tian, 2009). There are several papers devoted to unlocking the polyadenylation events which depend on non-canonical polyadenylation signals. Nunes et al., 2010 unveiled that melanocortin 4 receptor (MC4R) mRNAs utilizes an upstream A-rich polyadenylation signal and does not possess an AWUAAA sequence or U/GU-rich DSE. During this study, they further identified that A-rich signal-dependent polyadenylation may occupy up to one third of non-canonical polyadenylation pathways. One of the polyadenylation signals they identified is the jun B proto-oncogene (JUNB) which, just like MC4R gene, can undergo

successful polyadenylation with A-rich polyadenylation signals. Another well-documented non-canonical signal can be found in the poly(A) polymerase- γ (PAPOLG) gene (Venkataraman et al., 2005). PAPOLG gene lacks an AWUAAA canonical polyadenylation signal and uses UGUAN (where N can be any ribonucleotide) for efficient polyadenylation. UGUAN is a known binding site for mammalian Cleavage Factor I (CFI_m) and point mutations in the motif abolish efficient polyadenylation.

The site of cleavage is defined by the sequence elements that flank it – the polyadenylation signal and downstream U-rich DSE (Chen et al., 1995). Although the sequences immediately around the cleavage site are not highly conserved, studies have shown that adenine is found at the cleavage site of 70 % of mRNAs (Sheets et al., 1990). This finding implies that the first adenine in the poly(A) tail is likely to be template-encoded (Sheets et al., 1990). They have also shown that a cytosine residue is the most frequent nucleotide preceding the A residue in the cleavage site, thus a CA dinucleotide is a favored poly(A) site for many mRNAs (Sheets et al., 1990).

The third element of the core poly(A) signal is the U-rich or GU-rich DSE which lies ~15-30 nt downstream of the cleavage site and is not as conserved as the AAUAAA sequence (Chou et al., 1994). Analyses indicate that the DSE may consist of a 4 out of 5 base U tract (Chou et al., 1994). Point mutations in DSE usually have only a slight negative effect on cleavage efficiency and a more extensive deletion/mutation of the element is often necessary to completely eradicate the function (Chou et al., 1994). This may suggest functional redundancy in the downstream elements (Sittler et al., 1994; Zarkower and Wickens, 1988).

Other *cis*-elements involved in the 3' end formation are auxiliary USEs and auxiliary DSEs. The auxiliary USEs, located upstream of the core poly(A) signal, do not have a consensus sequence but often consist of UUUU (Zhao et al., 1999) or similar

sequences such as UGUA and UAUA (Hu et al., 2005). The efficiency of 3' end processing is enhanced by the presence of USEs as it is the binding site for general and regulatory polyadenylation factors such as Polypyrimidine Tract-Binding protein, PTBP1 (Moreira et al., 1998; Huang et al., 1999). Auxiliary DSEs can be G-rich and are also involved in regulating cleavage/polyadenylation efficiency (Arhin et al., 2002; Bagga et al., 1995; Dalziel et al., 2007). Our understanding of *cis* elements in the process of 3' end formation will be surely augmented as technologies advance and become more affordable.

Trans-acting factors in the cleavage reaction

Figure 2 portrays the factors involved in the cleavage/polyadenylation reaction in mammalian cells. The cleavage reaction in mammalian cells requires several factors – CPSF, CstF, CFI_m, CFII_m, RNAPII-CTD and PAP – which are described in detail below.

Cleavage Polyadenylation Specificity Factor is a hetero-pentameric protein complex, composed of CPSF160, 100, 73, 30 and hFip1 (Takagaki et al., 1988, 1989; Christofori and Keller, 1988; Gilmartin et al., 1989). CPSF160 binds strongly to the AAUAAA element (Christofori and Keller, 1988). It is required for both cleavage and polyadenylation reactions (Takagaki et al., 1988). All six nucleotides of AAUAAA are necessary for binding CPSF and RNAs as short as 10 nt can be recognized specifically (Keller et al., 1991). Mammalian CPSF100 possesses an RNA binding domain but has lost the ability to bind RNA (Callebaut et al., 2002; Aravind, 1999). CPSF-73 has endoribonuclease activity, which is believed to catalyze the cleavage at the end of the pre-mRNA 3'UTR (Mandel et al., 2006). CPSF30 is required for both the cleavage and polyadenylation reactions and prefers binding to poly(U) sequence in *in vitro* RNA binding (gel shift) assays (Barabino et al., 1997, 2000). hFip1 protein binds to U-rich RNA sequences present in the Aux-USE and coordinates the correct interaction of PAP

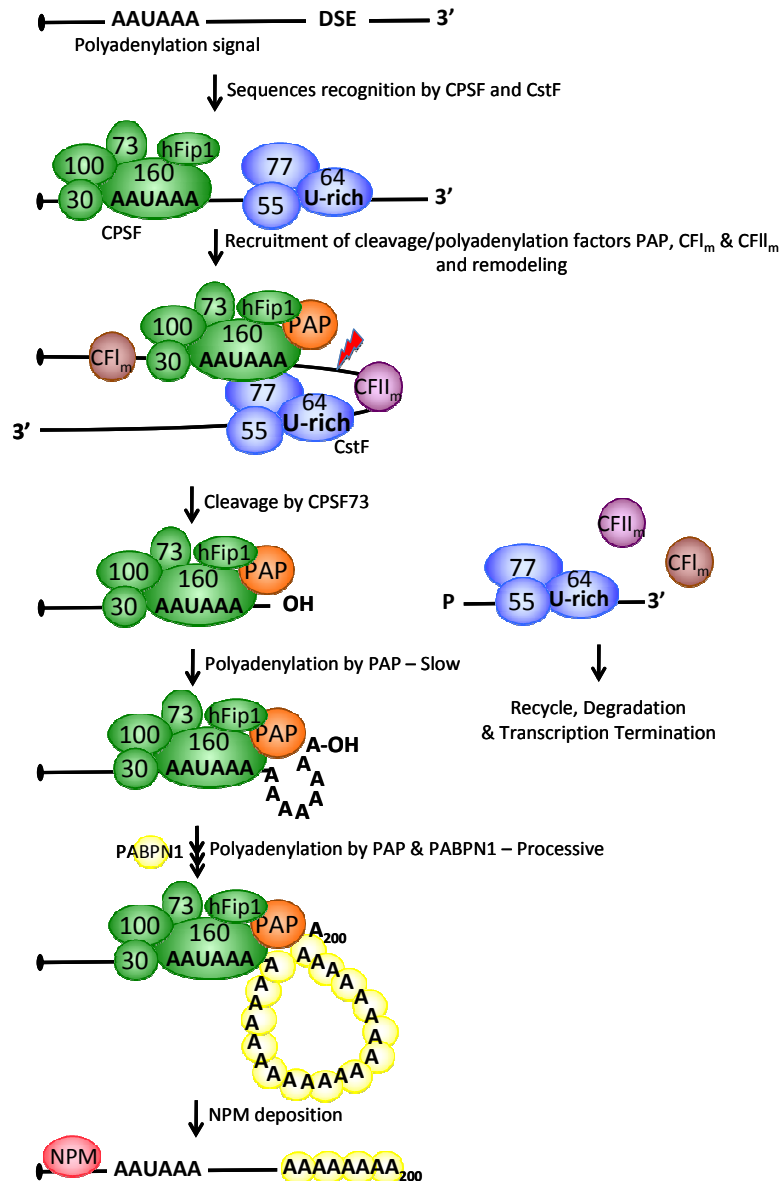


Figure 2: Diagram of Cleavage/Polyadenylation processing

During transcription, the polyadenylation signal (AAUAAA) is recognized by CPSF, mainly through binding by CPSF160. Approximately 20-30 nucleotides downstream of the core polyadenylation signal, U-rich sequences are then recognized by CstF. Other cleavage/polyadenylation factors – Poly(A) Polymerase (PAP) and Cleavage factors, CFI_m & CFII_m – are also recruited and facilitate the cleavage reaction which is catalyzed by the endoribonuclease CPSF73. 3' cleavage products help to terminate transcription and are rapidly degraded. CstF, CFI_m & CFII_m are recycled for another round of processing. The 5' cleavage product is, on the other hand, subsequently polyadenylated by PAP. Once the poly(A) tail grows long enough for PABPN1 to bind, it stimulates PAP activity and helps to elongate poly(A) tail in a processive fashion. Successful polyadenylation results in deposition of NPM on the RNA body, adjacent to AAUAAA.

with CPSF and the cleavage site (Kaufmann et al., 2004).

CstF, Cleavage stimulatory Factor, is a hetero-trimeric protein complex of CstF77, 64 and 50 and is required for cleavage but not for polyadenylation (Gilmartin and Nevins, 1989). CstF77 is a scaffold to connect CPSF160 (Bai et al., 2007) to CstF64 and 50 (Takagaki and Manley, 2000). CstF64 binds to the U-rich downstream element and enhances association of CPSF, thus promoting the cleavage reaction (Wilusz and Shenk, 1988). CstF50 interacts with both CstF77 (Takagaki and Manley, 2000) and the C-Terminal Domain of RNA Polymerase II (CTD of RNAP II CTD) (McCracken et al., 1997a; b).

CFI_m and CFII_m, mammalian Cleavage Factors I and II, are not as extensively explored as the other factors above. Studies indicate that they help cells recognize the polyadenylation signal of the pre-mRNA substrate (Takagaki et al., 1998; de Vries et al., 2000). As introduced above in the studies of PAPOLG gene, a UGUAN motif is a binding site for the CFI_m factor and point mutations in the motif diminish the polyadenylation efficiency (Venkataraman et al., 2005). Moreover, CFI_m aids in recruiting CPSF complex to PAPOLG pre-mRNA and initiates AWUAAA-independent polyadenylation through its interactions with CPSF and PAPOLA. This study reinforces the concept that the CPSF-PAP polyadenylation machinery can be recruited via other *trans*-acting factors which in turn provide the specificity as to which polyadenylation signals need to be processed. The RNA Polymerase II carboxy terminal domain (RNAP II-CTD) plays a crucial role in mRNA 3' end formation (Hirose and Manley, 1998). It acts as a platform for CPSF, CstF and CF II_m subunits (McCracken et al., 1997a; b). Mammalian RNAP II-CTD is composed of 52 repeats of Y¹-S²-P³-T⁴-S⁵-P⁶-S⁷ where a series of phosphorylation and dephosphorylation events can take place to modulate association of RNA processing factors (Schroeder et al., 2004). During transcription initiation and the 5' capping reaction, S⁵ of CTD-RNAP II is highly phosphorylated and S²

is dephosphorylated (Gu and Lima, 2005; Licatalosi et al., 2002). As transcription continues and 3' end processing gets closer to taking place, cleavage/polyadenylation factors are recruited to the CTD while S² becomes phosphorylated and S⁵ becomes dephosphorylated (Ryan et al., 2002).

Although the role of poly(A) polymerase (PAP) in the cleavage reaction is not fully understood, PAP is recruited by CPSF and required for the *in vitro* cleavage reaction (Shi et al., 2009). One notable exception is the SV40 late cleavage site that does not absolutely require the PAP activity (Chrislip et al., 1991).

Alternative polyadenylation sites

As illustrated above, definition of the precise cleavage site is carefully supervised by both *cis* elements and *trans*-acting factors. Surprisingly, over 50% of genes contain alternative poly(A) signals (Tian et al., 2005; Ozsolak et al., 2010) and the choice of which poly(A) site to use is dynamically regulated based on cell growth, developmental stage and cancerous phenotype (Sandberg et al., 2008; Ji et al., 2009; Mayr and Bartel, 2009). For example, stimulation of B lymphocytes, T cells and monocytes generally results in the increased expression of shorter 3'UTR isoforms compared to non-stimulated cells, suggesting the isoforms generated by alternative polyadenylation are required for effective cell cycle progression (Sandberg et al., 2008). Mayr and Bartel in 2009 also showed that cancer cells express many mRNAs with shorter 3'UTRs due to alternative polyadenylation. Most notably, IMP1 is an RNA-binding protein over-expressed in a variety of human cancers (Ross et al., 1997; Doyle et al., 1998; Nielsen et al., 1999; Noubissi et al., 2006). When expressed in cells, an IMP1 mRNA with a shortened 3'UTR gives up-regulated expression and more effective transformation than the same ORF with the normal, full length 3'UTR. This indicates that alternative polyadenylation can activate oncogenes and contribute to the pathogenesis. Although it

is has been challenging to unlock the mechanisms of alternative polyadenylation site selection, there are clues that core polyadenylation factors may be involved. The Handa laboratory showed that knockdown of the 25 kDa subunit of CFI_m alters polyadenylation site usage in HeLa cells (Kubo et al., 2006). On the other hand, in mouse primary B cells, CstF64 is specifically down-regulated and the over expression of CstF64 protein is sufficient to switch Ig heavy chain expression via alternative polyadenylation sites (Takagaki et al., 1996).

Trans-acting factors involved in polyadenylation

Following successful cleavage, polyadenylation takes place. The addition of A residues to the new 3' end, which is carried out by PAP, is relatively slow at first but once the poly(A) tail becomes 20-25 nt long, nuclear Poly(A)-binding protein 1 (PABPN1) associates with the nascent tail and PAP activity becomes highly processive (Bienroth et al., 1993). Once the poly(A) tail reaches ~200 adenines in length, PAP dissociates and PABPN1 remains bound to the tail (Wahle, 1995).

In yeast, a number of factors have been linked directly to poly(A) tail length control, while studies in mammalian system in this area are still at an early stage. For instance yeast Nab2p, which contains a zinc-finger RNA binding domain, has been proposed to play a critical role in regulating poly(A) tail length (Hector et al., 2002; Dheur et al., 2005). The mammalian homolog of Nab2p, ZC3H14, also associates with poly(A)⁺ RNAs, but has not yet been shown to regulate poly(A) tail length (Kelly et al., 2007). Yeast poly(A) binding protein Pab1p and Pab1p-dependent poly(A)-specific nuclease Pan2p/3p are also reported to be involved in defining the poly(A) tail length in an mRNA-specific manner (Brown and Sachs, 1998). In mammalian cells, PABPN1 seems to be the key factor in controlling the poly(A) tail during elongation in an *in vitro* reconstituted system (Wahle, 1991; Kerwitz et al., 2003; Kuhn et al., 2009). In these

studies, PABPN1 appears to strengthen the interaction between CPSF160 and the AAUAAA motif. Elongation by PAP is dependent on the presence of PABPN1 as PABPN1 stabilizes the interaction between CPSF160 and PAP.

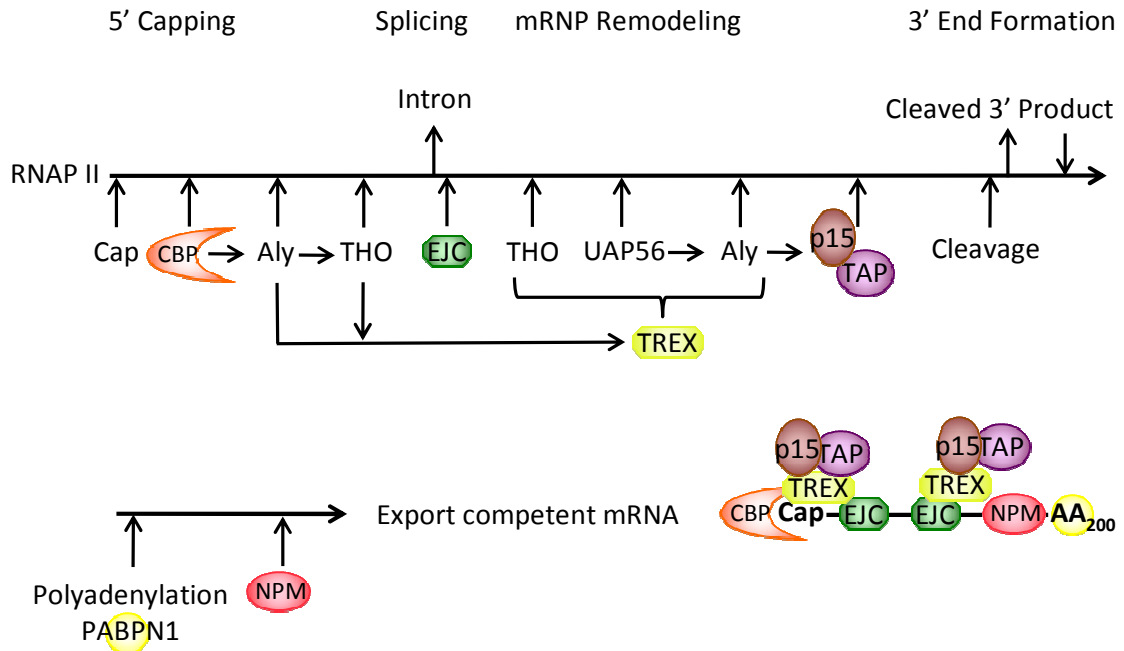


Figure 3: Diagrams of co-transcriptional nuclear processing and mRNA export through the nuclear pore complex in mammalian cells

Panel A. RNA polymerase II traverses 5'-3' along the gene and interfaces with capping, splicing and 3' end formation machinery. Capping enzymes modify the 5' end of a nascent transcript to become a 7-methylguanosine triphosphate, which is then recognized by CBP. Once bound to 5' cap, CBP partners with TREX complex through Aly and the first EJC complex. As transcription proceeds, splicing removes introns and joins exons together, resulting in the deposition of the EJC as well as the Tho complex. As a part of EJC, UAP56 recruits Aly to the transcript to form TREX complex with THO complex. In concert, Aly engages TAP/p15 onto the transcript. 3' end formation requires cleavage of 3'UTR of transcript into a 5' and 3' product. The 3' product aids in terminating transcription while undergoing degradation. The 3' end of the 5' product is subsequently polyadenylated. The poly(A) tail is coated by PABPN1 and NPM is deposited on the polyadenylated RNA. These co-transcriptional events transform the nascent RNAP II transcript into an export-competent mRNA.

Mammalian mRNA export

Nuclear mRNA processing is dedicated to preparing transcripts for transport to the cytoplasm where mRNA can be further localized, translated or degraded. Figure 3 illustrates the general maturation of nascent transcripts into export-competent mRNPs in mammalian cells. Capping, splicing and 3' end formation all contribute to making export-competent mRNPs and, at the same time, the mRNP goes through cascades of remodeling to recruit one export factor after another. The Reed lab reported that CBC, the nuclear Cap Binding Complex, is recognized by Aly (mRNA export adaptor), which brings in THO complex to form the TREX (TRanscription-Export) complex (Rondon et al., 2003; Strasser et al., 2002; Cheng et al., 2006). The TREX complex engages TAP/p15 (heterodimeric mRNA export factor) onto the transcript (Stutz et al., 2000). Following capping, splicing takes place and a multi-protein complex called the Exon Junction Complex (EJC) is deposited ~20-24 nt upstream of each exon-exon junction (Le Hir et al., 2000). A component of the EJC, UAP56 (the ATP-dependent RNA helicase) recruits the Aly protein which together with the THO complex forms the TREX complex (Rondon et al., 2003; Strasser et al., 2002). Aly binds the TAP/p15 onto the transcript (Stutz et al., 2000). The connections between 3' end processing and mRNA export in mammalian cells is still largely understudied. However, in the yeast, Nab2p not only aids in defining the poly(A) tail but also binds to yeast mRNA export factors Mex67/Mtr2 protein and the yeast mRNA export adaptor Yra1p to promote nuclear mRNA export (Iglesias et al., 2008), illustrating the contribution of 3' end processing to mRNA export. Additionally, in mammalian cells reporter transcripts which encode the poly(A) in the gene and thus create it co-transcriptionally instead of being processed by the 3' end formation machinery have been shown to be poorly exported to the cytoplasm in some instances (Huang and Carmichael, 1996).

Significance of polyadenylation and the poly(A) tail

Although polyadenylation appears at first glance to be the simple addition of adenines, it requires numerous protein factors and is tightly regulated for several reasons. PAP can be a sequence-independent enzyme and, in principle, is able to add adenines to the 3' end of any RNA (Butler and Platt, 1988). This could be disastrous for the cell as 3' polyadenosine tailing is also associated with RNA degradation (LaCava et al., 2005; Vanacova et al., 2005). The specific docking of PAP to the 3' end of nascent pre-mRNAs is achieved in part through association of 3' end formation factors with the C-terminal domain of the transcribing RNA polymerase II, and through coordination with splicing and 5' capping events (Murthy and Manley, 1992; 1995; Luna et al., 2008). Most importantly, the CPSF160 protein, which binds strongly and specifically to AAUAAA core polyadenylation signal, seems to be primarily responsible for assigning the PAP to the correct 3' end prior to the cleavage/polyadenylation reaction (Murthy and Manley, 1992; 1995).

The poly(A) tail is a key player in initiating translation. The mRNA forms a closed-loop where the 5' cap is connected to the 3' end of the mRNA through interaction of PABPC1 on the poly(A) tail with eIF4F associated with the cap. This serves to bring in the translation initiation factors (Kapp and Lorsch, 2004) and increase translation efficiency. Furthermore, among the other events that polyadenylation influences are transcription termination (West and Proudfoot, 2009), transcription re-initiation at upstream promoters (Mapendano et al., 2010), splicing efficiency of the last exon (Cooke and Alwine, 1996) and recruitment of export factors (Johnson et al., 2009).

On the other hand, the removal of poly(A) tail (deadenylation) is the first step in the decay of the majority of mRNAs in mammalian cells (Garneau et al., 2007; Gao et al., 2000). Due to the intricate networking of polyadenylation with other RNA processing

events, it is perhaps not surprising that close to 85 proteins form the machinery required to drive 3' end processing (Shi et al., 2009).

Significance of other 3' end modifications

It should be also mentioned that what is on the 3' end of an RNA can dictate the fate of the transcript in many species. Mammalian replication-dependent histone mRNAs which possess a stem-loop structure and lack the poly(A) tail are subject to oligouridylation at the 3' end prior to degradation (Mullen and Marzluff, 2008; Schmidt et al., 2011). Mammalian miRNAs, let-7 miRNA in particular, are also the target of uridylation prior to degradation (Song and Kiledjian, 2007; Heo et al., 2008).

In contrast to the mammalian mRNA poly(A) tail, addition of adenosine to the 3' end of bacterial RNAs promotes their rapid decay (Cohen, 1995; Cao and Sarker, 1992). In the chloroplast of higher plants, a poly(A)-rich sequence consisting of ~70% adenosines and ~25% guanosines is post-transcriptionally added to 3' end of mRNAs, which in turn promotes the endonuclease cleavage of plant transcripts for degradation (Lisitsky et al., 1996). In yeast, the TRAMP protein complex named after the components – Trf4(5)p/Air1(2)p/Mtr4p – was identified as an exosome-activating factor (Lacava et al., 2005). The Trf proteins belong to the same protein family as the yeast poly(A) polymerase, Pap1p (Vanacova et al., 2005). Studies have illustrated that Trf proteins can adenylate misfolded or aberrant tRNA and pre-rRNAs (Vanacova et al., 2005) and that the nuclear exosome is activated by TRAMP modification of the 3' end of these transcripts (Dreyfus and Regnier, 2002). These data show that the addition of ribonucleotides to the 3' end of RNAs in message- and species-specific manners promote the degradation of otherwise structurally inaccessible, toxic or unwanted RNA substrates.

Polyadenylation and surveillance

In addition to the roles of the poly(A) tail outlined above, it plays an essential part in mRNA quality control. Generation of a mature mRNA requires a series of elaborate events and is therefore naturally prone to error (Sagues et al., 2005). Cells have developed mechanisms of mRNA surveillance to monitor the status of the mRNA pool. These mechanisms eliminate mRNAs that are incorrectly processed or function erroneously due to mutations within the encoding gene or mistakes made during mRNA maturation (Garneau et al., 2007). The surveillance systems help to stop cells from translating mRNAs that could encode truncated proteins with deleterious effects (Sommer and Nehrbass, 2005).

One well-characterized co-transcriptional event that is intricately associated with the quality control mechanism is EJC deposition during splicing (Le Hir et al., 2000). The EJC is a multifunctional complex whose activity influences many aspects of mRNA metabolism from mRNA export, to nuclear RNA decay to translation and mRNA localization (Tange et al., 2004; Le Hir et al., 2003; Hachet et al., 2004; Le Hir et al., 2001). The presence of the EJC enhances mRNA export efficiency through its association with mRNA export factors (Tange et al., 2004; Le Hir et al., 2003) and incorrect positioning of the EJC relative to translational stop codons can result in rapid mRNA decay (Tange et al., 2004; Le Hir et al., 2003).

As polyadenylation is the last step in maturation of an mRNA, it is likely to be intimately linked with mRNA surveillance processes. Surveillance within the nucleus is understudied, particularly in mammalian cells. Studies in yeast have shown that various factors interact with one another to clearly link transcription and 3' end processing to nuclear mRNA surveillance and mRNA export. The most extensively researched among them are the THO/TREX, rrp6 protein, hyperadenylation and BRCA1/BARD1/PARN in mammalian cells.

THO/TREX and RRP6

As mentioned above, the THO complex is a key component in mRNP assembly and export through its interactions with mRNA export factors which altogether form the TREX complex (Rondon et al., 2003). In yeast, mutations in any of the individual components of the THO/TREX complex result in a decreased level of several mRNAs (Rougemaille et al., 2007) and the rapid accumulation of transcripts with extended poly(A) tails in the nucleus (Jensen et al., 2001). Intriguingly, this phenotype is dependent on the RRP6 protein, an enzymatically active component of the nuclear exosome which is involved in processing and decay of nuclear transcripts including rRNA and mRNAs (Libri et al., 2001). In a yeast THO-deletion mutant, the retention of polyadenylated reporter RNAs was restored upon deletion of RRP6 (Libri et al., 2001), suggesting that RRP6 participates in events responsible for the retention of aberrant mRNAs.

Hyperadenylation

Regulation of poly(A) tail length is also a crucial determinant of valid mRNA maturation. Qu and Moore demonstrated in 2009 that mutations in the yeast mRNA export factors, Yra1p (Aly in mammals), Sac3p and Mex67p/Mtr2p (Tap/p15 in mammals) lead to accumulation of hyperadenylated mRNAs and retention of the poly(A)⁺ RNAs in the nucleus. Interestingly, these mutations also cause the delayed release of the Rna15p (cleavage factor I) from polyadenylated transcripts (Qu et al., 2009). In contrast, mutations in cytoplasmic export factors such as Dbp5p, Rat7p and Fle1p led to hyperadenylation and nuclear retention of mRNAs, but no defects in release of Rna15p were observed. These results infer that there is a reciprocal relationship between export and polyadenylation. The formation of a proper 3' end allows the nascent mRNA to cooperate with specific factors which enable export. In addition, the

proper assembly of mRNA export factors is required for disbanding the 3' end formation factors once the poly(A) tail reaches the proper size. This implies that proper 3' end formation facilitates the removal of a withholding anchor to allow export. There is, therefore, a sensing system in the cells to detect aberrant 3' end formation of mRNPs and prevent their possible toxic expression.

DNA Damage Response

Recently Cevher et al., 2010 uncovered another role of the poly(A) tail in maintaining cellular homeostasis in response to DNA damage. At steady state (i.e. in the absence of UV-induced DNA damage), CBP80 binds to the deadenylase PARN and prevents it initiating degradation of the nascent poly(A) tail. In response to DNA damage by UV treatment, RNAP II transcription stalls at the site of damage, the 3' end processing factor CstF50 is recognized by BRCA1/BARD1, which then promotes the degradation of RNAP II via ubiquitination. PARN dissociates from CBP80 and instead associates with CstF50. This CstF50-PARN complex, greatly enhanced by BARD1 association through CstF50, not only initiates the degradation of stalled transcripts but also inhibits the cleavage reaction (Cevher et al., 2010).

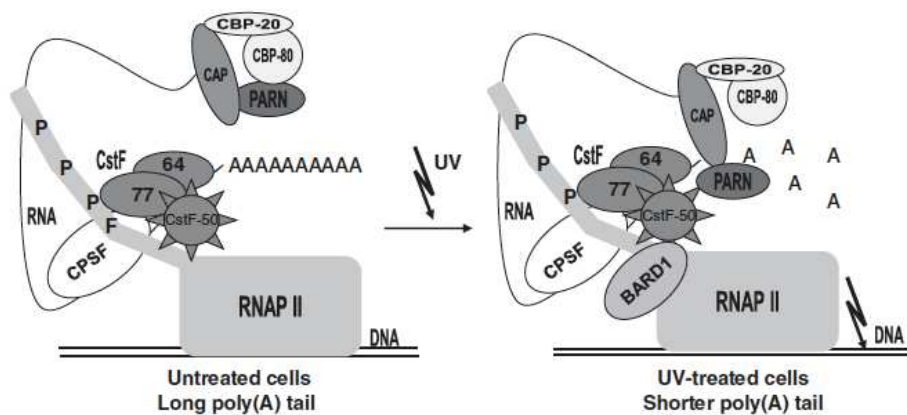


Figure 4: Model of poly(A) tail dynamics after DNA damage; directly adapted from Cevher et al., 2010.

In the absence of DNA damage, CBP80 prevents nuclear PARN deadenylation activity. After exposure to UV treatment, the elongating RNAP II-CstF complex stalls at the sites of damage. Under those conditions, becoming free of CBP restriction, PARN-dependent decay pathway is initiated.

Identification of NPM as a polyadenylation mark

The poly(A) tail is indispensable but it is not clear if the poly(A) tail itself is sufficient to mark 3' end formation as complete as the mere presence of poly(A) in transcripts can fail to promote the mRNA export (Huang and Carmichael, 1996). The studies described above led to the hypothesis that the process of 3' end formation may result in deposition of a protein or protein complex that marks the mRNA as accurately processed and facilitates downstream events such as export and translation.

Previously, the Wilusz Laboratory demonstrated that the polyadenylation reaction deposits a protein called nucleophosmin (NPM) on the body of RNA substrates bearing viral poly(A) signals *in vitro* (Palaniswamy et al., 2006).

Detailed studies of the requirements for NPM deposition *in vitro* led to several significant insights. First, NPM deposition requires only the polyadenylation reaction to become associated with mRNA body - the cleavage process is dispensable. Secondly, NPM deposition requires the actual process of polyadenylation as it does not associate with RNAs that have been artificially polyadenylated. Thirdly, NPM binding seems to be sequence independent as it binds to unrelated sequences upstream of the AAUAAA in three different RNA substrates. In addition, NPM was found to be associated with nuclear poly(A)⁺ RNA isolated from living cells.

NPM is a multi-functional protein

NPM is often highly over-expressed in cancer cells (Grisendi et al., 2006) and induced pluripotent stem cells (Ashley Neff, personal communication), while its expression is maintained at a lower level in normal tissue. It is a crucial protein that

plays a role in a variety of cellular activities. It has been implicated in many cellular events including regulation of cell proliferation (Zhang, 2004), gene expression (Dhar et al., 2004) and embryonic development (Grisendi et al., 2005). NPM is also proposed to act as a molecular chaperone (Okuwaki et al., 2001), and has been implicated in processes such as nuclear import of proteins (Szebeni et al., 1995), response to UV damage (Latonen and Laiho, 2005) and regulation of apoptosis (Ahn et al., 2005). On top of that, NPM has also been linked to tumorigenesis and is involved in translocations that cause hematological disorders (Nakagawa et al., 2005). NPM is normally predominantly localized to the nucleolus, but due to frameshift mutations in exon 12, is exclusively found in the cytoplasm in 60% of patients with a distinctive type of acute myelogenous leukemia (Nakagawa et al., 2005).

Another study (Colombo et al., 2002) has shown that the overexpression of NPM in murine primary fibroblasts leads to a substantial reduction in proliferation and cell division. In this study, NPM was found to interact directly with a tumor suppressor, p53, to regulate its stability and enhance transcriptional activation by p53. Furthermore, NPM overexpression in *p53*^{-/-} fibroblasts does not induce the inhibition of cell proliferation, suggesting that p53-dependent senescence requires NPM up-regulation in fibroblasts.

The post-translational modification of NPM is crucial to determine the roles of NPM in other RNA processing. CDK/cyclin E phosphorylates NPM at Thr¹⁹⁹ residue (Tarapore et al., 2006). When NPM is phosphorylated at Thr¹⁹⁹ and added to the nuclear extracts, the extracts fail to splice a reporter pre-mRNA as effectively as unphosphorylated NPM does, demonstrating that post-translational modification partakes actively in NPM functions (Tarapore et al., 2006).

Interestingly, NPM and the 50 kDa protein of CstF are both candidate substrates of the BRCA1/BARD1 ubiquitin ligase (Sato et al., 2004; Kleiman et al., 1999). As mentioned earlier, in response to DNA damage, 3' end processing is temporarily but

specifically inhibited, while the formation of CstF-BRCA1/BARD1 protein complex increases although the individual protein levels are kept the same. These data imply that the formation of the CstF-BRCA1/BARD1 complex inhibits CstF from acting in 3' end processing (Kleiman et al., 1999). The expression of NPM is up-regulated and NPM translocates from the nucleolus to the nucleoplasm upon DNA damage (Latonen and Laiho, 2005, Higuchi et al., 1998; Wu and Yung., 2002) and we have shown NPM functions as a polyadenylation mark (Palaniswamy et al., 2006). Together these two pieces of data strongly insinuate that 3' end processing and the cellular response to DNA damage are closely linked.

Hypotheses

Based on the information mentioned above that polyadenylation, like other aspects of RNA biogenesis, is very much intertwined with downstream processing and NPM is the polyadenylation marker, we strived to pursue answers for the following hypotheses.

Hypothesis I: NPM deposition occurs regardless of the type of polyadenylation signal.

Rationale: Non-canonical polyadenylation signals are ubiquitously seen in pre-mRNA. Thus it is important to determine whether or not the type of polyadenylation signal influences NPM deposition.

Hypothesis II: NPM deposition likely occurs at polyadenylation initiation, elongation of the tail, or termination of poly(A) synthesis.

Rationale: NPM deposition occurs on the RNAs that undergo the successful polyadenylation. The polyadenylation is a 3-step process – initiation, elongation and

termination. It is not known at which step NPM binds to RNAs. This mechanistic understanding may lead insights into how NPM deposition occurs.

Hypothesis III: Given that NPM is deposited during polyadenylation, NPM may interact with other known polyadenylation factors to influence polyadenylation efficiency and downstream events such as export.

Rationale: As polyadenylation requires numerous proteins, NPM may also play the role of a polyadenylation factor. Hypothesis II implies that NPM may act at a specific step of the polyadenylation process.

Hypothesis IV: Since polyadenylation is networked to so many processes, reduced NPM deposition may result in defects in mRNA export from the nucleus which is strongly linked to polyadenylation.

Rationale: The NPM polyadenylation mark likely has downstream functional implications for mRNA biogenesis. These will be surveyed in NPM knockdown experiments.

Hypothesis V: As the majority of factors involved in mRNP maturation are multi-subunit complexes, NPM may not be the only component of the polyadenylation mark.

Rationale: The Wilusz Lab showed previously that in a similar fashion as NPM deposition, a protein of ~14kDa binds to RNA bodies after the successful polyadenylation in *in vitro* cell-free polyadenylation systems. This observation will be further pursued in this project.

Results

Polyadenylation mediated by a variety of cellular polyadenylation signals causes deposition of nucleophosmin on transcripts.

Previously, the Wilusz Lab used three independent viral polyadenylation signals (Palaniswamy et al., 2006), the bovine growth hormone poly(A) signal and a cellular CPSF6 polyadenylation signal (Morrison, 2007) to demonstrate the deposition of NPM on RNA substrates undergoing polyadenylation in HeLa nuclear extracts. All of these poly(A) signals bear the canonical AAUAAA element and therefore likely undergo polyadenylation by very similar mechanisms. We wondered whether NPM could be deposited on an RNA with a non-conventional (non-AAUAAA) polyadenylation signal upon successful polyadenylation. Melanocortin 4 receptor (MC4R) mRNA utilizes an upstream A-rich polyadenylation signal for the 3' processing (Nunes et al., 2010) and therefore was selected as a non-conventional polyadenylation signal (Fig. 5). Pre-cleaved RNAs containing the SV40 late (SVL) poly(A) signal were used as a positive control. As shown in Figure 5A, top panel, the MC4R polyadenylation signal, could be polyadenylated in our HeLa nuclear extracts, albeit less efficiently than the SVL substrate. Additionally, NPM was specifically associated with the body of MC4R RNA substrates following polyadenylation as anti-NPM antibodies immunoprecipitated a 32 kDa cross linked band from the samples that had gone through polyadenylation but not from the sample taken before incubation at 30°C (Fig. 5A, lower panel). Therefore, we conclude that non-canonical polyadenylation can also result in NPM deposition.

We next assessed whether individual cellular mRNAs could be found associated

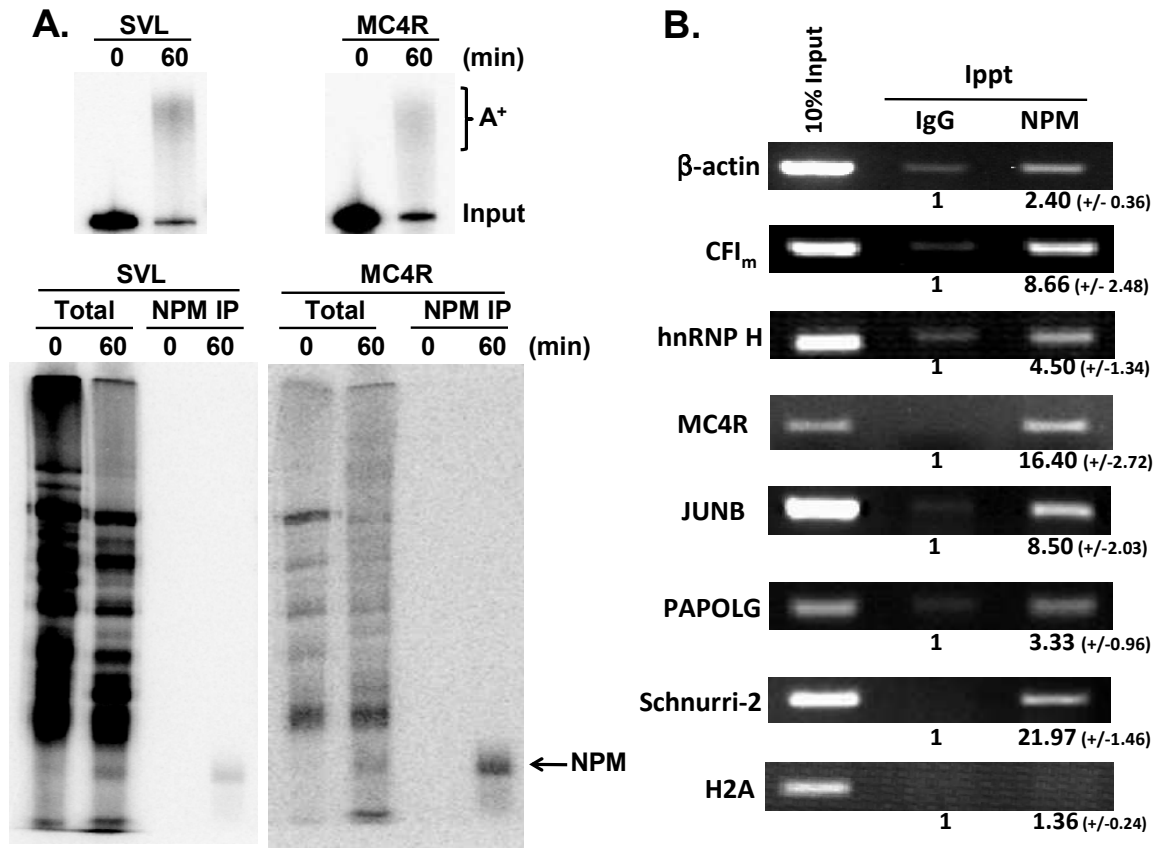


Figure 5: Nucleophosmin is deposited on cellular poly(A)⁺ mRNAs both in an *in vitro* polyadenylation system and dividing cells.

Panels A. Radiolabeled RNAs (Input) containing polyadenylation signals from the SV40 late (SVL), melanocortin 4 receptor (MC4R) were incubated with HeLa nuclear extract in an *in vitro* polyadenylation assay for the times indicated. RNA products were analyzed on a 5% acrylamide gel containing urea (top panel). Input indicates the size of the RNA substrate while A⁺ indicates the migration of the polyadenylated product RNAs. In the lower panel, in parallel experiments under identical reaction conditions, radioactive RNAs were cross linked by UV light to closely associated proteins, treated with RNase and total cross linked proteins were analyzed by SDS-PAGE (Total lanes) or immunoprecipitated using an anti-NPM antisera prior to electrophoresis (NPM IP lanes). The arrow on the right indicates the migration of the NPM cross linked product while molecular weight markers are indicated on the left. Panel B. HeLa cells were treated with formaldehyde to stabilize mRNP complexes and lysed. Lysates were immunoprecipitated using equal amounts of either IgG control sera or NPM specific antibodies. Immunoprecipitated RNA was extracted and analyzed by RT-PCR using primers specific for the indicated transcripts and products were resolved on 2% agarose gels. The numbers below each band in the immunoprecipitated lanes represent the relative fold enrichment of PCR product obtained compared to the control IgG lanes. Results shown are the mean of three experiments with the standard deviations indicated.

CPSF6 (CFI_m) – NM_007007.2:

1999 GAAAAAAGUCAAGUAAAUGCUUGUUUUUGUAGUAGUUUGUUCUUGUUAA
2049 AAAUGUUUAUAUGAUAAUGUCUGUAAACAGCAUCACUUUGAUUACAAUAG
2099 AUGUAGUGUUGU**AAUAAAC**UGUUUAAUGGGGC

hnRNP H – NM_005520.2:

2119 AGGAUUUUGGUCUUGGUGUUUGUAUGAAAUUCUGAGGCCUUGAUUUAAAU
2169 CUUUCAUUGUAUUGUGAUUUCCUUUAGGUUAUUGCGCUAAGUGAAACU
2219 UGUCA**AAUAAU**CCUCCUUUUAAAACUGCA

β -Actin – NM_001101.3:

1700 AACUUGAGAUGUAUGAAGGCUUUUGGUCUCCUGGGAGUGGGUGGAGGCA
1750 GCCAGGGCUUACCUGUACACUGACUUGAGACCAGUUG**AAUAAA**AGUGCAC
1800 ACCUAAAAAUGA

MC4R – NG_016441.1:

6594 AUUAUUUCCAAUGUCAUGCUACUUUUUUGGCCAUAAAUAUGAAUCUAUG
6644 UUAUAGGUUGUAGGCACUGUGGAUUUAC**AAAAAGAAA**AGUCCUUUUAAA
6694 AGCUUAACAAUGUC

JUNB – NM002229.2:

1673 CCCUGCCCUCUCCUCUCUGCACCGUACUGUGGAAAAGAAACACGCACUUA
1723 GUCUCUAAAGAGUUUUAUUUUAAGACGUGUUUGUGUUUGUGUGUUUGUU
1773 CUUUUUUAUUGAAUCUAUUUAAGU**AAAAAAAAAA**UUGGUUCUUUA

PAPOLG – NM_022894.3:

3612 UUUCAUGAAUGCAUGCUCAGUUUAUUAAAAUCCAUAACCAUGUAAUUCUU
3662 **GUAAU**AUGUUGAUUCAGUGUUU**UGUAA**UGAAGUCGUA**UGUAU**UUUCAGA
3712 GUUUUU**UGUAUGUACUGUA**AGAUACCAUCUUUUCAAAGAGAAACGUUUA
3782 AAACCUUUA

Schnurri-2 – NM_006734.3:

8045 AAGCA**AAGAUCCUUC**AUCAG**AAAAGAG**UCAGCUACAUUGAUCUAUGAUGC
1500 nt omitted
9695 UUAAGGAGUGUUCUUUAAAAGAGAA**UAAU**AUACAAAUACAUGCUUGA

Figure 6: Sequences of various polyadenylation signals.

Partial 3'UTR sequences of mRNAs and their accession number are displayed. Numbers on the left side represent the sequence position. These upstream elements of the polyadenylation signals are marked in bold. CPSF6, hnRNP H, β -Actin and Schnurri-2 mRNAs use the canonical AAUAAA polyadenylation signal (Gu et al, 1999). MC4R and JUNB use an A-rich sequence, while PAPOLG use UGUAN as their polyadenylation signal (Nunes et al., 2010; Venkataraman et al., 2005). For MC4R, the underlined bases represents the pre-cleaved sequence used for our *in vitro* polyadenylation assay. In each case, the last ribonucleotide corresponds to the presumed cleavage site.

with NPM in dividing cells. HeLa cells were treated with formaldehyde to stabilize protein-RNA complexes. Cell lysates were subject to immunoprecipitation using NPM-specific or control antisera and co-precipitated mRNAs were assessed using RT-PCR analysis. As seen in Fig. 5B, seven polyadenylated mRNAs including MC4R mRNA, were specifically co-precipitated using NPM antiserum. This set of mRNAs was chosen (Fig. 6) to represent mRNAs with conventional AAUAAA-driven polyadenylation signals (β -actin, CPSF6 (CFI_m) and hnRNP H), signals containing a core upstream UGUAN motif, which lacks AAUAAA motif (PAPOLG; Venkataraman et al., 2005), an upstream A-rich core motif (JUNB (AAAAAGAAAA) and MC4R (AAAAAAAAAAAA); Nunes et al., 2010), or a putative 'poly(A) limiting element' that restricts the overall size of the tail (Schnurri-2; Gu et al., 1999). As a negative control, histone H2A mRNAs, the vast majority of which lack a poly(A) tail, failed to significantly interact with NPM. Collectively these data suggest that NPM is deposited on poly(A)⁺ cellular mRNAs independent of the type of polyadenylation signal they possess and the machinery(ies) responsible for NPM deposition must be shared between all the signals tested in this study. Significant enrichment of snRNAs was seen in NPM IP samples (data not shown). This is likely due to the by-products of formaldehyde treatment which crosslink snRNAs to pre-mRNAs as snRNAs are involved in splicing of pre-mRNAs. While the significance of the differences in the overall efficiency of NPM co-precipitation among individual polyadenylated mRNAs remains to be elucidated, the mode of recognition used to initiate 3' end processing does not appear to play a role in deposition of NPM.

Nucleophosmin is deposited on mRNAs as a result of the natural process of termination of polyadenylation

Previous results clearly indicated that NPM deposition on mRNAs was associated with the process of poly(A) tail addition rather than 3' end cleavage of pre-

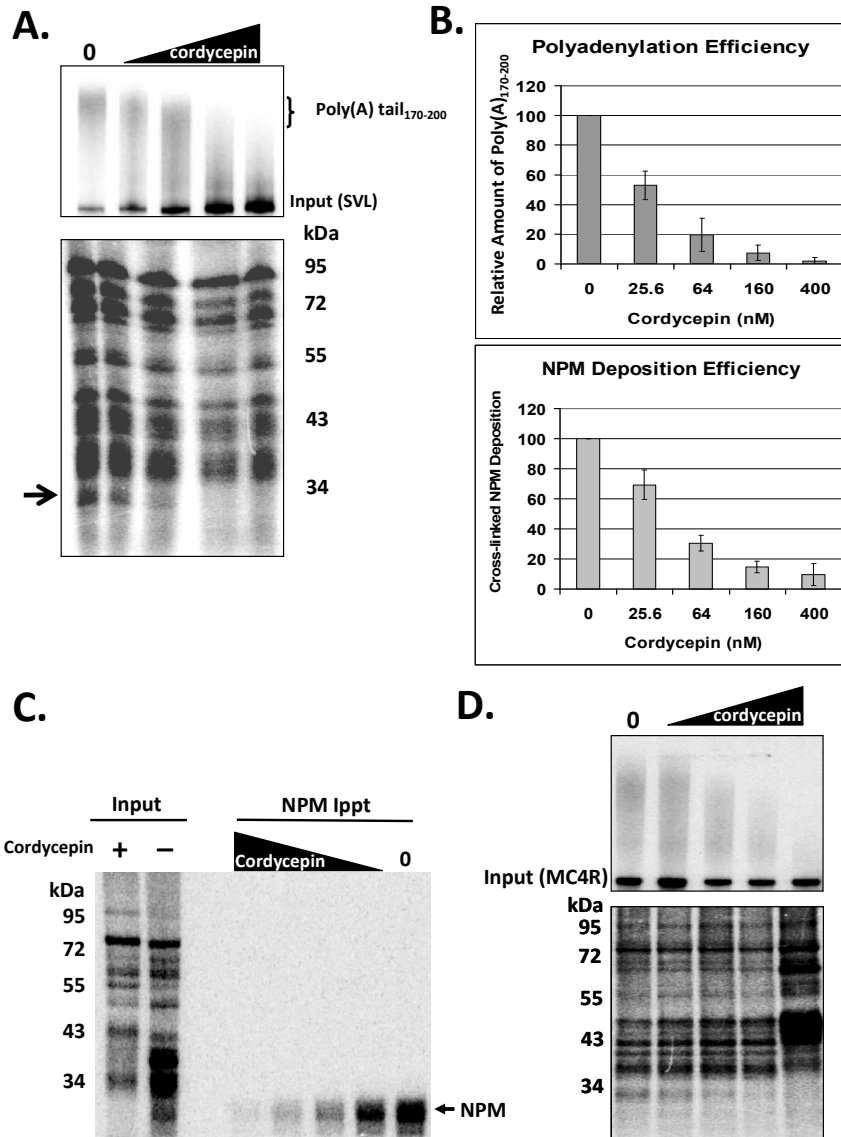


Figure 7: Deposition of NPM on RNAs is associated with natural termination of poly(A) synthesis.

Panel A. RNAs containing the SVL polyadenylation signal were incubated in cell free polyadenylation reactions using HeLa nuclear extract in the presence of the indicated amount of cordycepin. RNA products of the reaction were analyzed on a 5% denaturing acrylamide gel (top); total proteins that were UV cross linked to the radioactive body of the RNA were analyzed by 10% SDS PAGE (middle gel); and cross linked proteins immunoprecipitated with NPM-specific antisera were analyzed by 10% SDS PAGE (Panel C). The arrow in the middle gel indicates the position of NPM. Panel B. Quantification of the results shown in Panel A. Error bars represent the standard deviation of three experiments. Panel D. RNAs containing the MC4R polyadenylation signal were incubated in cell free polyadenylation reactions using HeLa nuclear extract in the presence of the indicated amount of cordycepin. RNA products of the reaction were analyzed on a 5% denaturing acrylamide gel (top); total proteins that were UV cross linked to the radioactive body of the RNA were analyzed by 10% SDS PAGE (bottom).

mRNA substrates (Palaniswamy et al., 2006). In order to begin to gain more mechanistic insight into NPM-mRNA interactions, we addressed which step of the polyadenylation process (initiation, elongation, or termination of poly(A) synthesis) was associated with NPM deposition. We approached this experimentally via the addition of increasing amounts of cordycepin triphosphate into *in vitro* polyadenylation reactions. Cordycepin will act as a chain terminator when incorporated into the growing adenylate tract by poly(A) polymerase, allowing us to determine the effect of artificially terminating poly(A) synthesis on NPM deposition. As seen in Fig. 7A and D, when cordycepin is added in sufficient concentrations to terminate polyadenylation prematurely, NPM was no longer deposited on either the SVL or the MC4R RNA substrate. This suggests that NPM deposition does not occur during the initiation or elongation steps of poly(A) tail synthesis. However, when cordycepin is added to the polyadenylation reactions in sufficient quantities to cause a complete block in poly(A) tail elongation and then gradually decreased to allow for the natural termination of poly(A) tail synthesis, a direct correlation between NPM deposition and natural poly(A) tract termination can be observed (Fig. 7B). Cross linking/immunoprecipitation was also conducted to ensure that the 32kDa band was indeed NPM (Fig. 7C). Thus, we conclude that deposition of NPM on RNAs undergoing polyadenylation is closely associated with the termination step of poly(A) tail synthesis.

Nucleophosmin interacts with factors directly implicated in the determination of poly(A) tail length

Based on the results described above, which indicate that NPM is deposited on mRNAs as polyadenylation is completed, we hypothesized that it may interact with factors required for poly(A) tail addition. As introduced previously, there are three factors that play a major role in the polyadenylation step: CPSF160 (a component of

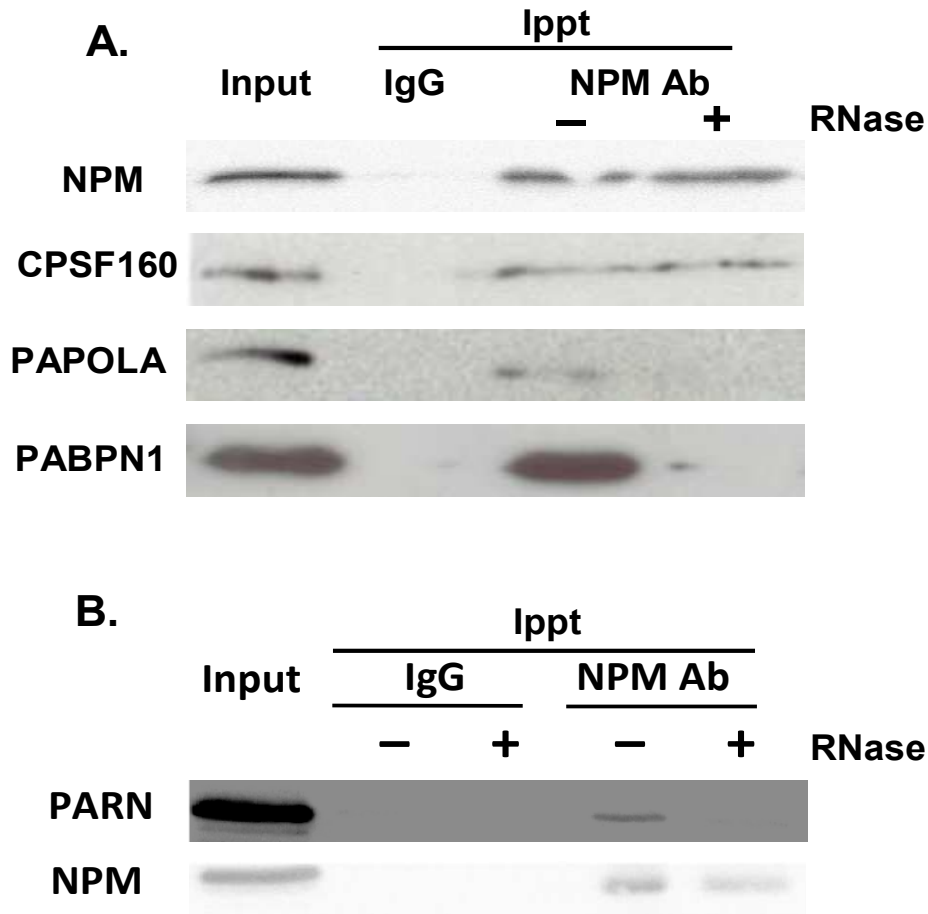


Figure 8: NPM is associated with the core polyadenylation factor CPSF.

Panel A. HeLa cell lysates were immunoprecipitated with either control mouse IgG or NPM antibodies before (- lanes) or after (+ lanes) treatment with RNase ONE. Precipitated proteins were separated on a 10% SDS-acrylamide gel and analyzed by western blotting using the antisera indicated on the left. Input lanes represent 10% of the total amount of protein used for the immunoprecipitation reactions. Panel B. HeLa cell were treated with formaldehyde and lysates were immunoprecipitated with either control mouse IgG or NPM antibodies before (- lanes) or after (+ lanes) treatment with RNase A. Precipitated proteins were separated on a 10% SDS-acrylamide gel and analyzed by western blotting using the antisera indicated on the left. Input lanes represent 10% of the total amount of protein used for the immunoprecipitation reaction

CPSF complex of which interacts with the AAUAAA core upstream element of the poly(A) signal), PABPN1 (which interacts with CPSF and the growing adenylate tail), and Poly(A) Polymerase (PAP) (which is the enzyme responsible for adding adenylate

residues; Millevoi and Vagner, 2010). Additionally, PARN deadenylase was also examined as the Pan2p/3p deadenylase controls the poly(A) tail length of subsets of mRNAs in yeast (Brown and Sachs, 1996) and PARN has previously been linked with the polyadenylation process (Cevher et al., 2010). In order to gain further insight into the mechanism of NPM deposition on polyadenylated mRNAs, we determined whether NPM associates with factors known to have an influence on polyadenylation and poly(A) tail length.

Immunoprecipitations were performed in HeLa nuclear extracts using antisera specific for NPM and western blots were probed for a variety of polyadenylation factors – CPSF160, PABPN1, PAP and PARN. As seen in Fig. 8A, NPM specifically co-precipitated only with CPSF160. The interaction between NPM and the CPSF complex was insensitive to degradation of RNA by RNase ONE, which cleaves the phosphodiester bond between any ribonucleotides. Interestingly, the major nuclear poly(A) polymerase PAP and PABPN1 were also co-immunoprecipitated with NPM antibody, but in an RNase-sensitive fashion (Fig. 8A). Only trace amounts of the nuclear deadenylase PARN was immunoprecipitated with NPM, but this weak interaction was most likely RNA-mediated as it was sensitive to ribonuclease (Fig. 8B). Thus we conclude that NPM can interact directly with the complex that binds the AAUAAA element in the 3' UTR of the pre-mRNA. In addition, NPM interacts indirectly through RNA bridging with the enzyme that adds adenylate residues to the 3' end of the pre-mRNA (PAP) as well as a key factor in poly(A) length determination (PABPN1). Thus NPM may be, through the CPSF160 interaction, a part of the complex present on pre-mRNAs during polyadenylation initiation and elongation. Only when the reaction nears termination, can NPM be detected bound directly to the RNA body.

Knock down of nucleophosmin in cells results in hyperadenylation of mRNA in HeLa cells

If NPM does play a role in the termination of poly(A) synthesis, then one might predict that poly(A) tail length would be affected in the absence of the protein. In order to address this, we examined poly(A) tail length of mRNAs isolated from HeLa cells stably depleted of NPM using shRNAs. We used two independent NPM knock down HeLa cell lines established in the lab previously using the Mission® pLKO-1 shRNA expression system (Zhang et al., 2008). As seen in Fig. 9A and B, NPM protein and RNA levels were knocked down >90% in these cells (Hend Ibrahim, personal communication). Similar levels of NPM depletion were achieved with other shRNAs that target independent regions of the mRNA (Hend Ibrahim, personal communication). We performed linker ligation-mediated poly(A) tail length assays (LLM-PAT; Garneau et al, 2008) for three independent mRNAs. As seen in Fig. 10, the length of the poly(A) tail on the β -actin, hnRNP H and rps5 mRNAs was clearly increased in NPM knock down cells compared to control cell lines. The effect was specific for mRNAs as no evidence was obtained for an increase in polyadenylated subforms of rRNAs (Fig. 11). Therefore we conclude that knock down of NPM in HeLa cells results in hyperadenylation of mRNAs.

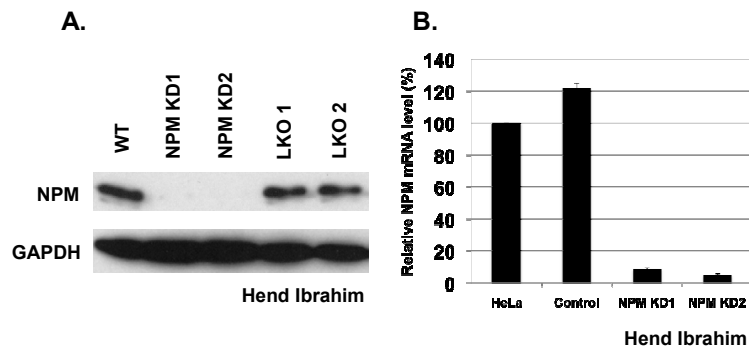


Figure 9: Verification of stable NPM KD in HeLa cells by an NPM-specific shRNA. Panel A. Western analysis of total cell proteins isolated from the indicated cell lines using either NPM or GAPDH-specific antisera. Control lanes represent independent HeLa cell lines stably transfected with an empty vector. Panel B. Quantification of the relative level KD of NPM mRNA in the indicated cell lines using qRT-PCR. Error bars are generated from the pipetting errors in qRT-PCR reactions.

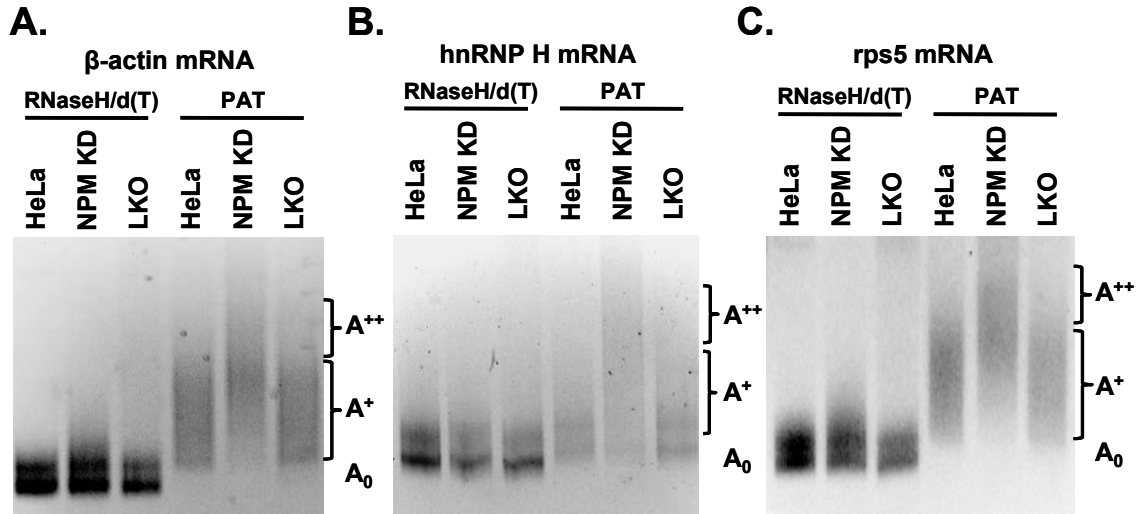


Figure 10: Stable knock down of NPM results in an increase in mRNA poly(A) tail length in cells.

Total RNA was isolated from untreated WT (HeLa lanes), HeLa cells stably transfected with an empty vector (LKO1 lanes) or stable NPM KD HeLa cells (NPM KD lanes) and analyzed by linker-ligation-mediated PCR-based poly(A) tail length assay. A set of samples was treated with oligo dT and RNase H to remove the poly(A) tail prior to analysis (RNase H/d(T) lanes). The PAT lanes represent samples where mRNAs with intact poly(A) tails were analyzed. Primers for β -actin mRNA were used in panel A, hnRNP H mRNA in panel B and rps5 mRNA in panel C. PCR products were analyzed on a 5% acrylamide gel. The positions of the unadenylated RNA (A_0), normally polyadenylated (pA) and hyperadenylated (pA $^{++}$) are indicated on the right.

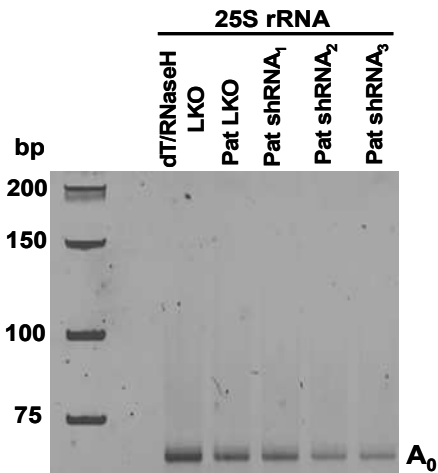


Figure 11: Transient transfection with independent NPM shRNA does not result in an increase of polyadenylated forms of 25S rRNA.

Twenty-four hours post-transfection with LKO empty vector or indicated NPM-specific shRNA vectors in HeLa cells, total RNA was purified and used for LLM-Pat assay to examine the poly(A) tail status of 25S rRNA. A set of samples was treated with oligo d(T) and RNase H to remove the poly(A) tail prior to analysis (RNase H/d(T) lanes). PCR products were analyzed on a 5% acrylamide gel. The position of the unadenylated RNA (A_0) is indicated on right.

Quite interestingly, transient knock down of NPM by independent shRNAs did not give the same results. GAPDH and β -actin have normal poly(A) tail lengths under these conditions as shown in Fig. 12. However, the transient NPM knock down resulted in hyperadenylation of the poly(A) tail of puromycin N-acetyltransferase (PAC) mRNA (Fig. 13B) which is encoded on the shRNA-bearing plasmid and confers puromycin resistance to transfected cells. We suggest that the stable mRNAs which encode for house-keeping genes and presumably reside in the cytoplasm are not as susceptible to the short-term NPM depletion in the nucleus as nascently transcribed mRNA derived from the newly introduced PAC gene. However, during the continuous rounds of selection for NPM KD cell lines, mRNAs encoding house-keeping genes are turned over and replaced by hyperadenylated forms generated in the absence of NPM (Fig. 10). Additionally, as shown in Fig. 5C, although the techniques are not absolutely quantitative, NPM does not associate significantly with β -actin mRNAs and the prolonged NPM depletion is possibly necessary to affect these mRNAs. It is also noted that the level of NPM protein reduction in the transient experiments could well be insufficient to cause the poly(A) tail defects.

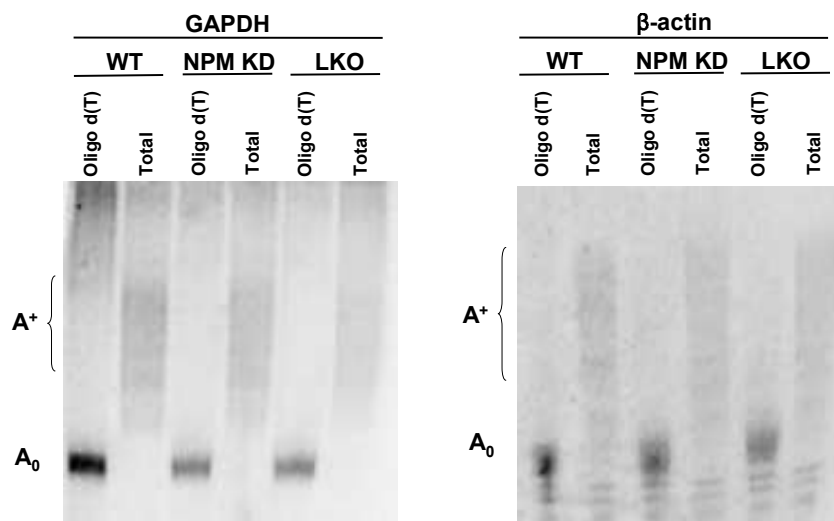


Figure 12: Transient knock down using NPM shRNAs does not induce the hyperadenylation of GAPDH or β -actin mRNAs.

Twenty-four hours post-transfection with LKO empty vector or NPM-specific shRNA vector in HeLa cells, total RNA was purified and was hybridized with DNA-oligonucleotides specific to GAPDH or β -actin mRNA followed by RNase H digestion to shorten the mRNA length prior to analysis. Lanes marked with oligo d(T) were also hybridized with oligo d(T) to remove poly(A) tail prior to analysis. Reaction products were separated on 5% polyacrylamide gel, transferred to Hybond-XL membranes and visualized with a GAPDH or β -actin-specific radioactive probe. The positions of the unadenylated RNA (A_0) and polyadenylated (A^+) are indicated.

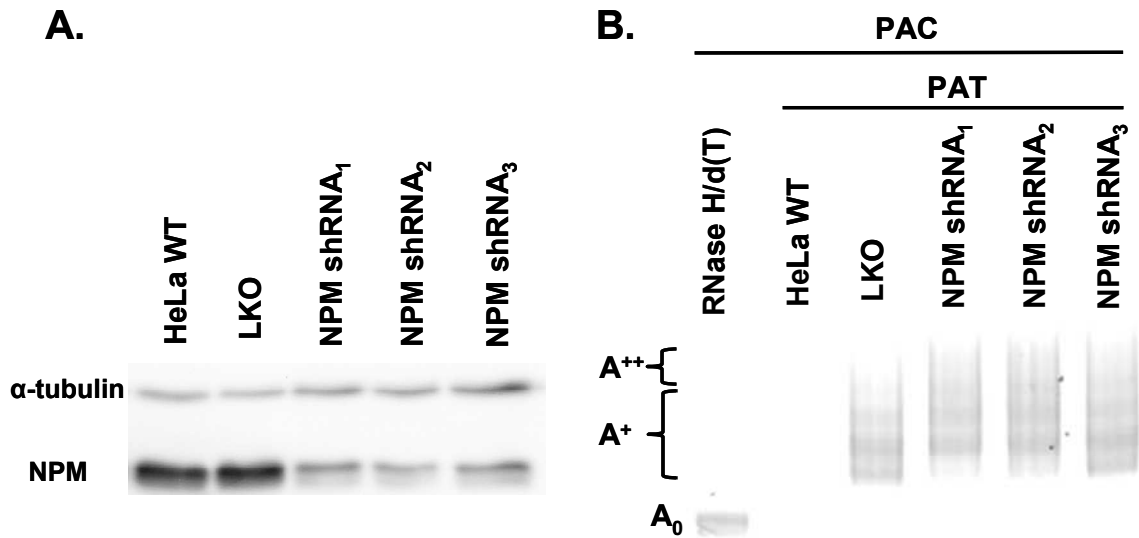


Figure 13: Transient NPM knock down using NPM shRNAs results in the hyperadenylation of puromycin N-acetyltransferase (PAC) mRNAs.

Panel A. Twenty-four hours post-transfection with either a LKO empty vector or indicated NPM-specific shRNA vectors in HeLa cells, whole cell extracts were made, separated by 10% SDS-PAGE gels and subjected to western blot analysis using either NPM or α -tubulin-specific antisera. Panel B. Twenty-four hours post-transfection with LKO empty vector or indicated NPM-specific shRNA vectors in HeLa cells, total RNA was purified and used for LLM-Pat assay to measure the poly(A) tail length of PAC mRNA. A set of samples was treated with oligo d(T) and RNase H to remove the poly(A) tail prior to analysis (RNase H/d(T) lanes). The PAT lanes represent samples where mRNAs with intact poly(A) tails were analyzed. Primers for PAC mRNA were used. PCR products were analyzed on a 5% acrylamide gel. The positions of the unadenylated RNA (A_0) and polyadenylated (A^+) are indicated.

Hyperadenylation of RNA could be recapitulated in an *in vitro* polyadenylation assays from NPM knock down extracts.

We hypothesized that the hyperadenylation of mRNAs observed in NPM knock down cells is due to a direct disruption in regulation of poly(A) tail length during synthesis or remodeling. Alternatively, hyperadenylation could be an indirect effect of a block in nuclear export or as a consequence of aberrant mRNA quality control. In order to begin to differentiate between these mechanistic possibilities, we prepared nuclear extracts from wild type, control and NPM KD HeLa cells. Pre-cleaved RNAs containing the SVL poly(A) signal were incubated in cell-free polyadenylation reactions using nuclear extracts and poly(A) tail length was assessed on acrylamide gels. As seen in Fig. 14A, while extracts from untransfected HeLa WT cells and LKO control cells stably transfected with an empty LKO vector gave polyadenylated products of similar size, nuclear extracts from stably transfected NPM KD lines gave hyperadenylated tails ~80 bases longer than those seen in control extracts. Importantly, independent extracts gave similar, highly reproducible results (Fig. 14A). There is a noticeable difference in polyadenylation efficiency between HeLa WT and NPM KD extracts, but we did not actively pursue the difference as it is not uncommon that the independent extracts give different polyadenylation efficiency. A similar hyperadenylation of RNA substrates in NPM knock down extracts was observed for other poly(A) signals, including adenoviral signals IVA2 (Fig. 14B) and E1B (14C).

The hyperadenylation observed in extracts made from NPM depleted cells was not simply due to differences in the kinetics of poly(A) tail addition. As seen in Fig. 14D and E, once a maximal poly(A) tail length was obtained in extracts from control HeLa cells at around 10 mins, no notable additional length increase occurred in the poly(A) tail.

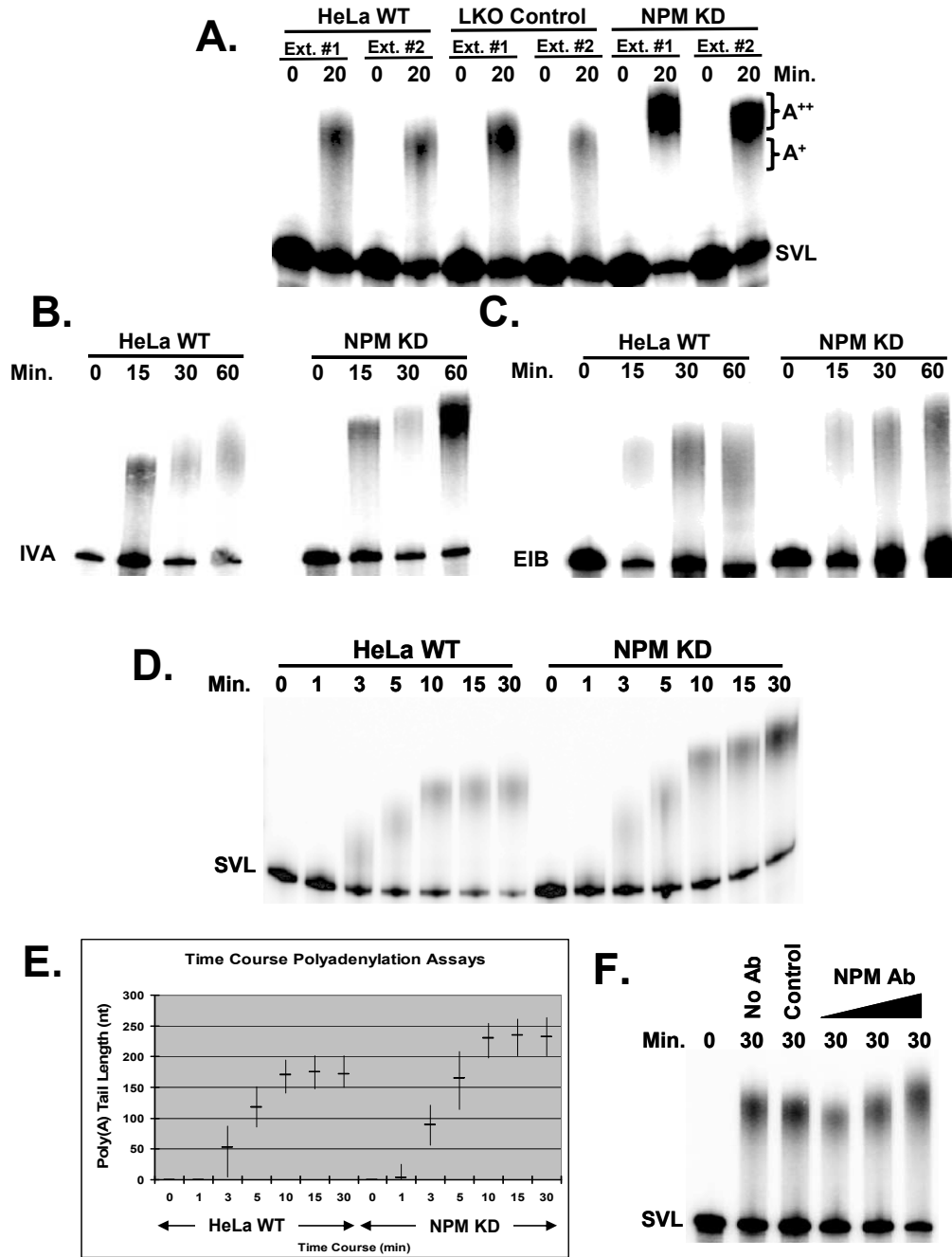


Figure 14: Hyperadenylation can be demonstrated in nuclear extract-based polyadenylation assays when NPM is depleted.

Panel A. RNAs containing the SVL polyadenylation signal were incubated for the indicated times in extracts from either untreated WT, stable LKO control cells or stable NPM KD HeLa cells. Ext #1 and #2 denote independent extracts made from each of the indicated cell types. Polyadenylated products were analyzed on a 5% denaturing acrylamide gel. The positions of the input, normally polyadenylated and hyperadenylated RNAs are indicated on the right. Panel B and C. Same as the previous panel except input RNAs containing the IVA2 (Panel B) and EIB (Panel C) polyadenylation signal were used. Panel D. Time course of an *in vitro* polyadenylation

reaction using nuclear extracts derived from untreated WT or NPM KD HeLa cells and the SVL RNA substrate. Panel E. Panel D was quantified and graphed. Horizontal bars represents the mean poly(A) tail length at each time points whereas vertical bars represent the 80% of polyadenylated RNA population at each time points. Panel F. HeLa nuclear extracts were used untreated (No Ab lane), depleted with protein A Sepharose beads with control IgG prior to use (Control lane), or depleted with increasing amounts of NPM-specific antisera prior to removal of antigen-antibody complexes with protein A beads (NPM Ab lanes). The SVL RNA substrate was incubated in these treated extracts for the time indicated and polyadenylated products were analyzed on a 5% acrylamide gel.

In extracts from NPM-depleted cells, on the other hand, maximal tail length was clearly increased compared to control cells although it was reached at approximately the same time point. Furthermore, immunodepletion studies performed by adding increasing amounts of Protein-A Sepharose beads bearing NPM-specific antibodies to HeLa nuclear extracts also resulted in a dose-dependent increase in poly(A) tail length (Fig. 14E). Control Protein A Sepharose beads with non-specific IgG had no influence on polyadenylation.

In principle, hyperadenylation could be caused by either a failure to terminate polyadenylation effectively, or a failure to trim the poly(A) tail to the correct length after polyadenylation is complete. In the latter case, one might expect a deadenylase such as PARN to be involved. Indeed, Pan2p/3p, a yeast, deadenylase was shown to be responsible for maintaining the poly(A) tail length of specific mRNAs and Pan2p and/or 3p-deficient yeast strains exhibit hyperadenylation on these mRNAs (Brown and Sachs., 1998). Based on their observation, we pursued whether or not NPM could recruit PARN deadenylase to control the length of poly(A) tail during the polyadenylation. First, we sought to see whether PARN can be localized in the nucleus in HeLa cells. Immunofluorescence assays showed that PARN was found in both nucleus and cytoplasm (Fig. 15A) in HeLa cells.

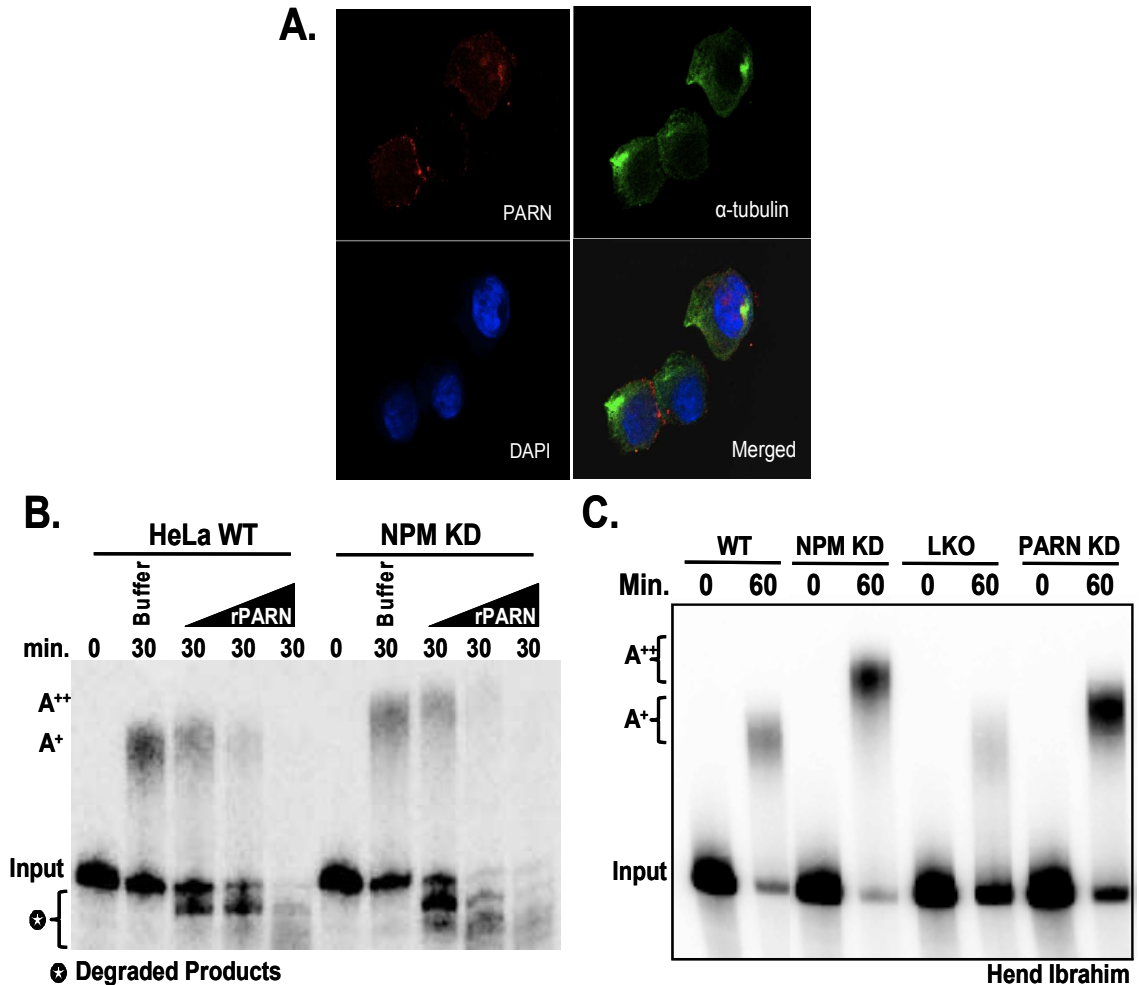


Figure 15A: PARN deadenylase is found in both nucleus and cytoplasm.

HeLa cells were grown on coverslips, fixed and analyzed by immunofluorescence assays using anti-PARN sera, anti α -tubulin antibodies and DAPI stain.

B: Addition of rPARN into NPM KD nuclear extracts fails to rescue the hyperadenylation defect. Prior to *in vitro* polyadenylation assays, increasing amounts of recombinant PARN deadenylase was added to WT and NPM KD HeLa nuclear extracts. The SVL RNA substrates were incubated in the treated extracts for the time indicated. Reaction products were analyzed on a 5% acrylamide gel. Position of the input, polyadenylated products and degraded products are indicated.

C: PARN knock down nuclear extract does not recapitulate the NPM knock down nuclear extracts.

RNAs containing the SVL polyadenylation signal were incubated for the indicated times in extracts from either untreated WT, LKO control, NPM KD or PARN KD HeLa cells in which PARN was knocked down using a specific shRNA. Polyadenylated products were analyzed on a 5% denaturing acrylamide gel. The positions of the input, normally polyadenylated and hyperadenylated RNAs are indicated on the left.

If PARN is involved in the hyperadenylation defects as a result of the inefficient recruitment of PARN to RNAs in the reduced level of NPM, the addition of excess amounts of recombinant PARN to the NPM KD nuclear extracts should aid in trimming the NPM KD poly(A) tail back to the WT poly(A) tail. Figure 15B illustrates that the addition of increasing amounts of recombinant PARN deadenylase failed to rescue the hyperadenylation defects in the NPM KD nuclear extracts. Interpretation is however complicated by the fact that large amounts of PARN result in complete degradation of the RNA substrate. We also examined the effects of PARN knock down on polyadenylation *in vitro*. Unlike NPM knockdown, PARN knockdown failed to induce a strong hyperadenylation phenotype (Fig. 15C, Hend Ibrahim). Furthermore, Fig. 8 shows that only small amounts of PARN are associated with NPM-bound RNAs and the interaction was RNase-sensitive.

These data suggested that hyperadenylation is a result of excess poly(A) synthesis rather than reduced poly(A) shortening. Therefore, contributions of poly(A) binding proteins to the NPM-KD defects were tested as PABPN1 protein can modulate the poly(A) elongation reaction in reconstitution systems (Keller et al., 2000). Chemically synthesized poly(A) was added to the nuclear extracts to sequester the poly(A) binding protein(s) and prevent their influence on poly(A) tail synthesis. Fig. 16 shows that both WT and NPM KD extract-generated poly(A) tail are shortened in a dose-dependent manner as increasing amounts of poly(A) are added, suggesting that poly(A) binding proteins were indeed required for poly(A) elongation but were not a major player in NPM KD defects.

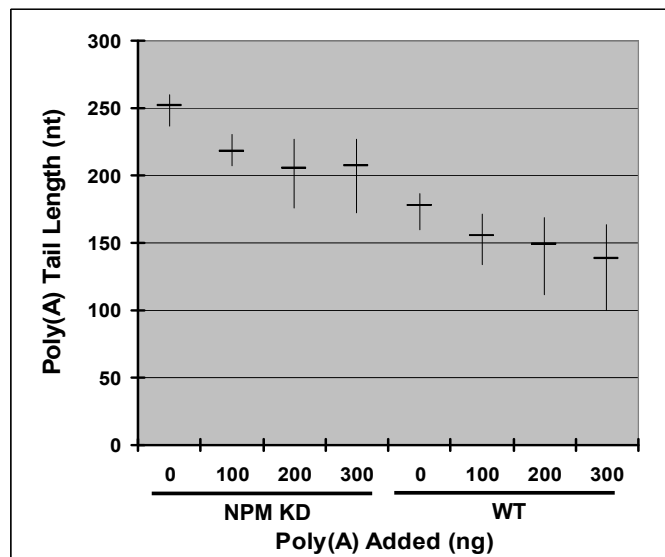
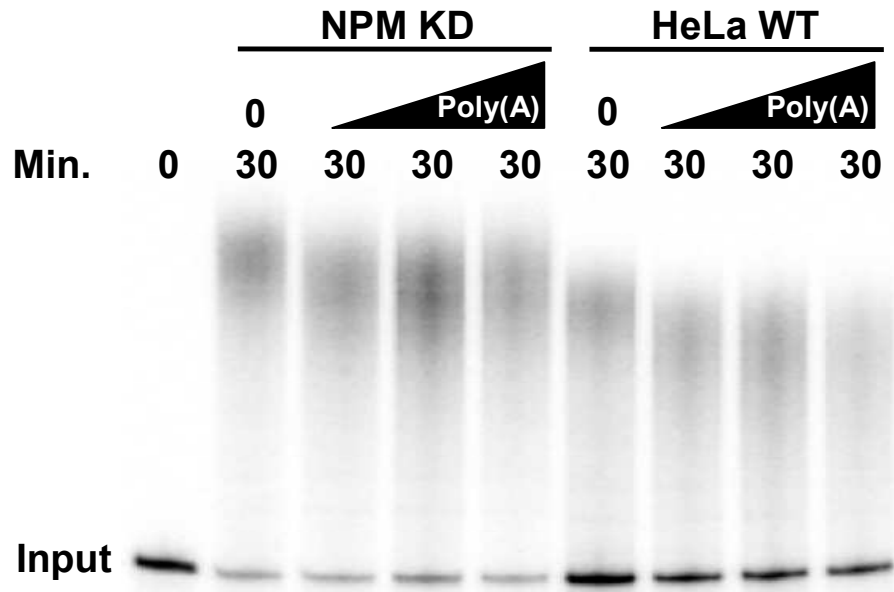


Figure 16: WT and NPM KD HeLa nuclear extracts are similarly sensitive to addition of exogenous poly(A).

Prior to *in vitro* polyadenylation assays, poly(A) (100, 200 and 300ng) was added in WT and NPM KD HeLa nuclear extracts. The SVL RNA substrates were incubated in the treated extracts for the time indicated. Reaction products were analyzed on a 5% acrylamide gel. Position of the input RNA is indicated. Poly(A) tail length was quantified. Horizontal bars represent the mean poly(A) tail length and vertical bars represent 80% of the poly(A) tail length generated from the extracts in the presence of the indicated amounts of poly(A) added to the extracts. The gel picture above was quantified in to graph. Horizontal bars represent mean poly(A) tail length at each amounts of poly(A) added whereas vertical bars represent the 80% of polyadenylated RNA population.

It is quite possible that during the generation of NPM KD cell lines, hyperadenylation defects developed due to changes in expression of polyadenylation factors – such as CPSF, PAP or PABPN1 – induced by NPM KD. Western blots revealed that NPM-specific shRNA did not produce dramatic indirect or secondary changes in the expression level of CPSF-160, PAP or PABPN1 (Fig. 17). Therefore we conclude that the mRNA hyperadenylation observed in NPM KD cells is likely a direct effect of the reduction in NPM levels on the efficiency of poly(A) tail termination.

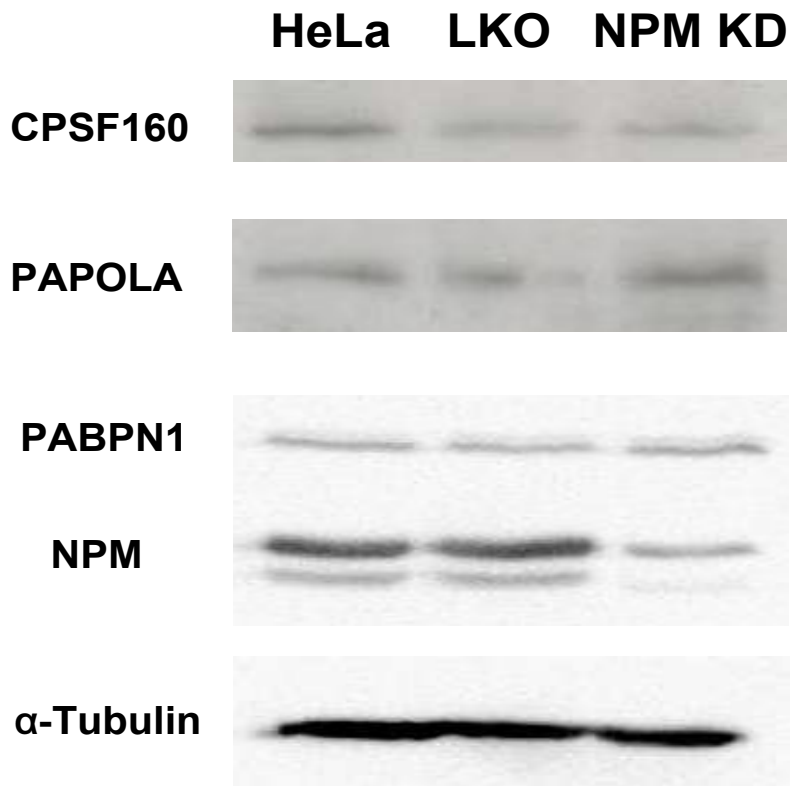


Figure 17: NPM knock down does not affect the expression level of CPSF160, PAP, PABPN1 and α -tubulin.

Whole cell proteins were made from WT, stable LKO control (LKO) and stable NPM KD HeLa cell lines, separated by 10% SDS-PAGE gels and analyzed by western blotting using either CPSF160, PAP, PABPN1, NPM or α -tubulin-specific antisera.

Knock down of nucleophosmin in dividing cells results in reduced mRNA export to the cytoplasm

In the yeast *Saccharomyces cerevisiae*, hyperadenylation is associated with a block in mRNA export from the nucleus (Jensen et al., 2001; Hilleren et al., 2001). In order to assess the overall localization of the poly(A)⁺ RNA population in NPM KD HeLa cells, we performed FISH analyses using Cy3-labeled oligo d(T) probes. As seen in Fig. 18A, while poly(A)⁺ RNA was largely cytoplasmic in control transfected HeLa cells, NPM reduction caused a dramatic accumulation of poly(A)⁺ RNA in the nucleus. Similar data were obtained using two additional shRNAs that targeted independent regions of the NPM mRNA (Fig. 18B), indicating the effects of these shRNAs were likely specific to NPM. The nuclear retention observed in NPM KD cells was specific for mRNA as 25S rRNA (Fig. 19) showed no dramatic change in its relative nuclear/cytoplasmic distribution. Therefore we conclude that a reduction in the level of NPM in HeLa cells results in a failure of mRNA to exit the nucleus, presumably due to a block in export as a result of failure to correctly terminate poly(A) synthesis.

NPM depletion does not influence the relative use of alternative polyadenylation sites.

Since NPM is over-expressed in many kinds of tumors, it is of interest to investigate possible relationships between NPM expression and cancerous phenotypes (Lindstrom 2010). It has become clear that transformation causes the changes in poly(A) site choice, which consequently contribute to promote or activate oncogenes (Mayr and Bartel, 2009). Fig. 8 shows NPM could be associated with the AAUAAA binding factor CPSF160 in an RNase insensitive manner. As the CPSF complex is critical in both cleavage and polyadenylation we decided to examine the influences of NPM on choosing alternative polyadenylation sites of IMP1 and CCND1 mRNAs.

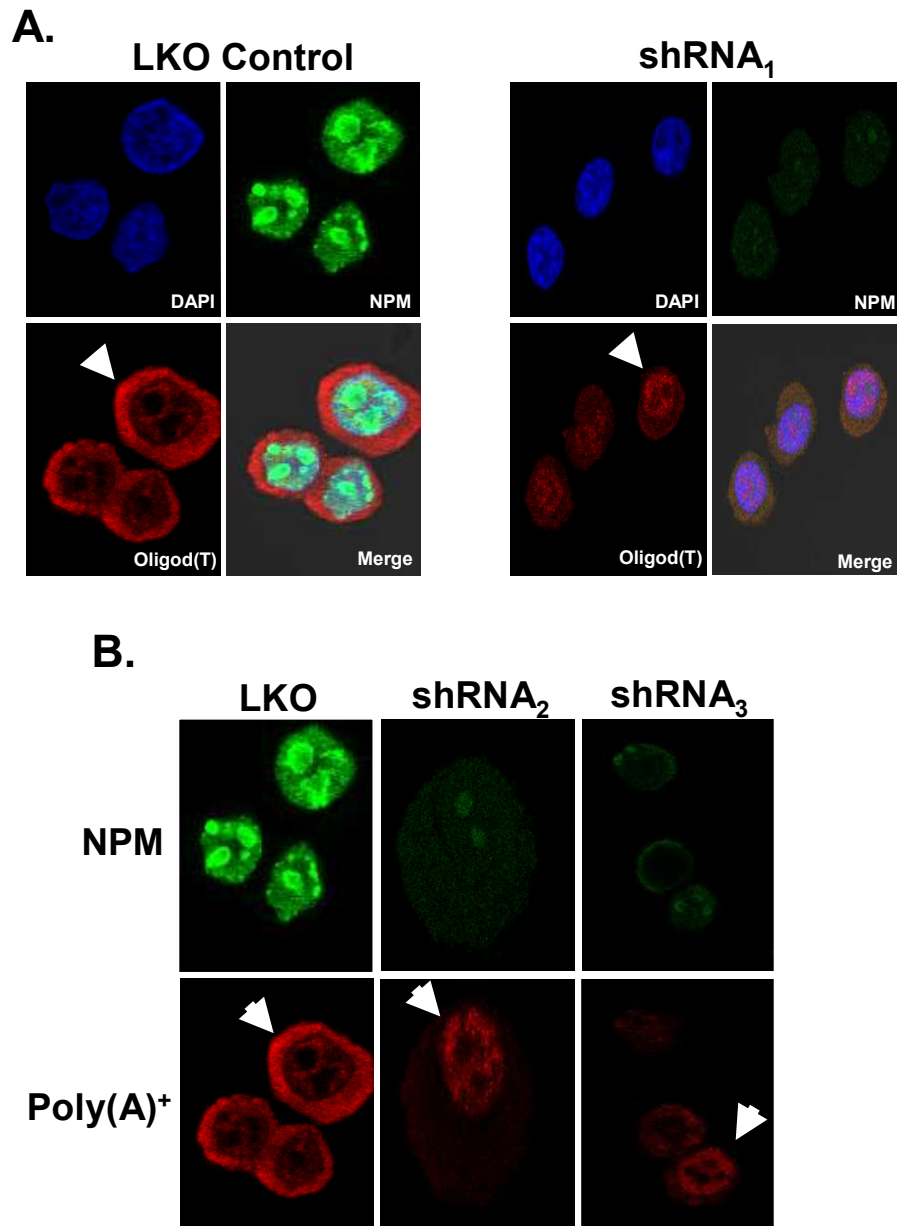


Figure 18: Reduction of NPM levels results in the accumulation of poly(A)⁺ RNAs in the nucleus.

Panel A. LKO control HeLa cells (transfected with an empty LKO vector) or NPM KD HeLa cells treated with an NPM-specific shRNA for 24 hours were analyzed by immunofluorescence using DAPI to mark nuclei, Cy3-oligo d(T) to identify poly(A)⁺ RNA or anti-NPM antibodies to visualize nucleophosmin. The arrow highlights a representative cell in which poly(A)⁺ RNA is largely cytoplasmic (LKO control cells) or is retained in the nucleus (NPM KD cells). Panel B. Same as panel A but cells were treated with two independent shRNAs targeting NPM prior to analysis (DAPI not shown).

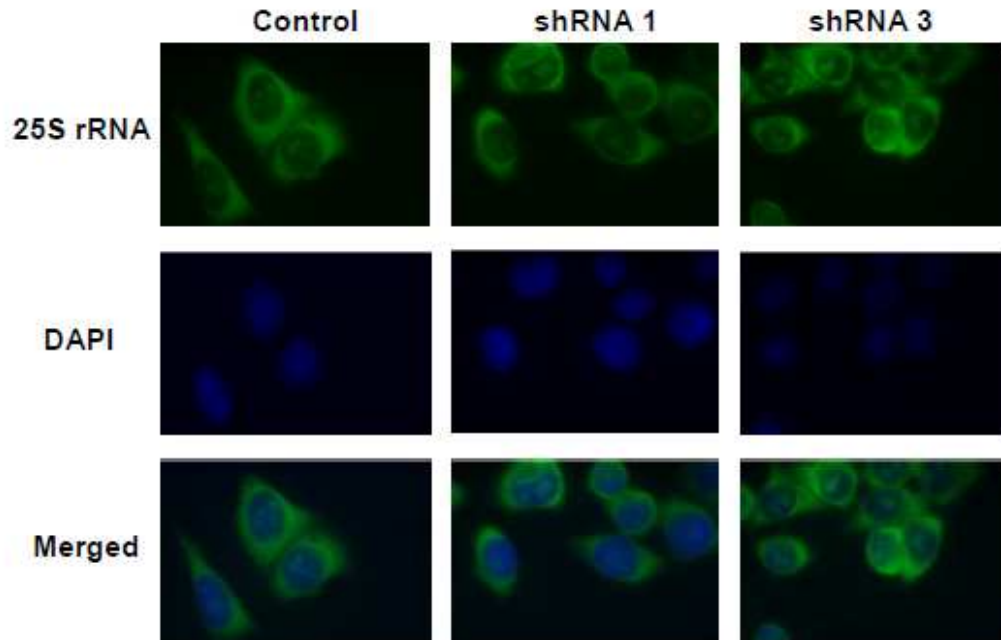


Figure 19: NPM knock down does not affect the subcellular localization of 25S rRNA.

LKO control cells or two NPM KD HeLa cell lines using independent NPM-specific shRNAs were grown on cover slips, fixed and analyzed by immunofluorescence using DAPI stain or a fluorescently labeled oligonucleotide specific for the 25S rRNA. The majority of 25S rRNA resides in the nucleolus and cytoplasm as expected.

These mRNAs were picked for the experiment since their 3'UTRs were demonstrated to be shortened in transformed cells (Mayr and Bartel, 2009). RNase Protection Assays (RPA) were used and Fig. 20 describes the experimental design. Briefly, in non-transformed cells, the CCND1 gene, for instance, produces two mRNA isoforms, one utilizing the distal AAUAAA and the other utilizing a proximal AAGAAA. Upon transformation, the AAGAAA proximal polyadenylation signal is more frequently used for 3' end processing and leads to the increase level of the shorter isoform. The two isoforms can be distinguished through RPA. The reaction products were separated on the gel and ratios of longer isoforms to shorter ones were quantified (Fig. 21).

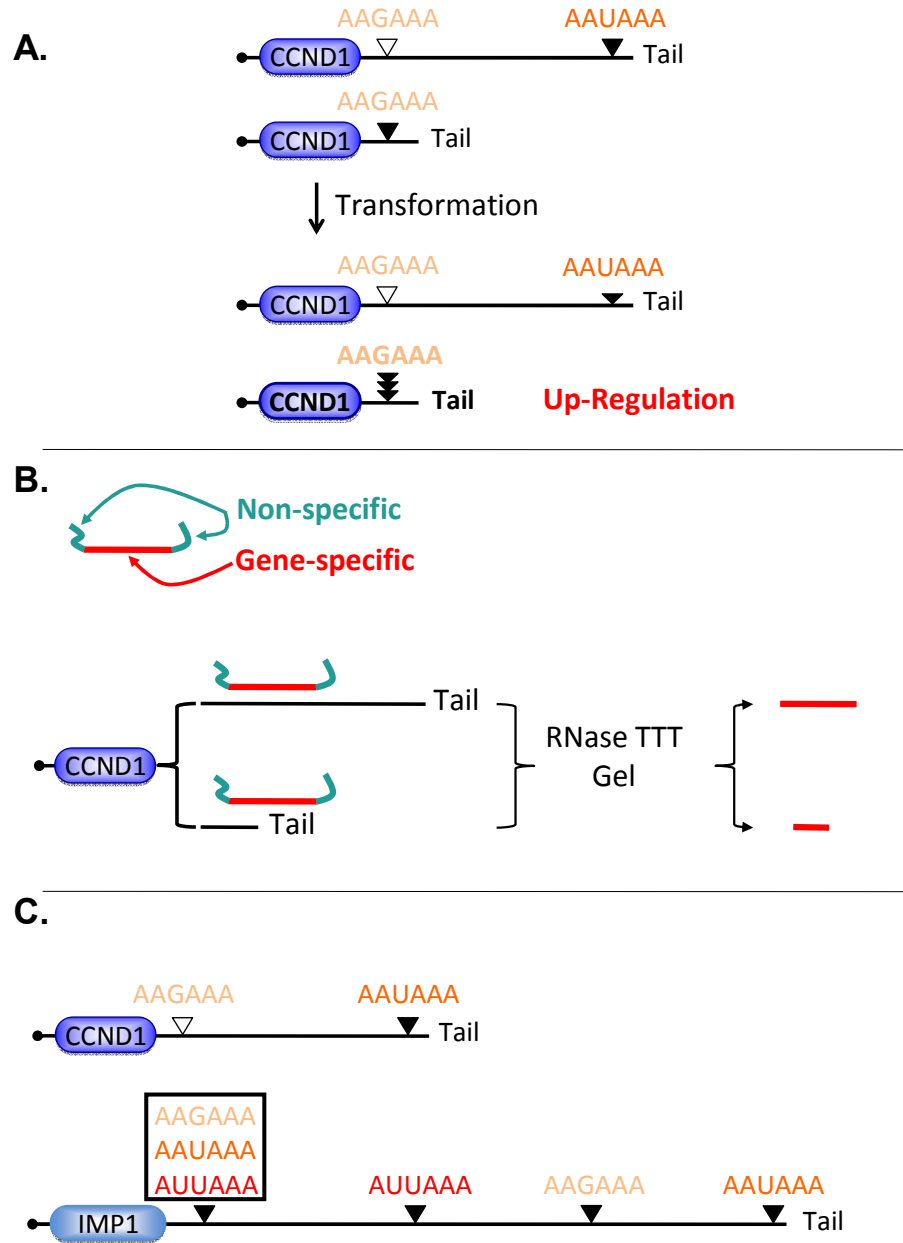


Figure 20: Schematic diagram of alternative polyadenylation sites in tumor cells, RPA assays to detect the sites and CCND1 and IMP1 mRNAs with known alternative polyadenylation sites

Panel A. CCND1 mRNAs contain two polyadenylation sites noted as proximal AAGAAA and distal AAUAAA sites, generating two isoforms. Following the transformation in non-transformed cells, the proximal AAGAAA site becomes the dominant polyadenylation site and generates more short isoforms. Panel B. Rationale for RPA assays to detect alternative polyadenylation sites. See details in main text. Panel C. Diagram of CCND1 mRNA and IMP1 mRNAs. CCND1 gene produces two isoforms. IMP1 gene produces several isoforms utilizing various polyadenylation signals. The polyadenylation signals marked in the box were examined here.

Figs. 21A and B clearly exhibit that NPM expression level did not influence the choice of polyadenylation sites in CCND1 and IMP1 mRNAs, no matter whether NPM was depleted transiently or stably. The assay itself sufficients to detect the alternative polyadenylation site usage in that HeLa and 293T cells utilize different polyadenylation sites (Fig. 21C). 293T cells prefer the proximal polyadenylation site for CCND1 mRNAs whereas HeLa cells prefer the distal sites.

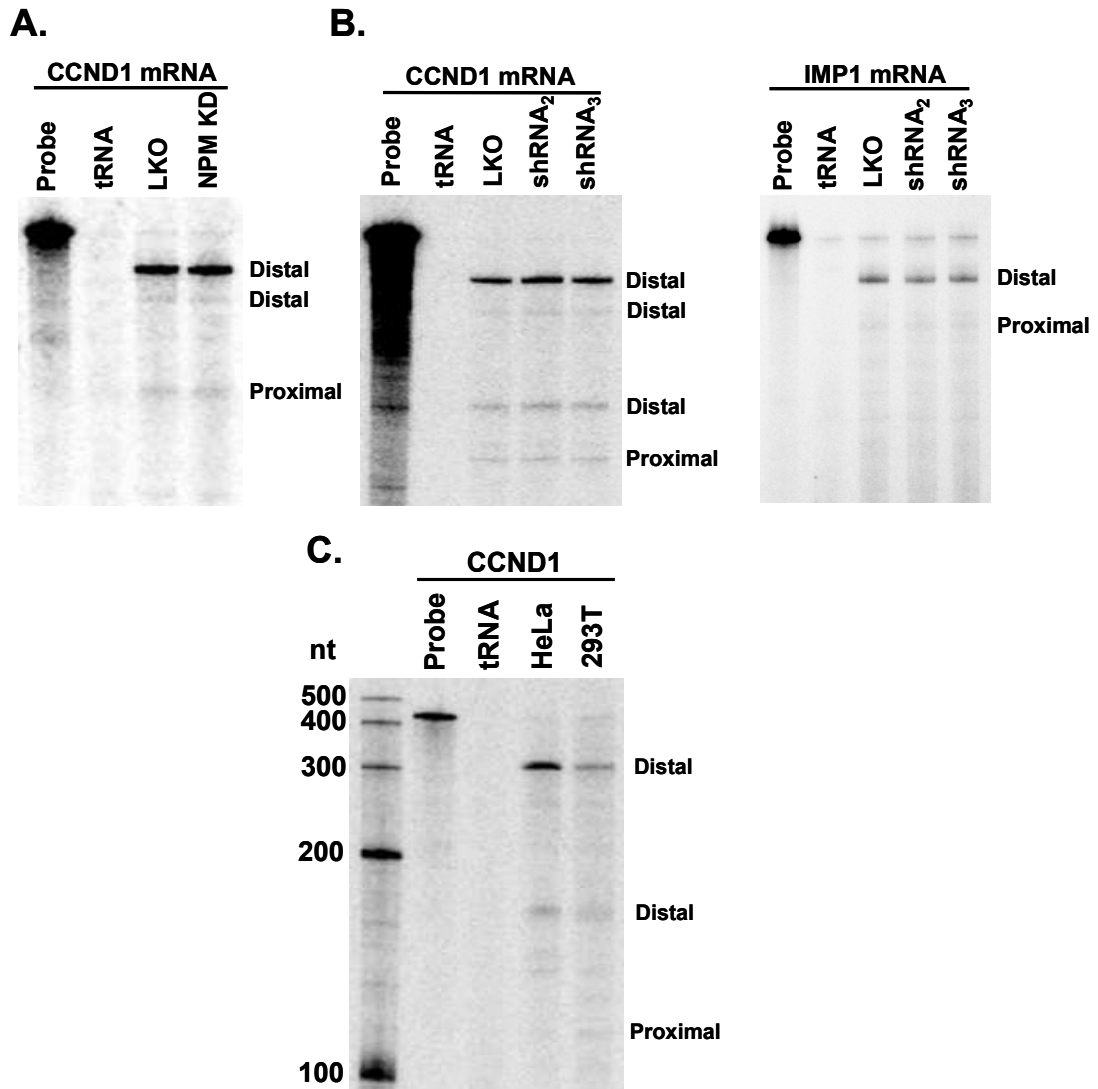


Figure 21: NPM knockdown does not lead to alternative polyadenylation site usage.

Panel A. Total RNA from stable LKO control (LKO) and stable NPM KD HeLa cell lines was purified and probed for CCND1 by RPA. Reaction products were separated on a 5% acrylamide gel containing urea and visualized by phosphorimaging. The lane

labeled as tRNA represents the results obtained when no total cellular RNA and only yeast tRNA was added to the reaction mixture, and the lane indicated “probe” represents the RPA probe without RNases digestion. The lanes labeled LKO and NPM KD represents reaction samples using LKO total RNA and NPM KD total RNAs, respectively. Panel B. Twenty-four hours post-transfection with LKO empty vector or indicated NPM shRNA vectors in HeLa cells, total RNA was purified and probed for CCND1 and IMP1-specific radioactive transcripts by RPA. Reaction products were separated on a 5% acrylamide gel containing 7 M urea and visualized by phosphorimaging. Panel C. Total RNA from HeLa and 293T cell lines was purified and probed for CCND1-specific radioactive probe by RPA. Reaction products were separated on a 5% acrylamide gel containing urea and visualized by phosphorimager. Sites of proximal and distal polyadenylation sites are noted on the right.

NPM knock down leads to slow growth in HeLa cells.

An analysis of cell doubling rates indicated that while viable, NPM KD cell lines grew significantly slower than their wild type and control LKO cell lines (Fig. 22A). These data confirm previously published work indicating that NPM plays a significant role in cellular growth and metabolism (Grisendi et al., 2005; Brady et al., 2009). We also thought it would be interesting to challenge NPM KD cells with 5 FluoroUracil (5 FU), a widely used chemotherapeutic in the treatment of tumors. Several reports have suggested that 5 FU may exert its effects through interference with rRNA metabolism which includes PM/Scf100, a component of RNA exosome (Cory et al., 1979; Greenhalgh and Parish, 1990; Lum et al., 2004). When Rrp6, the yeast-homolog of PM/Scf100 as depleted in *Saccharomyces cerevisiae*, cells accumulated extended, polyadenylated precursors of snRNAs, snoRNAs and rRNAs, but not mRNAs. In humans, PM/Scf100-depleted cells show hypersensitivity to 5 FU treatment (Kammler et al., 2008), highlighting the potential of 5 FU/PM/Scf100 combined therapies in cancer treatment. The hypothesis was proven wrong as in Fig 13, polyadenylated isoforms of rRNAs did not exhibit marked changes in poly(A) tails following NPM KD. As shown in Fig. 22B, 5 FU treatment significantly inhibited growth of both LKO control and NPM KD cell lines. However, NPM KD cell lines did not show any altered sensitivity to 5 FU treatment.

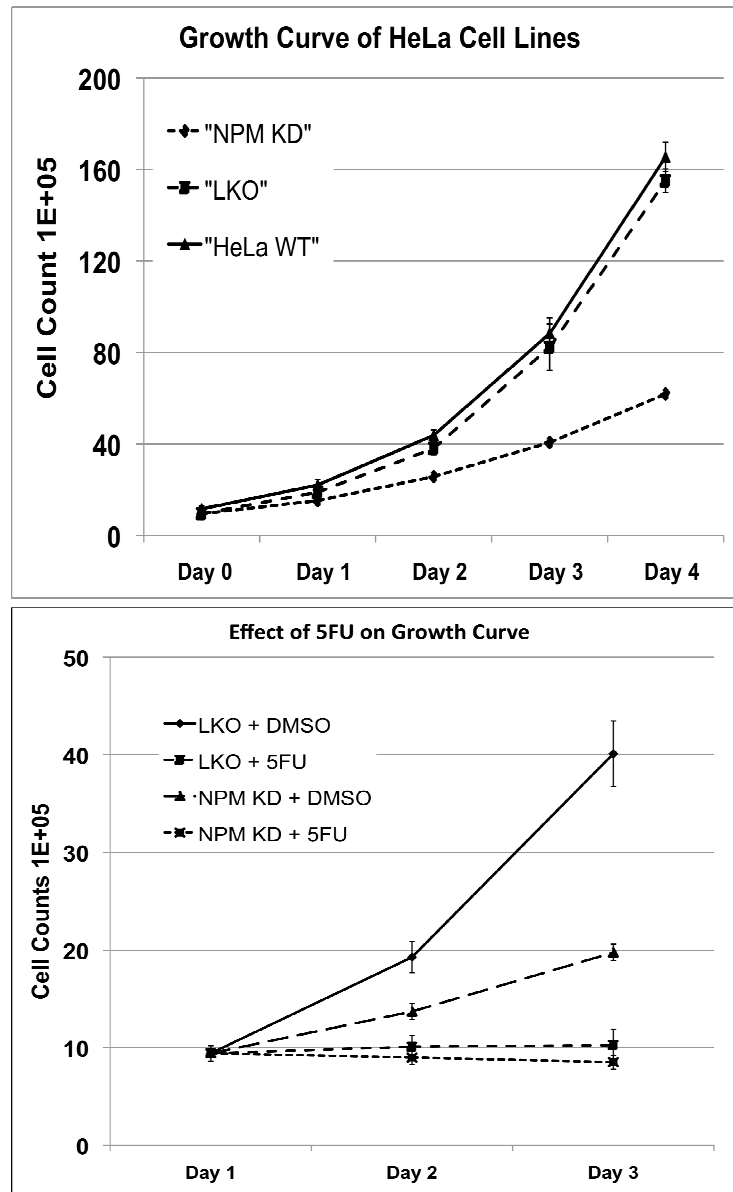


Figure 22: The NPM knock down HeLa cell line divides significantly slower than WT or LKO control HeLa cell lines, but is similarly sensitive to 5 FU treatment. Panel A. WT, stable LKO control and stable NPM KD HeLa cell lines were passaged in tissue culture and cell numbers were assessed on the days indicated. Error bars represent the standard deviation of three experiments. Panel B. LKO control and stable NPM KD HeLa cell lines were passaged in tissue culture and cell numbers were assessed on the days indicated with 0.05 mM of 5 FU and cell numbers were assessed on the days indicated. Error bars represent the standard deviation of three experiments.

Attempts/alternatives to purify a 14kDa protein that may also be a component of the polyadenylation mark.

Much like other RNA maturation events that involve a multi-protein complex, the polyadenylation mark may very well consist of more than just NPM. Identification of other components of the polyadenylation mark could give us important insights into its function. Angela Morrison previously observed a second protein at 14 kDa that behaves similarly to NPM in our *in vitro* polyadenylation systems in that it can be cross-linked following polyadenylation (Morrison, 2007). 40 nt-long 5' biotinylated RNA which contains a strong polyadenylation signal from SVL was used in our nuclear extracts for affinity purification. LLM-Pat assay (Fig. 23A) showed that biotinylated RNA was polyadenylated *in vitro* despite lacking the 5' cap structure. Western blotting analysis (Fig. 23B) showed that NPM could be pulled down using the affinity purification. As a negative control, TBP was not pulled down. ZC3H14, the human homolog of the yeast Nab2 protein could be also associated with the polyadenylated RNA. In Fig. 23C, affinity-purified protein samples were resolved on a 15% acrylamide gel and stained with silver staining to visualize bands. Although a western blotting showed NPM purification, a band of about 37kDa in size did not seem to be enriched in the silver staining. There are a couple of possible reasons for this. The washing conditions required to retain the 14kDa protein may not be stringent enough to remove the non-specific bands in the larger molecular size background (the previously published washing condition for NPM purification was too aggressive for a 14kDa protein to stay bound to RNA (data not shown)). Also a 15% acrylamide gel did not give the optimal resolution for NPM (32kDa) or larger molecules. As indicated by an arrow, a protein of an approximately 14 kDa protein is visible when a reaction contains biotinylated polyadenylated RNA. However, without the polyadenylation reaction or biotinylated RNA in the extract, this 14kDa protein failed to be affinity purified. However, this band was not sent for mass

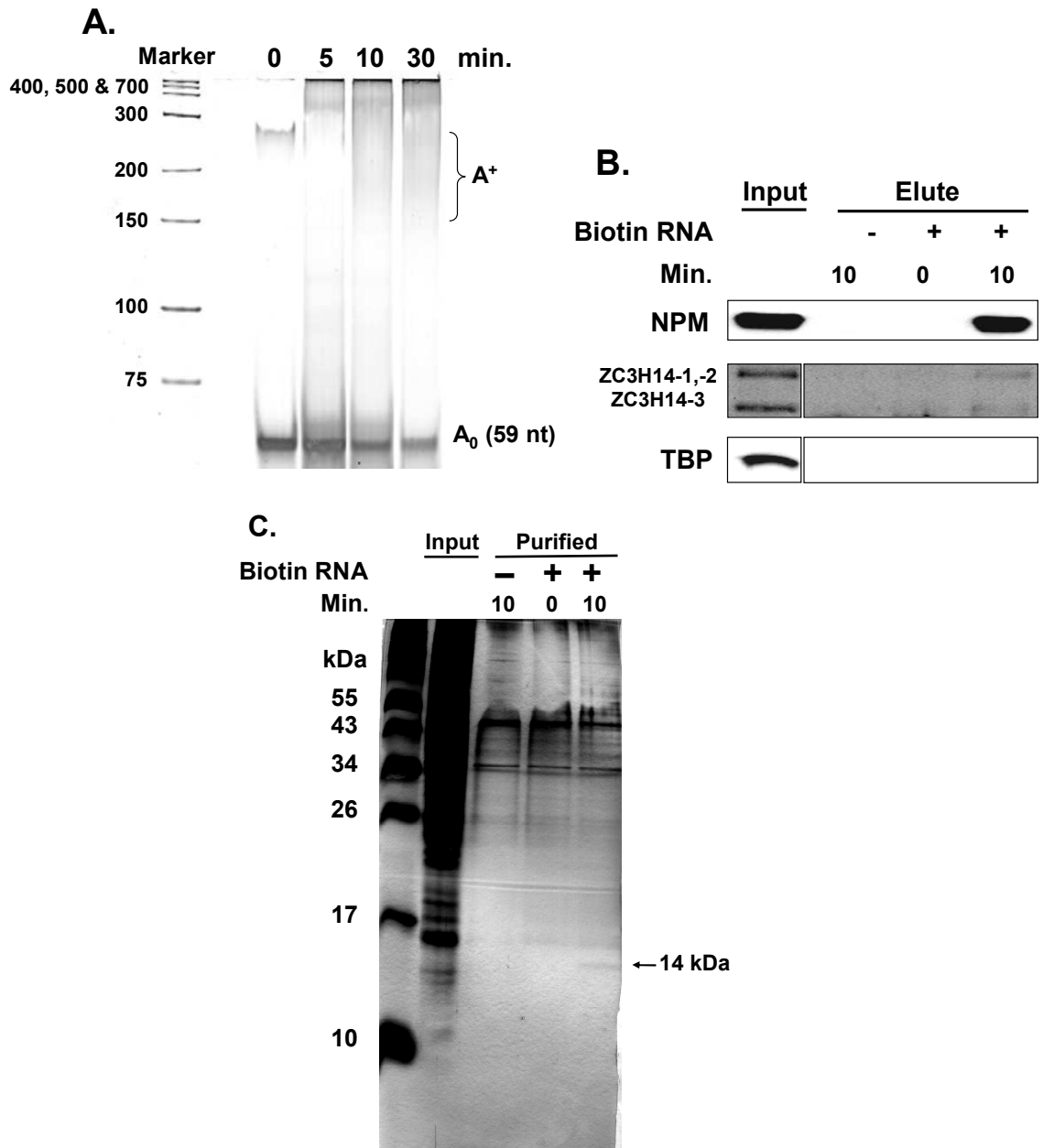


Figure 23: Biotinylated SVL RNA is polyadenylated in our *in vitro* polyadenylation assays.

Panel A. Biotinylated SVL RNA was incubated with WT HeLa nuclear extracts for the times indicated. Biotinylated RNA was then purified using streptavidin beads. LLM-PAT assay was used to examine the status of the affinity-purified RNAs. Reaction products were separated in 5% acrylamide gel and visualized by SYBRGreen staining using a Typhoon Trio imager. A₀ marker represents the size of the input biotinylated RNA. A⁺ represents the polyadenylated biotinylated RNA. Panel B. *In vitro* polyadenylation assays were performed with or without biotinylated RNAs as indicated. Following the incubation, samples were affinity-purified by streptavidin beads. The beads were washed three times and eluates were obtained by boiling the samples. Protein samples were separated on a 15% acrylamide gel and bands were visualized by silver staining.

spectrometric identification as it was extremely faint and we were not confident that MS analysis would produce meaningful results. As an alternative, we also searched for potential protein candidates, using available database from UniProtKB and ExPASy Proteomics Server – TagIdent tool. Searching parameters were ‘RNA binding’, ‘Homo sapiens’, ‘15000 Da with range of 33%’, which narrows down to proteins from 10kDa to 20kDa. We have found that there are several candidates for a 14kDa protein. Figure 24 summarizes the list of candidates for a 14kDa protein. Of particular interest were MAGOH and Y14 proteins, known components of an EJC. It has been shown that 3’ splice sites in the last exon increase the efficiency of polyadenylation, probably ensuring the nuclear pre-mRNA processing events are faithfully coordinated (Cooke et al 1996; 2002). Together with these observations, it makes sense that EJC components could also be part of the NPM-polyadenylation mark to send signals to the nuclear surveillance system that final splicing and polyadenylation complete. Although it is interesting that CBP20 was narrowed down to be a 14kDa candidate by software as well, it is probably not the right one as it is expected to bind to cap or cap analog not at the internal U-residues. In addition to the candidates above, the mRNA export factor P15 protein is also categorized in the search. P15 protein also makes sense immediately after NPM is deposited on the RNAs after the successful polyadenylation, P15 export factor binds to the NPM-marked RNA and initiates the nuclear export for the marked RNAs. Another candidate includes p14Arf protein. In the absence of DNA damaging, NPM retain p14ARF in nucleolous and prevents it from activating p53 pathways (Gjerset, 2006). Various anti-p14ARF antibodies were purchased and replacements were requested at no cost due to the poor quality of antibodies. However, none of the antibodies were of good enough quality to detect the p14ARF in our *in vitro* polyadenylation assays followed by the cross link/immunoprecipitation (data not shown).

Gene Name	Protein Name	kDa	pI	Known Function
MAGOH	Mago-nashi homolog	17.3	5.46	An EJC component; interacts with BPM8A/Y14
RBM8A/Y14	RNA binding motif protein 8A	19.9	5.5	An EJC component; interacts with MAGOH
CBP20	Cap Binding Protein 20 isoform 1	18	8.83	A small subunit of CBP which interact with TREX complex through Aly and CBP80
CBP20	Cap Binding Protein 20 isoform 2	11.9	8.67	A small subunit of CBP which interact with TREX complex through Aly and CBP80
P15	Nuclear mRNA export factor	15.5	4.91	A known mRNA export factor; heterodimerizes with another mRNA export factor, TAP.
p14ARF	Cyclin-dependent kinase inhibitor 2A, isoform 4	18.0	12.2	A known NPM binding partner; upon DNA damaging, localizes to nucleoplasm and interacts with mdm2 and activate p53.

Figure 24: List of candidates narrowed down for a 14kDa protein which behaves similarly to NPM in our *in vitro* polyadenylation assays

Protein candidates for a 14kDa protein were listed based on the available database search from UniProtKB and ExPASy Proteomics Server – TagIdent tool. Searching parameters were ‘RNA binding’, ‘Homo sapiens’, ‘15000 Da with range of 33%’, which narrows down molecular sizes of proteins between 10 and 20 kDa.

Microarray analyses on mRNAs following the transient depletion of NPM in HeLa cells.

The results shown above illustrate that NPM binds to the polyadenylated mRNAs regardless of the polyadenylation signals and NPM KD results in the hyperadenylation and nuclear retention of poly(A)⁺ RNA in cells. We also hoped to attain genome-wide expression profiles of mRNAs following the NPM KD. Fig. 25 portrays Gene Ontology (GO) terms for the most up-regulated and down-regulated mRNAs following the transient NPM KD in HeLa cells. This unveiled that the most up-regulated mRNAs expressed in NPM KD HeLa cells tend to encode factors participating in oxidation reduction, various cellular metabolism – lipid, amino acid, alcohol, macromolecules, precursor metabolites

Top ranked Gene Ontology terms associated with transient NPM KD in HeLa cells		
GO ID	P-value	GO Term
Up-regulated mRNAs		
GO:0055114	4.09E-11	oxidation reduction
GO:0044255	4.32E-09	cellular lipid metabolic process
GO:0008610	7.68E-09	lipid biosynthetic process
GO:0006520	1.77E-08	amino acid metabolic process
GO:0006066	1.14E-07	cellular alcohol metabolic process
GO:0016126	2.51E-07	sterol biosynthetic process
GO:0006091	2.71E-07	generation of precursor metabolites and energy
GO:0016125	9.18E-07	sterol metabolic process
GO:0006418	1.26E-06	tRNA aminoacylation for protein translation
GO:0043038	1.26E-06	amino acid activation
GO:0043039	1.26E-06	tRNA aminoacylation
GO:0006694	1.60E-06	steroid biosynthetic process
GO:0051186	4.26E-06	cofactor metabolic process
GO:0008104	7.88E-06	protein localization
GO:0015031	1.00E-05	protein transport
GO:0045184	1.05E-05	establishment of protein localization
GO:0033036	1.35E-05	macromolecule localization
GO:0008202	1.46E-05	steroid metabolic process
GO:0006695	2.41E-05	cholesterol biosynthetic process
GO:0006886	2.47E-05	intracellular protein transport
Down-regulated mRNAs		
GO:0009611	3.66E-09	response to wounding
GO:0002474	3.78E-07	antigen processing and presentation of peptide antigen via MHC class I
GO:0009615	4.22E-07	response to virus
GO:0051707	1.36E-06	response to other organism
GO:0006954	2.54E-06	inflammatory response
GO:0048002	3.32E-06	antigen processing and presentation of peptide antigen
GO:0009607	6.61E-06	response to biotic stimulus
GO:0019882	7.66E-06	antigen processing and presentation
GO:0012501	3.57E-05	programmed cell death
GO:0042127	3.67E-05	regulation of cell proliferation
GO:0006915	6.25E-05	apoptosis
GO:0051094	7.01E-05	positive regulation of developmental process
GO:0065009	8.78E-05	regulation of molecular function
GO:0008219	1.08E-04	cell death
GO:0016265	1.12E-04	death
GO:0008283	1.82E-04	cell proliferation
GO:0008285	2.00E-04	negative regulation of cell proliferation
GO:0030195	2.17E-04	negative regulation of blood coagulation
GO:0007243	2.49E-04	protein kinase cascade
GO:0050790	2.99E-04	regulation of catalytic activity

Figure 25: List of top ranked GO terms associated mRNAs that are misregulated upon transient NPM knock down in HeLa cells

Top 50 ranked mRNAs associated with transient NPM KD in HeLa cells							
Gene symbol	ACC #	P-value	Fold Change	Gene symbol	ACC #	P-value	Fold Change
Up-regulated mRNAs				Down-regulated mRNAs			
SCD	NM_005063	9.68E-03	20.37	CCL5	NM_002985	4.04E-06	146.91
ACSL1	NM_001995	7.69E-03	8.18	RSAD2	NM_080657	2.84E-06	137.80
SC4MOL	NM_006745	1.86E-05	8.10	CXCL10	NM_001565	4.77E-03	128.83
SQLE	NM_003129	1.51E-04	7.21	HRASLS2	NM_017878	1.02E-03	80.92
SLC16A6	NM_004694	3.11E-04	6.67	IFIT2	NM_001547	1.86E-03	52.79
DHCR7	NM_001360	3.59E-04	6.59	RARRES3	NM_004585	3.75E-05	38.31
TFRC	NM_003234	1.57E-06	6.40	NCF2	NM_000433	1.01E-04	27.66
EIF4B	NM_001417	7.88E-03	5.95	CCL3L1	NM_021006	9.95E-04	26.20
SLC2A3	NM_006931	6.18E-03	5.50	CCL3L1	NM_021006	9.95E-04	26.20
RNF182	NM_152737	3.58E-05	5.20	CCL3L1	NM_021006	9.95E-04	26.20
TBL1X	NM_005647	3.95E-04	5.12	SAMD9	NM_017654	4.48E-03	26.17
ATP7A	NM_000052	5.40E-05	5.11	CCL3	NM_002983	7.96E-04	25.42
PSG5	NM_002781	6.00E-04	5.04	XAF1	NM_017523	1.43E-04	23.39
SLC9A2	NM_003048	5.49E-04	4.94	IL6	NM_000600	1.56E-04	22.62
KIAA1715	NM_030650	4.43E-03	4.91	RAET1L	NM_130900	5.86E-04	21.27
RHOBTB3	NM_014899	1.22E-03	4.87	PTGER4	NM_000958	3.99E-04	20.86
SORBS2	NM_021069	1.95E-04	4.86	SDC4	NM_002999	1.94E-03	16.67
INSIG1	NM_005542	1.10E-05	4.79	JUN	NM_002228	4.71E-05	15.55
BDKRB1	NM_000710	7.95E-03	4.69	IFIT3	NM_0010316	4.27E-03	15.53
GLP2R	NM_004246	9.77E-03	4.62	KLF4	NM_004235	4.02E-05	14.87
CLCN3	NM_173872	4.39E-03	4.43	EPGN	NM_0010134	3.08E-05	14.65
SLC6A15	NM_182767	1.80E-04	4.37	NFKBIZ	NM_031419	1.95E-03	13.92
FDPS	NM_002004	3.02E-03	4.13	ISG15	NM_005101	5.47E-04	13.72
CYP51A1	NM_000786	2.95E-03	4.08	IFIT1	NM_001548	2.68E-06	13.52
FASN	NM_004104	6.53E-03	4.06	BIRC3	NM_001165	3.45E-04	12.58
ME1	NM_002395	8.51E-03	4.05	PMAIP1	NM_021127	1.94E-05	12.56
PDK3	NM_005391	1.47E-03	4.03	STEAP4	NM_024636	4.30E-03	12.31
ERMP1	NM_024896	1.33E-03	3.99	CRLF2	NM_022148	4.22E-04	11.86
FITM2	NM_0010804	1.66E-03	3.87	HIP1R	NM_003959	1.10E-04	11.68
FDFT1	NM_004462	1.94E-04	3.83	EDN1	NM_001955	1.55E-03	11.20
PSAT1	NM_058179	1.97E-03	3.77	HERC5	NM_016323	2.92E-04	10.45
ACACA	NM_198839	4.57E-05	3.63	CSAG2	NM_0010808	8.77E-04	10.01
MTO1	NM_133645	2.86E-03	3.61	KRT17	NM_000422	7.57E-04	9.90
ABCD3	NM_002858	2.94E-04	3.60	OAS2	NM_002535	1.07E-04	9.74
ACO1	NM_002197	9.15E-04	3.54	CSAG2	NM_0010808	5.77E-03	9.68
ACAT2	NM_005891	4.28E-04	3.53	SEMA3A	NM_006080	9.12E-05	9.28
KLRK1	NM_007360	7.96E-03	3.52	ZFP36L2	NM_006887	2.68E-03	9.15
EBP	NM_006579	1.59E-03	3.46	BAMBI	NM_012342	8.26E-04	9.12
CXCR4	NM_0010085	3.20E-04	3.41	IGFBP6	NM_002178	4.70E-04	8.90
HMGCR	NM_000859	6.39E-04	3.40	GBP3	NM_018284	1.11E-03	8.90
CALU	NM_001219	1.35E-03	3.37	TRIM22	NM_006074	3.21E-05	8.86
FGFBP1	NM_005130	8.76E-03	3.36	GSDMB	NM_0010424	7.08E-03	8.14
EIF4B	NM_001417	9.96E-04	3.34	PPP1R15A	NM_014330	2.62E-04	8.11
PRKDC	NM_006904	2.80E-03	3.32	NR4A2	NM_006186	3.19E-04	7.84
EMP2	NM_001424	6.01E-04	3.29	MUC13	NM_033049	5.16E-05	7.73
SETD7	NM_030648	5.27E-05	3.28	GRB10	NM_0010015	1.97E-04	7.44
FADS1	NM_013402	1.11E-03	3.24	ZNFX1	NM_021035	4.56E-03	7.43
DAD1	NM_001344	1.12E-03	3.24	CYR61	NM_001554	9.05E-03	7.42
MMGT1	NM_173470	6.12E-03	3.22	SERPINE1	NM_000602	4.73E-03	7.39
FDPSL2A	NR_003262	3.43E-03	3.19	TXNIP	NM_006472	2.55E-05	7.31

Figure 26: List of top 50 ranked mRNAs up-regulated or down-regulated following transient NPM knock down in HeLa cells

and energy and other cofactors – macromolecule transport and tRNA activation. In contrast, the GO terms for the most down-regulated mRNAs include response to inflammation, viruses and other organisms, antigen processing, programmed cell death, positive and negative regulation of cell proliferation, protein kinase cascade and regulation of catalytic activity. Figure 26 contain the top 50 most up-regulated or down-regulated mRNAs associated with NPM KD in HeLa cell from which GO terms were generated.

Discussion

Much like any other step in RNA biogenesis, polyadenylation is carefully regulated and coordinated with other events involved in nuclear mRNA processing. This thesis characterizes the oncoprotein nucleophosmin as a factor that influences the length of the poly(A) tail as well as mRNA export from the nucleus to the cytoplasm. These observations attribute important new functions to this abundant nuclear/nucleolar chaperone and significantly expand our insight into the overall impact of nucleophosmin on cellular metabolism. There are several possible models for how NPM influences poly(A) tail length. First, by binding CPSF, NPM may influence CPSF interactions with PABPN1 and PAP (Fig. 8). As the poly(A) tail gets longer and interactions between CPSF and the other factors become more difficult to maintain because of physical distance (Kuhn et al., 2009), NPM could provide added strain to these interactions and favor dissociation. When CPSF can no longer effectively interact with PAP/PABPN1, poly(A) tail synthesis terminates and NPM may simultaneously be released to bind to the 3' UTR of the mRNA as a polyadenylation mark. Thus binding of NPM to the 3' UTR may also assist in the release of the core poly(A) factors such as CPSF, PAP and PABPN1 from the nascent mRNA. If this is the case, in NPM KD cells, the core poly(A) factors noted above should be persistently attached on the RNAs long after they should have been removed. This hypothesis is quite attractive and testable because in yeast cells assembly of the mRNA export factors is a pre-requisite for the efficient release of poly(A) factors and thus mRNA export (Hilleren and Parker, 2001; Qu et al., 2009). Our working model is consistent with the data in Fig. 8 showing that an RNase insensitive interaction exists between NPM and CPSF complex as well as with the requirement for natural

termination of poly(A) tail synthesis for NPM deposition (Fig. 7). Alternative models exist which are less likely but cannot be formally ruled out. NPM, for instance, may modulate poly(A) tail size by assisting with the recruitment of a deadenylase to remodel the poly(A) tail. There seems to be an RNA bridging between NPM and a nuclear poly(A)-specific ribonuclease, PARN but the interaction is readily eliminated following RNase treatment (Fig. 8). In addition, there is evidence for a role for PARN activity influencing poly(A) tail length in our nuclear extract-based polyadenylation assays where NPM regulation of poly(A) tail length could be recapitulated (Fig. 15). Nevertheless, we cannot rule out that other deadenylases may be involved. Perhaps, NPM may interact with nuclear poly(A) binding factor(s) which in turn manage poly(A) elongation (Keller et al., 2000; Kuhn et al., 2009). However this scenario is not the most likely as NPM interacts with PABPN1 protein in an RNase sensitive manner, possibly through CPSF160 (Fig. 8). In addition, sequestration of poly(A) binding proteins causes the shortening of poly(A) tails synthesized in both WT and NPM KD nuclear extracts (Fig. 16). These observations suggest that hyperadenylation defects stem from the depletion of NPM, rather than the defects in poly(A) remodeling or elongation. It is very possible that NPM may influence the association of other proteins in the large complex of ~85 putative factors involved in polyadenylation via its chaperone activity (Shi et al., 2009) and thus influence poly(A) tail length indirectly. Given the lack of known functions for other factors besides CPSF, PAP and PABPN1 in poly(A) length regulation (Kuhn et al., 2009), assessment of this alternative model awaits additional experimental insight into the functions of these other putative poly(A) factors in the Wilusz lab as well as by our colleagues. Nonetheless, this thesis points strongly toward that NPM may act as a polyadenylation terminator.

Since NPM could directly associate with the AAUAAA binding factor CPSF, we investigated whether NPM influences alternative polyadenylation. Given the

overexpression of NPM in cancer cells and the altered use of upstream poly(A) signals on many genes (Sandberg et al., 2008; Ji et al., 2009; Mayr and Bartel, 2009), we considered this an attractive experiment to test. Fig 21 demonstrates that NPM does not seem to be involved in alternative polyadenylation sites as poly(A) site choice was not altered in NPM KD cell lines. This remark would be consistent with the mechanistic data that NPM is not deposited during the mRNA cleavage event (Palaniswamy et al., 2006), but rather at later times in the poly(A) tail synthesis (Fig. 7), long after the choice of polyadenylation signals on the pre-mRNA has been made.

In addition to an overall block in mRNA export by hyperadenylation (Jensen et al., 2001), there are several hypotheses for how NPM may directly influence mRNA movement from the nucleus to the cytoplasm. First, NPM is a known nucleocytoplasmic shuttling protein (Maggi et al., 2008) and could play a direct role in chaperoning the movement of mature mRNAs from the nucleus to the cytoplasm when it is deposited on transcripts that have been properly polyadenylated. NPM is known to play a key role in ribosome export from the nucleus (Maggi et al., 2008) and has recently been implicated in miRNA export from cells (Wang et al., 2010), thus it may be generally involved in RNP movement in the cell. It will be interesting to investigate whether NPM takes part in all mRNA export whether some mRNAs such as those that utilize Crm1-mediated pathways are exempt from NPM influence (Brennan et al., 2000; Culkovic et al., 2006; Prechtel et al., 2006). Second, NPM has been shown to associate with the nuclear pore, specifically through interactions with Nup98 (Crockett et al, 2004). NPM could therefore directly assist in the loading of mRNA export complexes at the pore. Third, there have been a variety of connections between polyadenylation and mRNA export (Rougemaille et al., 2008; Johnson et al., 2009; Qu et al., 2009; Ruepp et al., 2009), and exploring the connections between NPM and these export factors could provide significant insight – NPM/Aly, NPM/EJC and NPM/CBP to name a few. Finally, NPM-influenced mRNA

export could be a regulated process in the cell. The tumor suppressor ARF blocks NPM shuttling, affects ribosome biogenesis and reduces polysome formation (Gallagher et al., 2006). It will be informative to assess whether activation of ARF also affects mRNA export from the nucleus, which could contribute to the translational effects that have been observed (Li and Hann, 2009). Could NPM be involved in the networking of polyadenylation to other aspects of nuclear mRNA biogenesis? Tarapore et al (2006) have demonstrated that NPM phosphorylated on Thr 199 can localize to nuclear speckles and repress mRNA splicing. It will be attractive to investigate the role of NPM deposition by polyadenylation in the connections between splicing and 3' end formation as NPM-bound RNAs should experience the successful polyadenylation and may also complete splicing.

There are numerous interesting potential implications in the observations made in this study to cancer-related cellular processes. First, DNA damage results in increased NPM synthesis as well as accumulation of NPM in the nucleoplasm (Wu et al., 2002). Given the changes in polyadenylation that have been noted in response to DNA damage (Cevher et al., 2010), it will be worthwhile to determine whether NPM contributes to any alterations in 3' end processing seen under these conditions – delayed or unsuccessful NPM deposition to retain the poly(A)⁺ RNAs in the nucleus and thus halt gene expression. Second, NPM undergoes mutations, translocations and significant up-regulation in cancer cells and has been implicated as both an oncogene and as a tumor suppressor (Grisendi et al., 2006). Many if not all cancer cells show a dramatic increase in NPM expression (Pianta et al., 2010). As the experiments performed in this study are in tissue culture cells (HeLa and 293T cells) that express high levels of NPM, it may be informative to compare NPM deposition, poly(A) tail length regulation and mRNA export in normal human cells. These studies could provide important insight into novel roles for NPM in the regulation and quality control of mRNA

biogenesis and the promotion of tumorigenic phenotypes. Third, the N-terminal half of NPM is a common target for chromosomal translocations that generate oncogenic fusion proteins (Grisendi et al., 2006). Whether and how these NPM fusion proteins function as polyadenylation marks will be interesting fodder for future studies. One can envision the scenario where NPM-fused proteins may still bind to RNAs as a polyadenylation mark and activate the aberrant gene expression due to the NPM-fused partners such as NPM-ALK (Morris et al., 1994) and NPM-MLF1 (Yoneda-Kato et al., 1996). Finally, about a third of adult acute myeloid leukemias (AML) possess a frameshift in the C-terminal portion of NPM that results in an aberrant cytoplasmic accumulation of the protein (Grisendi et al., 2006; Lindström, 2011). The challenge to study this model is that while *in vivo* AML patients exhibits the NPM localization exclusively in the cytoplasm, AML tissue-culture adapted cell lines, in unknown manners, localize NPM both in the nucleus and cytoplasm, making it extremely difficult to selectively study cytoplasmic-NPM and envision how the NPM localization changes the *in vivo* phenotypes (Quentmeier et al., 2005). How this altered NPM subcellular localization influences mRNA poly(A) tails and mRNA export regulation in AML cells will also be an interesting question for future studies.

Experimental Procedures

Cell Culture and Transfection

Adherent HeLa cell lines were grown at 37°C in 5% CO₂ in Dulbecco's Modification of Eagle's Medium (DMEM) supplemented with 10% fetal bovine serum, 1 mM L-glutamine, 10U/mL penicillin and 10µg/mL streptomycin. HeLa S3 suspension cells were grown in Eagle's Minimum Essential Medium (MEM) supplemented with 10% horse serum. All plasmid DNA was treated with the MiraCLEAN endotoxin removal kit (Mirus Bio) prior to being used for transfection with Lipofectamine 2000 (Invitrogen). For establishment of the LKO and NPM Knock Down (KD) HeLa cell lines, either empty LKO-1 plasmid or LKO-1 plasmid containing an shRNA against the coding sequence of human NPM (shRNA 1: Sigma MISSION clone ID NM_002520.4-169s1c1) was transfected into cells. Two days post-transfection, cells were switched to media containing puromycin (5 µg/mL). Single colonies were selected, and expression of NPM was assessed by qRT-PCR using NPM-specific and GAPDH-specific oligonucleotides (Table 1) and corroborated by Western blot using NPM antibodies (Santa Cruz: SC-32256, 1:5000) and secondary goat anti-mouse IgG-HRP (Santa Cruz: SC-2005, 1:20000).

Name	Sequence	Expected Size	Accession Number	PCR Efficiency
NPM F	GGTCTGCCCTGGAGGT	148	NM_002520.6	108%
NPM R	GGCGCTTTTCTTCAGCTT			
GAPDH F	AAGGTGAAGGTCGGAGTCAA	108	NM_002046.3	97.8%
GAPDH R	AATGAAGGGGTCATTGATGG			

Table 1: list of oligonucleotides used for q-RT-PCR assays.

For growth analysis, cells were plated at 3.4×10^4 cells per mL and then trypsinized and counted daily using a hemocytometer. For the 5-Fluorouracil (5-FU) sensitivity test, 0.05 mM of 5-FU (Sigma Aldrich F6627 – dissolved in DMSO) was added to media. Cells were plated at 3.4×10^4 cells per mL and then trypsinized and counted daily using a hemocytometer and the media was changed for fresh media containing 0.05 mM 5-FU. For transient shRNA-mediated KD of NPM expression, either empty LKO-1 plasmid or NPM shRNA LKO-1 plasmids (shRNA 2: NM_002520.4-664s1c1; shRNA 3: NM_002520.4-819s1c1) were transfected into HeLa cells. Twenty-four hours post-transfection, cells were processed for fluorescence *in situ* hybridization (FISH) assays, western blotting, linker ligation-mediated poly(A) tail (LLM-PAT) assays, RNase protein assays and RNase H/northern assays. Transfection efficiency was routinely in the 70-80% range and was verified by cotransfection of a plasmid encoding eGFP.

Plasmids and RNAs

The templates for the 3'UTR of melanocortin 4 receptor (MC4R), poly(A) polymerase gamma (PAPOLG) were generated by hybridizing two DNA oligonucleotides with upstream SP6 polymerase recognition sequence listed in Table 2.

Name	Accession Number	Sequence
SP6 MC4R F	NG_016441.1	<u>ATTTAGGTGACACTATAGAATCTATGTTATAGGTTGTAGGCACTGTGG</u> <u>ATTTACAAAAAGAAAAGTCCTTATTAAAAGCTTAACAATGTC</u>
SP6 MC4R R		<u>GACATTGTTAAGCTTTTAATAAGGACTTTTCTTTTGTAAATCCACAG</u> <u>TGCCTACAACCTATAACATAGATTCTATAGTGTACACCTAAAT</u>
SP6 PAPOLG F	NM_022894.3	<u>ATTTAGGTGACACTATAGTGTGTTTGTAAATGAAGTCGTATGTATTTTC</u> <u>AGAGTATTTTGTATGTACTGTAAGATACCATCTTTTCAAAGAGAAAC</u> <u>GTTTAAACCTTTA</u>
SP6 PAPOLG R		<u>TAAAGGTTTTAAACGTTTCTCTTTGAAAAGATGGTATCTTACAGTACA</u> <u>TACAAAAATACTCTGAAAATACATACGACTTCATTTACAAAACACTAT</u> <u>AGTGTACCTAAAT</u>

Table 2: List of oligonucleotides hybridized to generate transcription templates for MC4R and PAPOLG polyadenylation signals. SP6 Polymerase recognition sequences are underlined

pSVL consists of a 241 bp BamHI-BclI fragment containing the SV40 late polyadenylation signal inserted into the BamHI site of pSP65 (Wilusz et al., 1988). Pre-cleaved SVL RNA was generated by SP6 transcription of pSVL that had been linearized with HpaI. pIVA2 contains the 155 bp BamHI-PvuII fragment of adenovirus pE1B cloned into pGem4 at the HincII and BamHI sites. SP6 transcription of BglI-linearized template yielded a 156 nt RNA (IVA2). To generate probes to detect cellular mRNAs by RNase protection assay, PCR products amplified from HeLa cDNA were cloned into pGem-4 at EcoRI and PstI sites and sequenced. The plasmids were linearized with BsrGI restriction enzyme and transcribed by T7 RNA polymerase.

RPA Probe			
Name	Sequence	Amplicon	Accession Number
EcoRI-CCND1 RPA F	CCGAATTCCTGACAGTCCCTC CTCTCC	1161-1474	NM_053056.2
PstI-CCND1 RPA R	AAACTGCAGCGCCTCCTTTGTG TTAATGC		
EcoRI-IMP1 RPA F	CCGAATTCATGCGTGGAGTTC CCCTCC	3601-3961	NM_006546.3
PstI-IMP1 RPA R	AAACTGCAGGGCCTGTTCTCCA TAGAGAG		
EcoRI-CPEB RPA F	CCGAATTCCTCAAGCCTCTTGTTT TTCACCA	1921-2154	NM_030594.3
PstI-CPEb RPA R	AAACTGCAGACTGGGGCAGATC TTGAAGT		

Table 3: List of oligonucleotides used to clone RPA probes

To generate probes to detect GAPDH and β -actin mRNA by RNase H northern blot, HeLa cDNA generated using HeLa total RNA and random hexamers were used for PCR and PCR products were cloned into pGem-4 at EcoRI and PstI sites and sequenced. The plasmids were linearized with EcoRI and transcribed by T7 RNA polymerase.

Northern Probe			
Name	Sequence	Binding Site	Accession Number
EcoRI-GAPDH Northern F	CCGAATTGCGCCACACTCAGTCCCCCACCACACT	1182-1310	NM_002046.3
PstI-GAPDH Northern R	AAACTGCAGGGTTGAGCACAGGGTACT		
EcoRI-ActB Northern F	CCGAATTCTGTCCCCCAACTTGAGATG	1693-1811	NM_001101.3
PstI-ActB Northern R	AAACTGCAGCATTMTTAAAGGTGTGCACTT		

Table 4: List of oligonucleotides used to clone northern probes

***In Vitro* Transcription**

Transcription reactions using SP6/T7 RNA polymerase were performed in the presence of α -³²P-UTP as described previously (Wilusz and Shenk, 1988). A typical transcription reaction contains 1 μ g of linearized template DNA, 500 μ M ATP and CTP, 50 μ M GTP and UTP, α -³²P UTP (800 Ci/mmol), 500 μ M 7^mGpppG cap analog (New England Biolabs, S1404), 20 U of Ribolock RNase Inhibitor (Fermentas) and 20 U SP6 RNA polymerase (Fermentas) in transcription buffer (40 mM Tris-HCl (pH 7.9), 6 mM MgCl₂, 10 mM DTT, 10 mM NaCl, 2 mM spermidine). All RNAs were gel-purified before use. For transcribing radioactive RNA probes for northern blot or RPA assays, transcription was conducted in the same manner as SP6 transcription except that the 500 μ M GTP was used, cap analog was omitted and 20 U T7 RNA polymerase was used.

RNase Protection Assays

Total RNA was purified from HeLa cell lines using the TRIzol (Invitrogen) method. 10 μ g of total RNA and 10 μ g of yeast tRNA was mixed with 1x10⁵ CPM internally labeled radioactive RPA probes and vacuum dried by Speed Vac to 1-2 μ L. RPA hybridization buffer (40 mM PIPES-HCl pH6.4, 400 mM NaCl, 1 mM EDTA and 20% formamide) was

added up to 30 μ L. The samples were heated at 85°C for 4 minutes and cooled down at -0.1°C/s to 45°C and kept at that temperature for at least 8 hours in a thermocycler (Eppendorf). Following the hybridization, the reaction was digested with 7 ng of RNase A and 100 U of RNase T1 (Ambion) for 30 minutes at 37°C in digestion buffer (10 mM Tris-HCl pH 7.5, 200 mM NaCl and 5 mM EDTA). These concentrations of RNases were optimized to give complete digestion of single-stranded probes while minimizing non-specific digestion of protected probes. The reaction was stopped by adding 20 μ L 20% SDS. The samples were phenol-chloroform extracted and precipitated by ethanol with 10 μ g glycogen as a carrier. Control samples that did not experience RNase treatment, or did not contain HeLa total RNA were also routinely analyzed. The digested samples were run on a 5% acrylamide gel containing 7 M urea. Gels were dried, exposed to a phosphor screen and visualized by a Typhoon Trio (GE Healthcare) phosphorimager.

RNase H/Northern assays

Total RNA samples prepared from HeLa cell lines as described above were hybridized to 500 ng of a DNA oligonucleotide designed to anneal to the 3' UTR of either GAPDH or β -actin and treated with 5 U RNase H (Fermentas). This step was performed to reduce the size of cellular RNAs that would be detected by Northern blotting so that the length of the poly(A) tail could be readily discerned on a polyacrylamide gel. Additional reactions also included 2 μ g oligo d(T) to generate a marker for fully deadenylated mRNAs. Reaction products were separated on a 5% denaturing polyacrylamide gel. RNA was then transferred to a Hybond-XL (GE Healthcare) membrane at 700 mA for 45 minute at 4°C in TBE buffer. RNA was cross linked to the membrane by exposing to Stratalinker for autocross link twice or 2400 micro joules. The membrane was blocked in 25 mL hybridization buffer (5X Denhardt's solution, 50% formamide, 5x SSC, 1% SDS,

0.5 mL SS-DNA) at 60°C for 30 minutes, followed by the overnight incubation with the gene-specific radioactive RNA probes described above. Following two washes with 2x SSC with 0.1% SDS and one wash with 1x SSC and 0.1% SDS, the membrane was exposed to the phosphor imager screen and analyzed by a Typhoon Trio phosphorimager.

RNase H oligo			
Name	Sequence	Binding Site	Accession Number
GAPDH RNase H	AGGGACTCCCCAGCAGTG	1163-1181	NM_002046.3
β -actin RNase H	AAAAAGGGGGAAGGGGG	1675-1692	NM_001101.3

Table 5: List of oligonucleotides used to hybridize to 3' UTR of mRNAs to trim the 3'UTR length in RNase H/Northern assays

Polyadenylation Assays

HeLa nuclear extracts were prepared and cell free polyadenylation assays were performed as previously described (Wilusz and Shenk, 1988). A typical reaction contained 3 % (w/v) polyvinyl alcohol (PVA), 1 mM ATP, 20 mM phosphocreatine, 12 mM HEPES (pH 7.9), 12 % (v/v) glycerol, 60 mM KCl, 0.12 mM EDTA, 0.3 mM DTT and 60% (v/v) nuclear extract in 12.5 μ L reaction. Cordycepin 5'-triphosphate (Sigma Aldrich C9137) was dissolved in water and added to polyadenylation assays at the concentrations indicated. Recombinant poly(A)-specific ribonuclease, PARN was added to nuclear extract where indicated. Chemically synthesized poly(A) RNA (Pharmacia) was resuspended in water and the indicated amounts were added to the HeLa wild type and NPM knockdown nuclear extracts. To immunodeplete NPM from HeLa nuclear extracts, either 2, 4, or 8 μ L NPM-specific antibody (Santa Cruz: sc-5564) or 16 μ L control normal rabbit IgG (Santa Cruz: sc-2027) was pre-bound with 20 μ L 50% Protein A- Sepharose beads (Sigma-Aldrich: P3391) in Buffer D (20 mM Hepes pH 7.6, 100 mM KCl 0.2 mM EDTA and 1 mM DTT) for 30 min at 4°C. Pre-bound complex was spun down at 16100xg for 30 sec and excess buffer was removed. 20 μ L HeLa nuclear

extracts were then added to the pre-bound complex and incubated for 30 minutes on ice with occasional mixing. Following the incubation, the extracts were spun at 16100xg for 30 sec and 7.25 μ L of supernatant was used for *in vitro* polyadenylation assays as described above. Reactions were incubated at 30°C for the indicated times and products were analyzed on 6% (w/v) acrylamide gels containing 7 M urea.

Protein-Protein Co-Immunoprecipitation Analysis

HeLa cells were lysed by douncing in 500 μ L lysis buffer (25 mM HEPES-HCl pH 7.6, 5 mM $MgCl_2$ 1.5 mM KCl and 0.5% NP-40) and nuclei were isolated by centrifugation at 900xg for 5 min at 4°C. The lysate was centrifuged at 16100xg for 10 min at 4°C to remove insoluble materials. The lysate was then pre-cleared using 20 μ L 25% Pansorbin cells (Calbiochem Cat# 507862). In some samples, 10 units of RNase ONE (Promega) was added to the pre-cleared lysate and incubated at 37°C for 15 min. The lysates were treated with either 10 μ L rabbit anti-nucleophosmin antibody (Santa Cruz, sc-5564) or 20 μ L rabbit IgG (Santa Cruz: sc-2027) as noted above and 20 μ L 25% Pansorbin cells. Following washing with NET-2 buffer, pellets were resuspended in SDS-loading dye (70 mM Tris-Cl pH 6.8, 6% glycerol, 2% SDS and 100 mM DTT) and were separated on a 10% SDS polyacrylamide gel and blotted to polyvinylidene difluoride (PVDF) membrane (Millipore). NPM was detected using mouse monoclonal antibody FC8791 (Santa Cruz Biotechnology, 1:5000). The loading control, GAPDH, was detected using mAb374 (Millipore, 1:10000). CPSF-160 was detected using a rabbit polyclonal serum (Wilusz Laboratory-made) (1:10000). PABPN1 was detected using rabbit anti-PABPN1 sera (1:10000) generously provided by Dr. David G. Bear (University of New Mexico). PAPOLA was detected using rabbit polyclonal antibodies (Abcam: ab72492, 1:1000). HRP-conjugated Goat anti-mouse IgG (Santa Cruz Biotechnology, sc-2005, 1:20000) was used to detect murine primary antibodies and HRP conjugated

goat anti-rabbit IgG (BIO RAD, 170-6515, 1:20000) was used to detect primary rabbit antibodies. Western blot was visualized by using SuperSignal® West Pico Chemiluminescent Substrate (Thermo SCIENTIFIC, 34080) according to the company's protocol. Results were visualized by CCD camera (BioRAD Versadoc) or by exposure to film.

UV Cross Linking and Immunoprecipitations

In a typical reaction, 50–200 fmol of ³²P-UTP-labeled RNA was incubated in the nuclear extract-based polyadenylation system for the time indicated. Reaction mixtures (10.5 µL) were transferred to MicroWell Mini Trays (Nunc: 439225), placed 11 cm away from UV source and irradiated for 2400 micro joules or 6 min on ice using a UV Stratalinker 2400 (Stratagene). RNase A was added to a final concentration of 1 mg/mL, incubated at 37°C for 15 min and reaction mixtures were incubated at 95°C for 10 min in SDS loading dye. Cross-linked proteins were separated by SDS-PAGE and visualized by phosphorimaging. In cross linking and immunoprecipitation experiments, after RNase treatment, reaction mixtures were diluted to 400 µL with NET2 buffer (noted above) and centrifuged at 16100xg for 10 min at 4°C. The supernatant was then incubated with 10 µL NPM antibody (Santa Cruz, sc-5564) for 1 hr at 4°C. Protein–antibody complexes were purified using 20 µL 25% Pansorbin cells as described above and washed vigorously four times in NET2 buffer. The precipitated proteins were then recovered by boiling in SDS-loading dye prior to separation on an SDS acrylamide gel.

LLM-PAT Poly(A) Tail Assays

Linker ligation-mediated poly(A) tail (LLM-PAT) assays were performed as described (Garneau et al., 2008). Total RNA was prepared from wild type, pLKO1 Control and NPM KD HeLa cell lines using TRIzol reagent (Invitrogen). The A0 marker was

generated by hybridizing 2 µg total RNA with 2 µg oligo d(T) (Integrated DNA Technologies), followed by RNase H (Fermentas) digestion (as described for the RNase Northern above). Both total RNA and RNase H/d(T) treated RNA were ligated to a 5' pppRNA linker (5'-rApppUUUAACCGCGAAUCCAG/3'ddC) by T4 RNA ligase (Home-made) at 16°C for 2 hrs in 50 mM Tris-HCl, pH 7.5, 10 mM MgCl₂, 20 mM DTT, 0.1 mg/mL bovine serum albumin. The ligated RNA was then reverse transcribed using 2.5 mM of a primer specific to the RNA linker in the reverse transcription buffer (50 mM Tris-HCl pH 8.3, 500 µM dNTPs, 3 mM MgCl₂, 50 mM KCl, 40 U RNase inhibitor (Fermentas, Ribolock), 1 µL reverse transcriptase (Promega, ImProm-II™ Reverse Transcriptase) and 10 mM DTT). The resulting cDNA was then amplified by PCR using the 3' primer and one of the following RNA-specific 5' primers: β-actin, rps5, hnRNP H, PAC or 25S rRNA. PCR products were separated on a 5% non-denaturing polyacrylamide gel. Following electrophoresis, the gel was soaked in TBE buffer (45 mM Tris, 45 mM Boric acid, 1 mM EDTA) with 0.001% ethidium bromide and visualized using a Typhoon Trio imager.

LLM-Pat assays			
Name	Sequence	Expected Size	Accession Number
RNA Linker	CTGGAATTCGCGGT	N/A	N/A
β-actin	GAATGATGAGCCTTCGTGCC	176 & Poly(A)	NM_001101.3
rps5	CTGAGTGCCTGGCAGATGAC	179 & Poly(A)	NM_001009.3
hnRNP H	TGAGACGCAATACCAATACT	171 & Poly(A)	NM_005520.2
PAC	CAGTGTGGAAAATCTCTAGC	160 & Poly(A)	N/A
25S rRNA	CTCCCTCGCTGCGATCTAT	69 & Poly(A)	NR_003287.2
SVL	GAATTTATTTGTAACCATTAT	59 & Poly(A)	NC_001669.1

Table 6: List of Oligonucleotides used for LLM-Pat assays

Immunofluorescence and FISH Assays

All procedures were performed at room temperature unless otherwise noted. Adherent cells were grown on cover slips and fixed for 10 min in 1% paraformaldehyde in PBS, for 10 min, in methanol and for 10 min in 70% ethanol. Cells were rehydrated for 5 min in 1 M Tris pH 8.0, followed by 1 hr incubation at 37°C with oligo d(T)-Cy3 probe (1:5000) or

an Alexa 647-rRNA probe (1:10000) (5'-ATCAGAGTAGTGGTATTTTC; IDT) in hybridization buffer (1 mg/mL yeast tRNA, 0.005% BSA, 10% dextran sulfate, 25% formamide and 2x SSC). Coverslips were washed once in 4x SSC and twice in 2x SSC. Mouse anti-NPM antibodies (Santa Cruz: SC-32256, 1:100), rabbit anti-PARN serum (Bioo Scientific, 1:500) and mouse anti- α -tubulin antibodies (Sigma-Aldrich, 1:500) were incubated for 2 hrs in the dark. Coverslips were washed three times with 2x SSC. Cy2-goat anti-mouse antibodies (Jackson ImmunoResearch, 1:3000) and Cy5-goat anti-rabbit antibodies (GE Healthcare life Sciences, 1:1000) were added for 1 hr in the dark. Coverslips were then washed four times with 2x SSC and mounted on ethanol-cleaned microscope slides with Prolong Gold antifade mounting reagent with DAPI (Invitrogen) and stored at 4°C until visualization. Images were obtained using a Zeiss Laser Scanning Axiovert Confocal microscope at foothills campus or a Nikon inverted epifluorescence microscope at the main CSU campus.

Analysis of mRNPs in HeLa Cells

Routinely $\sim 5.5 \times 10^6$ HeLa cells were used for each experiment. HeLa cells were grown on 10 cm² dishes overnight, washed three times with PBS (Cellgro: 21-040-CV), resuspended in a 0.1% formaldehyde solution in PBS, and incubated for 15 min at room temperature. The reaction was quenched by using 0.25 M glycine and kept at room temperature for 5 min. Fixed cells were washed with PBS and scraped off of dishes in 500 μ L RIPA buffer (50 mM Tris-HCl pH 7.5, 1% (v/v) NP-40, 0.5% (w/v) sodium deoxycholate, 0.05% (w/v) SDS, 1 mM EDTA, and 150 mM NaCl) using a cell lifter (Corning Incorporated). Cells were disrupted by sonication on ice for 3 x 3 sec with 1 min breaks and insoluble materials were removed via centrifugation at 16100xg for 10 min at 4°C. 200 μ L aliquots of supernatant each received 10 μ L anti-NPM antibodies (Santa Cruz, sc-5564) or 20 μ L control IgG (Santa Cruz: sc-2027) antibodies and were rocked

at 4°C for 2 hrs. Antibody-bound complexes were recovered using 20 µL 25% Pansorbin cells and washed seven times with RIPA buffer containing 1 M urea. Formaldehyde cross links were reversed by heating at 70°C for 45 min in a water bath while being mixed at 800 rpm (Eppendorf thermomixer). Total input samples were also heated along with the immunoprecipitated samples. Isolated RNAs were analyzed by RT-PCR to assess the amount of an individual RNA that was precipitated using the following primer sets: Schnurri-2, PAPOLG, H2A, MC4R, JunB, hnRNP H, CFIm (CPSF6), ActB, U1 snRNA, U3 snRNA and U4A snoRNA (See Table below for sequences).

RT-PCR			
Name	Sequence	Expected Size	Accession Number
β-actin F	GATGAGATTGGCATGGCTTT	100	NM_001101.3
β-actin R	CACCTTCACCGTTCCAGTTT		
CFIm F	TGAACCTGTAAGGATTCATGG	200	NM_007007.2
CFIm R	TGCACATCATAATGGCCAAA		
hnRNP H F	GGGAAAATTTGAGACGCAAT	135	NM_005520.2
hnRNP H R	GACAAGTTTCACTTAGCGCAAT		
JUNB F	TTAACAGGGAGGGGAAGAGG	140	NM_002229.2
JUNB R	TGCGTGTTCCTTTCCACAG		
MC4R F	GATTACCTTGACCATCCTGA	119	NG_016441.1
MC4R R	AGTGAGACATGAAGCACACA		
PAPOLG F	TTTCCAGATTGGCACATGAA	154	NM_022894.3
PAPOLG R	GCATTTCAAAGGCCTCCAT		
Schnurri-2 F	GGGAAAAGGAGATGGAGACC	192	NM_006734.3
Schnurri-2 R	CAGACATCCTCCCACGAGTT		
H2A F	AGCTCAACAAGCTTCTGGGCAA	~150	H2A family
H2A R	TTGTGGTGGCTCTCGGTCTTCTT		
U1 snRNA F	CTTACCTGGCAGGGGAGATA	119	NR_004430.2
U1 snRNA R	GCAGTCGAGTTTCCACATT		
U3 snoRNA F	CGAAAACCACGAGGAAGAGA	114	NR_006880.1
U3 snoRNA R	CAATACGGGGAGAAGAACGA		
U4A snRNA F	TGGCAGTATCGTAGCCAATG	117	NR_003925.1
U4A snRNA R	CTGTCAAAAATTGCCAATGC		

Table 7: List of oligonucleotides used to detect mRNA by RT-PCR assays

Affinity purification

Biotinylated SVL+25 RNA was designed and synthesized by IDT: 5'- biotin-internal spacer (C18)-GAAUUUAUUUGUAACCAUUAUAAGCUGCAAUAAACAAGUU. The biotin RNA was incubated in 3 separate 1.5 mL microcentrifuge tubes in our *in vitro* polyadenylation assays for the time indicated. Each tube contains 3% (w/v) polyvinyl alcohol (PVA), 1 mM ATP, 20 mM phosphocreatine, 12 mM HEPES pH 7.9, 12% (v/v) glycerol, 60 mM KCl, 0.12 mM EDTA, 0.3 mM DTT, 60% (v/v) nuclear extract and 40 fmole biotin RNA in 100 μ L reaction – 60 μ L of extract was used, which is approximately 600 μ g protein. The concentration of the biotin RNA used was chosen to deliver the maximal polyadenylation reaction to the RNA, otherwise too much biotin RNA inhibits the polyadenylation reaction (data not shown). For LLM-Pat assay to measure a poly(A) tail, at the time indicated the reaction was phenol-chloroform extracted and precipitated by ethanol with glycogen as a carrier. Precipitated RNA was processed for LLM-Pat assay using an SVL-specific primer. For protein purification, a control reaction was also performed without RNA substrate in the *in vitro* polyadenylation assays. Following the polyadenylation assays, samples were centrifuged at 16100xg for 10 min at 4°C. Supernatants were then incubated with 50 μ L 50% streptavidin beads for 20 min at 4°C on a rocker platform. The beads were spun down at 16100xg for 30 sec and washed three times with wash buffer (20 mM HEPES-HCl pH 7.5, 100 mM KCl and 0.2 mM MgCl₂ and 1 mM DTT). RNA-binding proteins were released by boiling the streptavidin beads in SDS sample buffer (2% (w/v) SDS, 50 mM Tris-HCl pH 6.8, 5% (v/v) DTT, 10% (v/v) glycerol and 0.01% (w/v) bromophenol blue) for 10 min and separated on a 15% SDS polyacrylamide gel. Protein samples were visualized by silver-staining (see below).

Silver-staining

SDS-PAGE gels were washed twice with plenty of water for 5 min at room temperature while being rocked. They were rocked for 20 min in fix solution (50% methanol, 5% acetate, 45% Millipore water), for 20 min in 50% methanol solution and washed twice with plenty of Millipore water for 10 min. Gels were soaked in 0.02% (w/v) sodium thiosulfate for 1 min with gentle shaking by hand and washed twice with plenty of water for 1 min. Gels were then soaked in 0.1% (w/v) AgNO_3 for 20 min while rocked and covered to shield gels from light and washed twice with plenty of water for 1 min. Protein bands were visualized by incubating gels in the developing solution (2% (w/v) sodium bicarbonate with 0.004% formaldehyde). Developing solution was changed for fresh as soon as a corner of gels turned yellow. The developing was stopped by 10% acetic acid.

Preparation of RNA samples and microarray hybridization

HeLa cells were transfected with either empty LKO control or NPM-specific shRNA vectors and total RNA was isolated. Total RNA was used for qRT-PCR to confirm the KD in NPM mRNA levels. Whole cell lysates were used to confirm the transient NPM KD by western blot. 10 μg of total RNA was separated on formaldehyde 1% agarose gels to ensure the RNA was intact. Following the quality control, 500 ng of total RNA was sent to the Rocky Mountain Research Center for Excellence (RMRCE) Genomics and Proteomics Core and was used to generate labeled cDNA fragments for hybridization to a Human Gene 1.0 ST Array (Affymetrix).

Analysis of microarray data (Gene 1.0 array)

Probe sets were normalized by utilizing GC-bin method for background correction and RMA (Robust Multi-array Analysis) normalization was applied by Affymetrix Power Tools (APT). Transcripts whose probe sets with detection above background (DABG) P-value < 0.05 in at least 2 out of 3 replicates were considered expressed and used for subsequent analyses.

Analysis of expression change using microarray data

To identify the genes whose expressions are significantly changed in nucleoplasmin knock down HeLa cells compared to control LKO HeLa cells, genes were selected when they 1) have fold change greater than 1.2 or less than 0.8 for up or down-regulation, 2) have p-value <0.05 (T-test)

Analysis of Gene Ontology (GO)

To identify gene functional groups that are significantly regulated, the NCBI Gene database was used to map genes to Gene Ontology (GO) biological process terms. GO terms for the genes encoding significantly up-regulated and down-regulated transcripts were examined. Fisher's exact test was performed to identify significantly enriched GO terms for selected genes. GO terms containing more than 500 genes were discarded, as they are too generic.

References

- Ahn, J. Y., X. Liu, D. Cheng, J. Peng, P. K. Chan, P. A. Wade, and K. Ye. 2005. Nucleophosmin/B23, a nuclear PI(3,4,5)P(3) receptor, mediates the antiapoptotic actions of NGF by inhibiting CAD. *Mol Cell*. 18:435-45.
- Aravind, L. 1998. An evolutionary classification of the metallo-b-lactamase fold proteins. *In Silico Biol*. 1:69-91.
- Arhin, G. K., M. Boots, P. S. Bagga, C. Milcarek, and J. Wilusz. 2002. Downstream sequence elements with different affinities for the hnRNP H/H' protein influence the processing efficiency of mammalian polyadenylation signals. *Nucleic Acids Res*. 30:1842-50.
- Bagga, P. S., L. P. Ford, F. Chen, J. Wilusz. 1995. The G-rich auxiliary downstream element has distinct sequence and position requirements and mediates efficient 3' end pre-mRNA processing through a trans-acting factor. *Nucleic Acids Res*. 23:1625-31.
- Bai, Y., T. C. Auperin, C. Y. Chou, G. G. Chang, J. L. Manley, and L. Tong. 2007. Crystal structure of murine CstF-77: dimeric association and implications for polyadenylation of mRNA precursors. *Mol Cell*. 25:863-75.
- Barabino, S. M., W. Hübner, A. Jenny, L. Minvielle-Sebastia, and W. Keller. 1997. The 30-kD subunit of mammalian cleavage and polyadenylation specificity factor and its yeast homolog are RNA-binding zinc finger proteins. *Genes Dev*. 11:1703-16.
- Barabino, S. M., M. Ohnacker, and W. Keller. 2000. Distinct roles of two Yth1p domains in 3'-end cleavage and polyadenylation of yeast pre-mRNAs. *EMBO J*. 19:3778-87.
- Beaudoing, E., S. Freier, J. R. Wyatt, J. M. Claverie, and D. Gautheret. 2000. Patterns of variant polyadenylation signal usage in human genes. *Genome Res*. 10:1001-1010.
- Bienroth, S., W. Keller, and E. Wahle. 1993. Assembly of a processive messenger RNA polyadenylation complex. *EMBO J*. 12:585-594.
- Brennan, C. M., I. E. Gallouzi, and J. A. Steitz. 2000. Protein ligands to HuR modulate its interaction with target mRNAs in vivo. *J. Cell Biol*. 151:1-14.
- Brown, C. E., and A. B. Sachs. 1998. Poly(A) tail length control in *Saccharomyces cerevisiae* occurs by message-specific deadenylation. *Mol. Cell Biol*. 18:6548-6559
- Brady, S. N., L. B. Maggi Jr, C. L. Winkeler, E. A. Toso, A. S. Gwinn, C. L. Pelletier, and J. D. Weber. 2009. Nucleophosmin protein expression level, but not threonine 198 phosphorylation, is essential in growth and proliferation. *Oncogene* 28:3209-20.
- Butler, J. S. and T. Platt. 1998. RNA processing generates the mature 3' end of yeast CYC1 messenger RNA in vitro. *Science* 242:1270-1274.

- Callebaut, I., D. Moshous, J. P. Mornon, and J. P. de Villartay. 2002. Metallo-beta-lactamase fold within nucleic acids processing enzymes: the beta-CASP family. *Nucleic Acids Res.* 30:3592-601.
- Cao, G. J., and N. Sarkar. 1992. Stationary phase-specific mRNAs in *Escherichia coli* are polyadenylated. *Proc Natl Acad Sci USA.* 89:10380–10384.
- Cevher, M. A., X. Zhang, S. Fernandez, S. Kim, J. Baquero, P. Nilsson, S. Lee, A. Virtanen, and F. E. Kleiman. 2010. Nuclear deadenylation/polyadenylation factors regulate 3' processing in response to DNA damage. *EMBO J.* 29:1674-87.
- Chen, F., C. C. MacDonald, and J. Wilusz. 1995. Cleavage site determinants in the mammalian polyadenylation signal. *Nucleic Acids Res.* 23:2614-2620
- Cheng, H., K. Dufu, C. S. Lee, J. L. Hsu, A. Dias, and R. Reed. 2006. Human mRNA export machinery recruited to the 5' end of mRNA. *Cell* 127:1389-400.
- Chou, Z. F., F. Chen, and J. Wilusz. 1994. Sequence and position requirements for uridylate-rich downstream elements of polyadenylation signals. *Nucleic Acids Res.* 22:2525-2531
- Chrislip, K. M., J. A. Hengst-Zhang, S. T. Jacob. 1991. Polyadenylation of SV40 late pre-mRNA is dependent on phosphorylation of an essential component associated with the 3' end processing machinery. *Gene Expr.* 1:197-206.
- Christofori, G., and W. Keller. 1988. 3' cleavage and polyadenylation of mRNA precursors in vitro requires a poly(A) polymerase, a cleavage factor, and a snRNP. *Cell* 54:875-889
- Cohen, S. N. 1995. Surprise at the 3' end of prokaryotic RNAs. *Cell* 80:829–832.
- Colombo, E., J. C. Marine, D. Danovi, B. Falini, and P. G. Pelicci. 2002. Nucleophosmin regulates the stability and transcriptional activity of p53. *Nat Cell Biol.* 4:529-33.
- Cooke, C., and J. C. Alwine. 1996. The cap and the 3' splice site similarly affect polyadenylation efficiency. *Mol Cell Biol.* 16:2579-84.
- Cooke, D., and J. C. Alwine. 2002. Characterization of specific protein-RNA complexes associated with the coupling of polyadenylation and last-intron removal. *Mol Cell Biol.* 13:4579-86.
- Cory, J. G., J. Crumley, and D. S. Wilkinson. 1976. Evidence for role of purine nucleoside phosphorylase in sensitivity of Novikoff hepatoma cells to 5-fluorouracil. *Adv Enzyme Regul.* 15:153-66.
- Crockett, D. K., Z. Lin, K. S. Elenitoba-Johnson, and M. S. Lim. 2004. Identification of NPM-ALK interacting proteins by tandem mass spectrometry. *Oncogene* 23:2617-29.
- Culjkovic, B., I. Topisirovic, L. Skrabanek, M. Ruiz-Gutierrez, and K. L. Borden. 2006. eIF4E is a central node of an RNA regulon that governs cellular proliferation. *J. Cell Biol.* 175:415-426.
- Dalziel, M., N. M. Nunes, and A. Furger. 2007. Two G-rich regulatory elements located adjacent to and 440 nucleotides downstream of the core poly(A) site of the intronless

- melanocortin receptor 1 gene are critical for efficient 3' end processing. *Mol Cell Biol.* 27:1568-80.
- de Vries, H., U. Rügsegger, W. Hübner, A. Friedlein, H. Langen, and W. Keller. 2000. Human pre-mRNA cleavage factor II(m) contains homologs of yeast proteins and bridges two other cleavage factors. *EMBO J.* 19:5895-904.
- Dhar, S. K., B. C. Lynn, C. Daosukho, and D. K. St Clair. 2004. Identification of nucleophosmin as an NF-kappaB co-activator for the induction of the human SOD2 gene. *J Biol Chem.* 279:28209-19.
- Dheur, S., K. R. Nykamp, N. Viphakone, M. S. Swanson, and L. Minvielle-Sebastia. 2005. Yeast mRNA Poly(A) tail length control can be reconstituted in vitro in the absence of Pab1p-dependent Poly(A) nuclease activity. *J Biol Chem.* 280:24532-8.
- Doyle, G. A., N. A. Betz, P. F. Leeds, A. J. Fleisig, R. D. Prokipcak, and J. Ross. 1998. The c-myc coding region determinant-binding protein: a member of a family of KH domain RNA-binding proteins. *Nucleic Acids Res.* 26:5036-5044.
- Dreyfus, M., and P. Régnier. 2002. The poly(A) tail of mRNAs: bodyguard in eukaryotes, scavenger in bacteria. *Cell* 111(5):611-3.
- Gallagher, S. J., R. F. Kefford, and H. Rizos. 2006. The ARF tumor suppressor. *Int J Biochem Cell Biol.* 38:1637-41.
- Garneau, N. L., J. Wilusz, and C. J. Wilusz. 2007. The highways and byways of mRNA decay. *Nat Rev Mol Cell Biol.* 8:113-26.
- Gao, M., D. T. Fritz, L. P. Ford, and J. Wilusz, 2000. Interaction between a poly(A)-specific ribonuclease and the 5' cap influences mRNA deadenylation rates in vitro. *Mol. Cell.* 5:479-488.
- Gilmartin, G. M., and J. R. Nevins. 1989. An ordered pathway of assembly of components required for polyadenylation site recognition and processing. *Genes Dev.* 3:2180-2189
- Gjerset, R. 2006. DNA damage, p14ARF, Nucleophosmin (NPM/B23) and cancer. *J Mol Hist.* 37:239-251
- Greenhalgh, D. L., and J. H. Parish. 1990. Effect of 5-fluorouracil combination therapy on RNA processing in human colonic carcinoma cells. *Br J Cancer.* 3:415-9.
- Grisendi, S., R. Bernardi, M. Rossi, K. Cheng, L. Khandker, K. Manova, and P. P. Pandolfi. 2005. Role of nucleophosmin in embryonic development and tumorigenesis. *Nature* 437:147-53.
- Grisendi, S., C. Mecucci, B. Falini, and P. P. Pandolfi. 2006. Nucleophosmin and cancer. *Nat Rev Cancer.* 6:493-505.
- Gu, H., J. Das Gupta, and D. R. Schoenberg. 1999. The poly(A)-limiting element is a conserved cis-acting sequence that regulates poly(A) tail length on nuclear pre-mRNAs. *Proc Natl Acad Sci USA.* 96:8943-8.

- Gu, M., and C. D. Lima. 2005. Processing the message: structural insights into capping and decapping mRNA. *Curr Opin Struct Biol.* 15:99-106.
- Hachet, O., and A. Ephrussi. 2004. Splicing of oskar RNA in the nucleus is coupled to its cytoplasmic localization. *Nature* 428:959-63.
- Hector, R. E., K. R. Nykamp, S. Dheur, J. T. Anderson, P. J. Non, C. R. Urbinati, S. M. Wilson, L. Minvielle-Sebastia, and M. S. Swanson. 2002 Dual requirement for yeast hnRNP Nab2p in mRNA poly(A) tail length control and nuclear export. *EMBO J.* 21:1800-10
- Heo, I., C. Joo, J. Cho, M. Ha, J. Han, and V. N. Kim. 2008. Lin28 mediates the terminal uridylation of let-7 precursor MicroRNA. *Mol Cell.* 32:276-84.
- Higuchi, Y., K. Kita, H. Nakanishi, X. L. Wang, S. Sugaya, H. Tanzawa, H. Yamamori, K. Sugita, A. Yamaura, and N. Suzuki. 1998. Search for genes involved in UV-resistance in human cells by mRNA differential display: increased transcriptional expression of nucleophosmin and T-plastin genes in association with the resistance. *Biochem Biophys Res Commun.* 248:597-602
- Hilleren, P., and R. Parker. 2001. Defects in the mRNA export factors Rat7p, Gle1p, Mex67p and Rat8p cause hyperadenylation during 3'-end formation of nascent transcripts. *RNA.* 7:753-64.
- Hirose, Y., and J. L. Manley. 1998. RNA polymerase II is an essential mRNA polyadenylation factor. *Nature* 395:93-6.
- Hu, J., C. S. Lutz, J. Wilusz, and B. Tian. 2005. Bioinformatic identification of candidate cis-regulatory elements involved in human mRNA polyadenylation. *RNA* 11:1485-93.
- Huang, Y., and G. G. Carmichael. 1996. Role of polyadenylation in nucleocytoplasmic transport of mRNA. *Mol Cell Biol.* 16:1534-42.
- Huang, Y., K. M. Wimler, and G. G. Carmichael. 1999. Intronless mRNA transport elements may affect multiple steps of pre-mRNA processing. *EMBO J.* 18:1642-52.
- Iglesias, N., and F. Stutz. 2008. Regulation of mRNP dynamics along the export pathway. *FEBS Lett.* 582:1987-96.
- Ji, Z., and B. Tian. 2009. Reprogramming of 3' untranslated regions of mRNAs by alternative polyadenylation in generation of pluripotent stem cells from different cell types. *PLoS One.* 4:e8419.
- Jensen, T. H., K. Patricio, T. McCarthy, and M. Rosbash. 2001. A block to mRNA nuclear export in *S. cerevisiae* leads to hyperadenylation of transcripts that accumulate at the site of transcription. *Mol Cell.* 7:887-98.
- Johnson, S. A., G. Cubberley, and D. L. Bentley. 2009. Cotranscriptional recruitment of the mRNA export factor Yra1 by direct interaction with the 3' end processing factor Pcf11. *Mol Cell.* 2009 33:215-256.
- Kammler, S., S. Lykke-Andersen, and T. H. Jensen. 2008. The RNA exosome component hRrp6 is a target for 5-fluorouracil in human cells. *Mol Cancer Res.* 6:990-5.

Kapp, L. D., and J. R. Lorsch. 2004. The molecular mechanics of eukaryotic translation. *Annu Rev Biochem.* 73:657-704.

Kaufmann, I., G. Martin, A. Friedlein, H. Langen, and W. Keller. 2004. Human Fip1 is a subunit of CPSF that binds to U-rich RNA elements and stimulates poly(A) polymerase. *EMBO J.* 23:616-26.

Keller, R. W., U. Kühn, M. Aragon, L. Bornikova, E. Wahle, and D. G. Bear. 2000. The nuclear poly(A) binding protein, PABP2, forms an oligomeric particle covering the poly(A) tail. *J Mol Biol.* 297:569-83

Keller, W., S. Bienroth, K. M. Lang, and G. Christofori. 1991. Cleavage and polyadenylation factor CPF specifically interacts with the pre-mRNA 3' processing signal AAUAAA. *EMBO J.* 10:4241-4249.

Kelly, S. M., S. A. Pabit, C. M. Kitchen, P. Guo, K. A. Marfatia, T. J. Murphy, A. H. Corbett, and K. M. Berland. 2007. Recognition of polyadenosine RNA by zinc finger proteins. *Proc Natl Acad Sci USA.* 104:12306-11.

Kerwitz, Y., U. Kühn, H. Lilie, A. Knoth, T. Scheuermann, H. Friedrich, E. Schwarz, and E. Wahle. 2003. Stimulation of poly(A) polymerase through a direct interaction with the nuclear poly(A) binding protein allosterically regulated by RNA. *EMBO J.* 22:3705-14.

Kleiman, F. E., and J. L. Manley. 1999. Functional interaction of BRCA1-associated BARD1 with polyadenylation factor CstF-50. *Science* 285:1576-9.

Kubo, T., T. Wada, Y. Yamaguchi, A. Shimizu, and H. Handa. 2006. Knock-down of 25 kDa subunit of cleavage factor Im in HeLa cells alters alternative polyadenylation within 3'-UTRs. *Nucleic Acids Res.* 34:6264-71.

Kühn, U., M. Gündel, A. Knoth, Y. Kerwitz, S. Rüdell, and E. Wahle. 2009. Poly(A) tail length is controlled by the nuclear poly(A)-binding protein regulating the interaction between poly(A) polymerase and the cleavage and polyadenylation specificity factor. *J Biol Chem.* 284:22803-14.

LaCava, J., J. Houseley, C. Saveanu, E. Petfalski, E. Thompson, A. Jacquier, and D. Tollervey. 2005. RNA degradation by the exosome is promoted by a nuclear polyadenylation complex. *Cell* 121:713-24.

Latonen, L., and M. Laiho. 2005. Cellular UV damage responses--functions of tumor suppressor p53. *Biochim Biophys Acta.* 1755:71-89.

Le Hir, H., D. Gatfield, E. Izaurralde, and M. J. Moore. 2001. The exon-exon junction complex provides a binding platform for factors involved in mRNA export and nonsense-mediated mRNA decay. *EMBO J.* 20:4987-97.

Le Hir, H., A. Nott, and M. J. Moore. 2003. How introns influence and enhance eukaryotic gene expression. *Trends Biochem Sci.* 28:215-20.

Le Hir, H., E. Izaurralde, L. E. Maquat, and M. J. Moore. 2000. The spliceosome deposits multiple proteins 20-24 nucleotides upstream of mRNA exon-exon junctions. *EMBO J.* 19:6860-6869.

- Li, Z., and S. R. Hann. 2009. The Myc-nucleophosmin-ARF network: a complex web unveiled. *Cell Cycle*. 8:2703-7.
- Libri, D., K. Dower, J. Boulay, R. Thomsen, M. Rosbash, and T. H. Jensen. 2002. Interactions between mRNA export commitment, 3'-end quality control, and nuclear degradation. *Mol Cell Biol*. 22:8254-66.
- Licatalosi, D. D., G. Geiger, M. Minet, S. Schroeder, K. Cilli, J. B. McNeil, and D. L. Bentley. 2002. Functional interaction of yeast pre-mRNA 3' end processing factors with RNA polymerase II. *Mol Cell*. 9:1101-11.
- Lindstrom, M. S. 2011. NPM1/B23: A Multifunctional Chaperone in Ribosome Biogenesis and Chromatin Remodeling. *Biochem Res Int*. 2011:195209.
- Lisitsky, I., P. Klaff, and G. Schuster. 1996. Addition of destabilizing poly (A)-rich sequences to endonuclease cleavage sites during the degradation of chloroplast mRNA. *Proc Natl Acad Sci USA*. 93:13398-403.
- Lum, P. Y., C. D. Armour, S. B. Stepaniants, G. Cavet, M. K. Wolf, J. S. Butler, J. C. Hinshaw, P. Garnier, G. D. Prestwich, A. Leonardson, P. Garrett-Engele, C. M. Rush, M. Bard, G. Schimmack, J. W. Phillips, C. J. Roberts, and D. D. Shoemaker. 2004. Discovering modes of action for therapeutic compounds using a genome-wide screen of yeast heterozygotes. *Cell* 116:121-37.
- Long, J. C., and J. F. Caceres. 2009. The SR protein family of splicing factors: master regulators of gene expression. *Biochem J*. 417:15-27.
- Luna, R., H. Gaillard, C. González-Aguilera, and A. Aguilera. 2008. Biogenesis of mRNPs: integrating different processes in the eukaryotic nucleus. *Chromosoma*. 117:319-31.
- Luo, W., and D. Bentley. 2004. A ribonucleolytic rat torpedo RNA polymerase II. *Cell* 119:911-4.
- Maggi Jr, L. B., M. Kuchenruether, D. Y. Dadey, R. M. Schwoppe, S. Grisendi, R. R. Twonsend, P. P. Pandolfi, and J. D. Weber. 2008. Nucleophosmin serves as a rate-limiting nuclear export chaperone for the Mammalian ribosome. *Mol Cell Biol*. 28:7050-65.
- Mandel, C. R., S. Kaneko, H. Zhang, D. Gebauer, V. Vethantham, J. L. Manley, L. Tong. 2006. Polyadenylation factor CPSF-73 is the pre-mRNA 3'-end-processing endonuclease. *Nature* 444:953-6.
- Mapendano, C. K., S. Lykke-Andersen, J. Kjems, E. Bertrand, and T. H. Jensen. 2010. Crosstalk between mRNA 3' end processing and transcription initiation. *Mol. Cell*. 40:410-22
- Mayr, C., and D. P. Bartel. 2009. Widespread shortening of 3'UTRs by alternative cleavage and polyadenylation activates oncogenes in cancer cells. *Cell* 138:673-84.
- McCracken, S., N. Fong, E. Rosonina, K. Yankulov, G. Brothers, D. Siderovski, A. Hessel, S. Foster, S. Shuman, and D. L. Bentley. 1997a. 5'-Capping enzymes are

targeted to pre-mRNA by binding to the phosphorylated carboxy-terminal domain of RNA polymerase II. *Genes Dev.* 11:3306-18.

McCracken, S., N. Fong, K. Yankulov, S. Ballantyne, G. Pan, J. Greenblatt, S. D. Patterson, M. Wickens, and D. L. Bentley. 1997b. The C-terminal domain of RNA polymerase II couples mRNA processing to transcription. *Nature* 385:357-61.

Meinhart, A., T. Kamenski, S. Hoepfner, S. Baumli, and P. Cramer. 2005. A structural perspective of CTD function. *Genes Dev.* 19:1401-15.

Millevoi, S., and S. Vagner. 2010. Molecular mechanisms of eukaryotic pre-mRNA 3' end processing regulation. *Nucleic Acids Res.* 9:2757-74.

Moreira, A., Y. Takagaki, S. Brackenridge, M. Wollerton, J. L. Manley, and N. J. Proudfoot. 1998. The upstream sequence element of the C2 complement poly(A) signal activates mRNA 3' end formation by two distinct mechanisms. *Genes Dev.* 12:2522-34.

Morris, S. W., M. N. Kirsten, M. B. Valentine, K. G. Dittmer, D. N. Shapiro, D. L. Saltman, and A. T. Look. 1994. Fusion of a kinase gene, *ALK*, to a nucleolar protein gene, *NPM*, in non-Hodgkin's lymphoma. *Science* 263:1281-84

Morrison, A. L. 2007. The role of a unique polyadenylation element and novel RNA-binding proteins in post-transcriptional control of gene expression. Masters Thesis. Colorado State University.

Mullen, T. E., and W. F. Marzluff. 2008. Degradation of histone mRNA requires oligouridylation followed by decapping and simultaneous degradation of the mRNA both 5' to 3' and 3' to 5'. *Genes Dev.* 22:50-65.

Murthy, K. G. K., and J. L. Manley. 1992. Characterization of the multisubunit cleavage-polyadenylation specificity factor from calf thymus. *J Biol Chem.* 267:14804-11.

Murthy, K. G. K., and J. L. Manley. 1995. The 160 kD subunit of human cleavage-polyadenylation specificity factor coordinates pre-mRNA 3' end formation. *Genes Dev.* 9:2672-83.

Nakagawa, M., Y. Kameoka, and R. Suzuki. 2005. Nucleophosmin in acute myelogenous leukemia. *N Engl J Med.* 352:1819-20

Neilson, J. R., and R. Sandberg. 2010. Heterogeneity in mammalian RNA 3' end formation. *Exp Cell Res.* 316:1357-64.

Nielsen, J., J. Christiansen, J. Lykke-Andersen, A. H. Johnsen, U. M. Wewer, and F. C. Nielsen. 1999. A family of insulin-like growth factor II mRNA-binding proteins represses translation in late development. *Mol Cell Biol.* 19:1262-70.

Noubissi, F. K., I. Elcheva, N. Bhatia, A. Shakoory, A. Ougolkov, J. Liu, T. Minamoto, L. Ross, S. Y. Fuchs, and V. S. Spiegelman. 2006. CRD-BP mediates stabilization of betaTrCP1 and c-myc mRNA in response to beta-catenin signalling. *Nature* 441:898-901.

Nunes, N. M., W. Li, B. Tian, and A. Furger. 2010. A functional human Poly(A) site requires only a potent DSE and an A-rich upstream sequence. *EMBO J.* 29:1523-36.

- Okuwaki, M., K. Matsumoto, M. Tsujimoto, and K. Nagata. 2001. Function of nucleophosmin/B23, a nucleolar acidic protein, as a histone chaperone. *FEBS Lett.* 506:272-6.
- Ozsolak, F., P. Kapranov, S. Foissac, S. W. Kim, E. Fishilevich, A. P. Monaghan, B. John, and P. M. Milos. 2010. Comprehensive polyadenylation site maps in yeast and human reveal pervasive alternative polyadenylation. *Cell* 143:1018-29.
- Palaniswamy, V., K. C. Moraes, C. J. Wilusz, and J. Wilusz. 2006. Nucleophosmin is selectively deposited on mRNA during polyadenylation. *Nat Struct Mol Biol.* 13:429-35.
- Pianta, A., C. Puppini, A. Franzoni, D. Fabbro, C. Di Loreto, S. Bulotta, M. Deganuto, I. Paron, G. Tell, E. Puzeddu, S. Filetti, D. Russo, and G. Damante. 2010. Nucleophosmin is overexpressed in thyroid tumors. *Biochem Biophys Res Commun.* 397:499-504.
- Prechtel, A. T., J. Chemnitz, S. Schirmer, C. Ehlers, I. Langbein-Detsch, J. Stulke, M. C. Dabauvalle, R. H. Kehlenbach, and J. Hauber. 2006. Expression of CD83 is regulated by HuR via a novel cis-acting coding region RNA element. *J Biol Chem.* 281:10912-25.
- Proudfoot, N. J., and G. G. Brownlee. 1976. 3' non-coding region sequences in eukaryotic messenger RNA. *Nature* 263:211-4.
- Qu, X., S. Lykke-Anderson, T. Nasser, C. Sagues, E. Bertrand, T. H. Jensen, and C. Moore. 2009. Assembly of an export-competent mRNPs is needed for efficient release of the 3'-end processing complex after polyadenylation. *Mol Cell Biol.* 29:5327-38.
- Quentmeier, H., M. P. Martelli, W. G. Dirks, N. Bolli, A. Liso, R. A. Macleod, I. Nicoletti, R. Mannucci, A. Pucciarini, B. Bigerna, M. F. Martelli, C. Mecucci, H. G. Drexler, and B. Falini. 2005. Cell lines OCI/AML3 bears exon-12 NPM gene mutation-A and cytoplasmic expression of nucleophosmin. *Leukemia.* 19:1760-7.
- Rondón, A. G., S. Jimeno, M. García-Rubio, and A. Aguilera. 2003. Molecular evidence that the eukaryotic THO/TREX complex is required for efficient transcription elongation. *J Biol Chem.* 278:39037-43.
- Ross, A. F., Y. Oleynikov, E. H. Kislaukis, K. L. Taneja, and R. H. Singer. 1997. Characterization of a beta-actin mRNA zipcode-binding protein. *Mol Cell Biol.* 17:2158-2165.
- Rougemaille, M., R. K. Gudipati, J. R. Olesen, R. Thomsen, B. Seraphin, D. Libri, and T. H. Jensen. 2007. Dissecting mechanisms of nuclear mRNA surveillance in THO/sub2 complex mutants. *EMBO J.* 26:2317-26.
- Ruepp, M. M., C. Aringhieri, S. Vivarelle, S. Cardinale, S. Paro, D. Schumperli, and S. M. Barabino. 2009. Mammalian pre-mrna 3' end processing factor CFIm68 functions in mRNA export. *Mol Biol Cell.* 20:5211-23.
- Ryan, K., K. G. Murthy, S. Kaneko, and J. L. Manley. 2002. Requirements of the RNA polymerase II C-terminal domain for reconstituting pre-mRNA 3' cleavage. *Mol Cell Biol.* 22:1684-92.

- Saguez, C., J. R. Olesen, and T. H. Jensen. 2005. Formation of export-competent mRNP: escaping nuclear destruction. *Curr Opin Cell Biol.* 17:287-93.
- Sandberg, R., J. R. Neilson, A. Sarma, P. A. Sharp, and C. B. Burge. 2008. Proliferating cells express mRNAs with shortened 3' untranslated regions and fewer microRNA target sites. *Science* 320:1643-7.
- Sato, K., R. Hayami, W. Wu, T. Nishikawa, H. Nishikawa, Y. Okuda, H. Ogata, M. Fukuda, and T. Ohta. 2004. Nucleophosmin/B23 is a candidate substrate for the BRCA1-BARD1 ubiquitin ligase. *J Biol Chem.* 279:30919-22.
- Schmidt, M. J., S. West, and C. J. Norbury. 2011. The human cytoplasmic RNA terminal U-transferase ZCCHC11 targets histone mRNAs for degradation. *RNA* 17:39-44.
- Schroeder, S. C., B. Schwer, S. Shuman, and D. Bentley. 2000. Dynamic association of capping enzymes with transcribing RNA polymerase II. *Genes Dev.* 14:2435-40.
- Shatkin, A. J. 1976. Capping of eucaryotic mRNAs. *Cell* 9:645-53.
- Sheets, M. D., S. C. Ogg, and M. P. Wickens. 1990. Point mutations in AAUAAA and the poly(A) addition site: effects on the accuracy and efficiency of cleavage and polyadenylation in vitro. *Nucleic Acids Res.* 18:5799-5805
- Shi, Y., D. C. Di Giammartino, D. Taylor, A. Sarkeshik, W. J. Rice, J. R. Yates, J. Frank, and J. L. Manley. 2009. Molecular architecture of the human pre-mRNA 3' processing complex. *Mol Cell.* 33:365-76
- Sittler, A., H. Gallinaro, and M. Jacob. 1994. Upstream and downstream cis-acting elements for cleavage at the L4 polyadenylation site of adenovirus-2. *Nucleic Acids Res.* 22:222-231
- Sommer, P., and U. Nehrbass. 2005. Quality control of messenger ribonucleoprotein particles in the nucleus and at the pore. *Curr Opin Cell Biol.* 17:294-301.
- Song, M. G., and M. Kiledjian. 2007. 3' Terminal oligo U-tract-mediated stimulation of decapping. *RNA.* 13:2356-65.
- Strässer, K., S. Masuda, P. Mason, J. Pfannstiel, M. Oppizzi, S. Rodriguez-Navarro, A. G. Rondón, A. Aguilera, K. Struhl, R. Reed, and E. Hurt. 2002. TREX is a conserved complex coupling transcription with messenger RNA export. *Nature* 417:304-8.
- Stutz, F., A. Bachi, T. Doerks, I. C. Braun, B. Séraphin, M. Wilm, P. Bork, and E. Izaurralde. 2000. REF, an evolutionary conserved family of hnRNP-like proteins, interacts with TAP/Mex67p and participates in mRNA nuclear export. *RNA* 6:638-50.
- Szebeni, A., J. E. Herrera, and M. O. Olson. 1995. Interaction of nucleolar protein B23 with peptides related to nuclear localization signals. *Biochemistry.* 34:8037-42.
- Takagaki, Y., and J. L. Manley. 2000. Complex protein interactions within the human polyadenylation machinery identify a novel component. *Mol Cell Biol.* 20:1515-25.
- Takagaki, Y., and J. L. Manley. 1998. Levels of polyadenylation factor CstF-64 control IgM heavy chain mRNA accumulation and other events associated with B cell differentiation. *Mol Cell.* 2:761-71.

- Takagaki, Y., L. C. Ryner, and J. L. Manley. 1988. Separation and characterization of a poly(A) polymerase and a cleavage/specificity factor required for pre-mRNA polyadenylation. *Cell* 52:731-42.
- Takagaki, Y., R. L. Seipelt, M. L. Peterson, and J. L. Manley. 1996. The polyadenylation factor CstF-64 regulates alternative processing of IgM heavy chain pre-mRNA during B cell differentiation. *Cell* 87:941-52.
- Takagaki, Y., L. C. Ryner, and J. L. Manley. 1989. Four factors are required for 3' end cleavage of pre-mRNAs. *Genes Dev.* 3:1711-1724
- Tange T., A. Nott, and M. J. Moore. 2004. The ever-increasing complexities of the exon junction complex. *Curr Opin Cell Biol.* 16:279-84.
- Tarapore, P., K. Shinmura, H. Suzuki, Y. Tokuyama, S. H. Kim, A. Mayeda, and K. Fukasawa. 2006. Thr199 phosphorylation targets nucleophosmin to nuclear speckles and represses pre-mRNA processing. *FEBS Lett.* 580:399-409.
- Tian, B., J. Hu, H. Zhang, and C. S. Lutz. 2005. A large-scale analysis of mRNA polyadenylation of human and mouse genes. *Nucleic Acids Res.* 33:201-12.
- Vanáčová, S., J. Wolf, G. Martin, D. Blank, S. Dettwiler, A. Friedlein, H. Langen, G. Keith, and W. Keller. 2005. A new yeast poly(A) polymerase complex involved in RNA quality control. *PLoS Biol.* 3:e189.
- Venkataraman, K., K. M. Brown, and G. M. Gilmartin. 2005. Analysis of a noncanonical poly(A) site reveals a tripartite mechanism for vertebrate poly(A) site recognition. *Genes Dev.* 19:1315-27.
- Wahle, E. 1991. A novel poly(A)-binding protein acts as a specificity factor in the second phase of messenger RNA polyadenylation. *Cell* 66:759-768
- Wahle, E. 1995. Poly(A) tail length control is caused by termination of processive synthesis. *J Biol Chem.* 270:2800–2808.
- Wang, K., S. Zhang, J. Weber, D. Baxter, and D. J. Galas. 2010. Export of microRNAs and microRNA-protective protein by mammalian cells. *Nucleic Acids Res.* 38:7248-59.
- West, S, N. J. Proudfoot, and M. J. Dye. 2008. Molecular dissection of mammalian RNA polymerase II transcriptional termination. *Mol Cell.* 29:600-10.
- West, S., and N. J. Proudfoot. 2009. Transcriptional termination enhances protein expression in human cells. *Mol Cell.* 33:354-64.
- Wickens, M., and P. Stephenson. 1984. Role of the conserved AAUAAA sequence: four point mutants prevent messenger RNA 3' end formation. *Science* 226:1045-1051
- Wilusz, J and T. Shenk. 1988. A 64 kd nuclear protein binds to RNA segments that include the AAUAAA polyadenylation motif. *Cell* 52:221-8.
- Wilusz, J., S. Pettine, and T. Shenk. 1989. Functional analysis of point mutations in the AAUAAA motif of the SV40 late polyadenylation signal. *Nucleic Acids Res.* 17:3899-3908

- Wu, M. H., and B. Y. Yung. 2002. UV stimulation of nucleophosmin/B23 expression is an immediate-early gene response induced by damaged DNA. *J Biol Chem.* 277:48234-40.
- Yoneda-Kato, N., A. T. Look, M. N. Kistein, M. B. Valentine, S. C. Raimondi, K. J. Cohen, A. J. Carroll and S. W. Morris. 1996. The t(3;5)(q25. 1;q34) of myelodysplastic syndrome and acute myeloid leukemia produces a novel fusion gene, NPM-MLF1. *Oncogene* 12:265-275.
- Zarkower, D., and M. Wickens. 1988. A functionally redundant downstream sequence in SV40 late pre-mRNA is required for mRNA 3' end formation and for assembly of a precleavage complex in vitro. *J. Biol. Chem.* 263:5780-5788
- Zhang, Y. 2004. The ARF-B23 connection: implications for growth control and cancer treatment. *Cell Cycle.* 3:259-62.
- Zhang, L., J. E. Lee, J. Wilusz, and C. J. Wilusz. 2008. The RNA-binding protein CUGBP1 regulates stability of tumor necrosis factor mRNA in muscle cells: implications for myotonic dystrophy. *J Biol Chem.* 33:22457-63.
- Zhao, J., L. Hyman, and C. Moore. 1999. Formation of mRNA 3' ends in eukaryotes: mechanism, regulation, and interrelationships with other steps in mRNA synthesis. *Microbiol Mol Biol Rev.* 2:405-45.